

**MATHEMATICAL MODELS OF VAPOR-COMPRESSOR SYSTEMS FOR  
MULTIVARIABLE CONTROL OF THE REFRIGERANT DYNAMICS AND  
INDOOR AIR CONDITIONS**

By

**Conrad Sanama**

*Submitted in partial fulfillment of the requirements for the degree*

Philosophiae Doctor (Electronic Engineering)

In the

Department of Electrical, Electronic and Computer Engineering

Faculty of Engineering, Built Environment and Information Technology

**UNIVERSITY OF PRETORIA**

November, 2022

# SUMMARY

---

## MATHEMATICAL MODELS OF VAPOR-COMPRESSION SYSTEMS FOR MULTIVARIABLE CONTROL OF THE REFRIGERANT DYNAMICS AND INDOOR AIR CONDITIONS

by

**Conrad Sanama**

Supervisor: Prof. Xiaohua Xia

Department: Electrical, Electronic and Computer Engineering

University: University of Pretoria

Degree: Philosophiae Doctor (Electronic Engineering)

Keywords: Vapor Compression System, Steady State Modelling, Transient State Modelling, Experimental Investigation, Control Volume Scheme, Navier-Stokes Equations, Finite Volume Method, Control-Oriented Modelling, Transfer Function, Cost Function, Superheat Control, Capacity Regulation, PID Control, State Space Formulation, MPC Implementation, Multivariable Control, Chiller-Fan Coil Unit.

Detailed steady and transient state models of vapor compression (VC) systems have been suggested in this work so that the governing parameters of the refrigerant dynamics such as pressure, enthalpy and temperature could be predicted at different operating conditions. The steady

and transient state models were validated with experimental data collected during startup and steady state operations. The experimental setup was equipped with a thermostatic expansion valve, a reciprocal compressor and plate heat exchangers for the condenser and evaporator. Recirculated water was adopted as secondary fluid for heat transfer with R-134a refrigerant.

The steady state model was developed from first principles with the refrigerant conditions being determined at each junction between the components of the VC system. A steady state matrix was built to determine the model outputs and it could be adopted for similar problems such as steady state modelling of single-condenser-and-multi-evaporators systems. The refrigerant pressures through the evaporator and condenser were in agreement with experiments. Other refrigerant conditions such as enthalpy and temperature through the components were also validated with experiments.

The evaporator and condenser modelling in transient state required special attention and Navier-Stokes equations were adopted for this purpose along with a finite volume scheme for discretization of the condenser and evaporator into 3 and  $n$ -control volumes. A transient state matrix was also built for outputs' prediction in transient operating conditions such as startup and shutdown. The refrigerant conditions namely pressure and enthalpy through the evaporator and condenser were validated with experiments.

The transient state model was then improved and converted into a control-oriented model with 12 state variables. The control-oriented model considered phase change in the condenser and evaporator namely, superheat, two-phase and subcooling. Model predictive control (MPC) was implemented on the control-oriented model after a model linearization around a steady state point

carefully selected from the steady state experiments performed for validation of the steady state modelling.

MPC implementation enabled to control superheat and evaporating pressure simultaneously with consideration of the coupling effect between superheat and capacity regulation. MPC was integrated in Simulink with satisfactory performances regarding disturbance rejection and reference tracking.

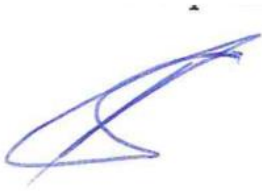
Building up on satisfactory MPC performance for multivariable control of the refrigerant dynamics, a proportional integral derivative (PID)-MPC controller was implemented on a Chiller-Fan coil unit (FCU) to control simultaneously, indoor temperature, humidity and CO<sub>2</sub> level with the coupling effect between humidity and temperature taken into consideration.

PID was implemented on a sub layer control loop located at the first heat exchanger and fresh air temperature was maintained within settings to level-out with room temperature to prevent from imbalanced loads. Disturbance rejection and set point tracking were satisfactory without necessarily increasing the supply fan and compressor speeds.

MPC was implemented on an upper layer control loop located at a secondary heat exchanger to regulate simultaneously indoor humidity, temperature and CO<sub>2</sub> level. The coupling effect between humidity and temperature was well taken care of by the MPC loop and CO<sub>2</sub> level regulation was performed without additional load as fresh air intake was carefully pre-cooled using the primary heat exchanger controlled with a PID loop. The performance of the sub layer PID was satisfactory with regards to stability, maximum overshoot and settling time whilst reference tracking and disturbance rejection were satisfactory with the upper layer MPC.

## STATEMENT OF SOURCES

To the best of my knowledge and belief, the work presented in this thesis is original, unless otherwise noted in the text. The information presented here has not previously been submitted, in whole or in part, for a degree offered by the University of Pretoria or any other university, I further declare.



Conrad Sanama

08<sup>th</sup> November 2022

## ACKNOWLEDGMENTS

Thanks are due to those who supported this thesis particularly to my research advisor Prof. Xiaohua Xia from the Department of Electrical, Electronic and Computer Engineering for his academic mentorship through the Centre of New Energy Systems (CNES) at the University of Pretoria, South Africa.

Thank you to Prof. Mohsen Sharifpur and Prof. Josua Meyer from the Department of Mechanical and Aeronautical Engineering who gave me my first research opportunity in the Clean Energy Research Group at the University of Pretoria, South Africa.

I also thank my peers from the CNES who supported me during my transition from the Department of Mechanical and Aeronautical Engineering to the Department of Electrical, Electronic and Computer Engineering.

Thank you to Prof. Robert Nzungwa from Ecole Nationale Supérieure Polytechnique of Douala, Cameroon who gave me my first glimpse of the engineering fields during my undergraduate studies.

I am also grateful to my undergraduate classmates at the Ecole Nationale Supérieure Polytechnique of Douala, Cameroon at the University of Douala for their friendship and support.

Thank you to my colleagues from Samsung Electronics Africa Regional Headquarters Johannesburg, South Africa especially to Dr. Yongbin Im who guided me during my beginnings in the field of HVAC.

Thank you to my colleagues from Samsung Electronics West Africa Limited Accra, Ghana for their friendship and encouragement during my time there.

Thank you to my colleagues at the International Finance Corporation (IFC) Abidjan, Côte d'Ivoire and abroad for their kindness during this process.

Very special thank you to my colleagues at GIGS, SOCIAM and Afrique Froid in Abidjan, Côte d'Ivoire for their trust in me.

Above all, to my family, I extend my gratitude especially to my parents in Douala, Cameroon and to my friends who supported me throughout my studies.

## LIST OF ABBREVIATIONS

<i>comp</i>	Compressor
<i>comp, out</i>	Compressor outlet
<i>comp, in</i>	Compressor inlet
<i>cond</i>	Condenser
<i>cond, out</i>	Condenser outlet
<i>cond, in</i>	Condenser inlet
<i>eff</i>	Effective
<i>evap</i>	Evaporator
<i>evap, in</i>	Evaporator inlet
<i>evap, out</i>	Evaporator outlet
<i>fin</i>	Condenser or evaporator fin
<i>in</i>	Inlet
<i>isen</i>	Isentropic
<i>isen, out</i>	Isentropic outlet
<i>out</i>	Outlet
<i>ref</i>	Refrigerant stream
<i>ref, in</i>	Inlet refrigerant
<i>ref, out</i>	Outlet refrigerant
<i>s</i>	Steady state
<i>Sh, operating</i>	Operating superheat



$Sh, static$	Static superheat
$T$	Transpose matrix
$tube$	Condenser or evaporator tube
$txv$	Thermostatic expansion valve
$txv, in$	Thermostatic expansion valve inlet
$txv, out$	Thermostatic expansion valve outlet
$v$	Volume
Vol	Volumetric
$wall, c, n$	Wall of $n^{th}$ -control volume of condenser
$wall, k$	Wall of $k^{th}$ -control volume of condenser
$water$	Water stream
$water, out$	Outlet water
$water, in$	Inlet water

## LIST OF SYMBOLS

$A_{cond,eff}$	Effective outer surface of condenser ( $m^2$ )
$A_{cond,tube}$	Outer surface of condenser tubes ( $m^2$ )
$A_{cond,fin}$	Surface of condenser fins ( $m^2$ )
$A_{c,n}$	Internal surface of $n^{th}$ -control volume in condenser ( $m^2$ )
$A_{evap}$	Evaporator surface ( $m^2$ )
$A_{cond}$	Condenser surface ( $m^2$ )
$A_{hx,dry}$	Heat transfer area at heat exchanger's dry zone ( $m^2$ )
$A_{hx,wet}$	Heat transfer area at heat exchanger's wet zone ( $m^2$ )
$C_{air}$	Specific heat of air ( $kJ\ kg^{-1}\ ^\circ C^{-1}$ )
$(C\rho A)_{cond,wall}$	Thermal capacitance at condenser wall ( $kJ\ ^\circ C^{-1}\ m^{-1}\ kg$ )
$(C\rho A)_{evap,wall}$	Thermal capacitance at evaporator wall ( $kJ\ ^\circ C^{-1}\ m^{-1}\ kg$ )
$C_{txv}$	Valve flow coefficient
$C_{water}$	Specific heat of water ( $kJ\ kg^{-1}\ ^\circ C^{-1}$ )
$d$	Disturbance ( $^\circ C$ )
$d_{cond}$	Inner diameter of condenser ( $m$ )
$d_{cond,in}$	Inner diameter of condenser ( $m$ )
$d_{cond,out}$	Outer diameter of condenser ( $m$ )
$d_{evap}$	Inner diameter of evaporator ( $m$ )
$d_{evap,in}$	Inner diameter of evaporator ( $m$ )

$d_{evap,out}$	Outer diameter of evaporator ( $m$ )
$D_v$	Displacement volume of compressor ( $m^3 s^{-1}$ )
$f_{cond}$	Friction factor in condenser
$f_{evap}$	Friction factor in evaporator
$G_{hxp}(s)$	Transfer function of primary heat exchanger
$G_{overall}(s)$	Overall transfer function
$G_{plant}(s)$	Plant's transfer function
$h$	Refrigerant enthalpy ( $kJ kg^{-1}$ )
$h_{air,supply}$	Enthalpy of supply air ( $kJ kg^{-1}$ )
$h_{comp,in}$	Refrigerant enthalpy at compressor inlet ( $kJ kg^{-1}$ )
$h_{comp,out}$	Refrigerant enthalpy at compressor outlet ( $kJ kg^{-1}$ )
$h_{cond,in}$	Refrigerant enthalpy at condenser inlet ( $kJ kg^{-1}$ )
$h_{cond,int,1}$	Refrigerant enthalpy at condenser interface 1 ( $kJ kg^{-1}$ )
$h_{cond,int,2}$	Refrigerant enthalpy at condenser interface 2 ( $kJ kg^{-1}$ )
$h_{cond,liq}$	Enthalpy of liquid refrigerant in condenser ( $kJ kg^{-1}$ )
$h_{cond,gas}$	Enthalpy of refrigerant gas in condenser ( $kJ kg^{-1}$ )
$h_{cond,out}$	Refrigerant enthalpy at condenser outlet ( $kJ kg^{-1}$ )
$h_{cond,sph}$	Enthalpy of superheated refrigerant in condenser ( $kJ kg^{-1}$ )
$h_{cond,sub}$	Enthalpy of subcooled refrigerant in condenser ( $kJ kg^{-1}$ )
$h_{evap,in}$	Refrigerant enthalpy at evaporator inlet ( $kJ kg^{-1}$ )
$h_{evap,int}$	Refrigerant enthalpy at evaporator interface ( $kJ kg^{-1}$ )
$h_{evap,liq}$	Enthalpy of liquid refrigerant in evaporator ( $kJ kg^{-1}$ )

$h_{evap,gas}$	Enthalpy of refrigerant gas in evaporator ( $kJ\ kg^{-1}$ )
$h_{evap,out}$	Refrigerant enthalpy at evaporator outlet ( $kJ\ kg^{-1}$ )
$h_{evap,sp}$	Enthalpy of superheated refrigerant in evaporator ( $kJ\ kg^{-1}$ )
$h_{hx,dry}$	Air enthalpy at heat exchanger's dry zone ( $kJ\ kg^{-1}$ )
$h_{hx,2ph}$	Refrigerant enthalpy at heat exchanger's two-phase zone ( $kJ\ kg^{-1}$ )
$h_{isen,out}$	Refrigerant isentropic enthalpy at compressor outlet ( $kJ\ kg^{-1}$ )
$h_{latent,vap}$	Water's latent heat of vaporization ( $kJ\ kg^{-1}$ )
$h_{ref,hx,in}$	Refrigerant enthalpy at heat exchanger's inlet ( $kJ\ kg^{-1}$ )
$h_{ref,hx,out}$	Refrigerant enthalpy at heat exchanger's outlet ( $kJ\ kg^{-1}$ )
$h_{txv,out}$	Refrigerant enthalpy at expansion valve outlet ( $kJ\ kg^{-1}$ )
$h_1$	Junction enthalpy at evaporator outlet ( $kJ\ kg^{-1}$ )
$h_2$	Junction enthalpy at condenser inlet ( $kJ\ kg^{-1}$ )
$h_3$	Junction enthalpy at condenser outlet ( $kJ\ kg^{-1}$ )
$h_4$	Junction enthalpy at evaporator inlet ( $kJ\ kg^{-1}$ )
$h_i$	Refrigerant enthalpy in $i^{th}$ -control volume ( $kJ\ kg^{-1}$ )
$h_i^0$	Initial refrigerant enthalpy in $i^{th}$ -control volume of condenser ( $kJ\ kg^{-1}$ )
$h_{c,n}$	Refrigerant enthalpy in $n^{th}$ -control volume of condenser ( $kJ\ kg^{-1}$ )
$h_{c,n}^0$	Initial refrigerant enthalpy in $n^{th}$ -control volume of condenser ( $kJ\ kg^{-1}$ )
$K_d$	Derivative gain
$K_i$	Integral gain
$K_p$	Proportional gain
$K_{plant}$	Plant's gain factor

$l_{cond}$	Condenser length ( $m$ )
$l_{cond,2ph}$	Two-phase length in condenser ( $m$ )
$l_{cond,sph}$	Superheat length in condenser ( $m$ )
$l_{cond,sub}$	Subcooled length in condenser ( $m$ )
$l_{evap}$	Evaporator length ( $m$ )
$l_{evap,2ph}$	Two-phase length in evaporator ( $m$ )
$l_{evap,sph}$	Superheat length in evaporator ( $m$ )
$M_{air,room}$	Moisture load generation in room ( $kg s^{-1}$ )
$m_{comp}$	Refrigerant mass flow rate in compressor ( $kg s^{-1}$ )
$(MC)_{cond}$	Thermal mass of condenser wall ( $kJ\ ^{\circ}C^{-1}$ )
$(m_{cond,ref})_{in}$	Refrigerant mass flow rate at condenser inlet ( $kg s^{-1}$ )
$(m_{cond,ref})_{int,1}$	Refrigerant mass flow rate at condenser interface 1 ( $kg s^{-1}$ )
$(m_{cond,ref})_{int,2}$	Refrigerant mass flow rate at condenser interface 2 ( $kg s^{-1}$ )
$(m_{cond,ref})_{out}$	Refrigerant mass flow rate at condenser outlet ( $kg s^{-1}$ )
$(m_{evap,ref})_{in}$	Refrigerant mass flow rate at evaporator inlet ( $kg s^{-1}$ )
$(m_{evap,ref})_{int}$	Refrigerant mass flow rate at evaporator interface ( $kg s^{-1}$ )
$(m_{evap,ref})_{out}$	Refrigerant mass flow rate at evaporator outlet ( $kg s^{-1}$ )
$\dot{m}_{ref}$	Refrigerant mass flow rate ( $kg s^{-1}$ )
$m_{txv}$	Refrigerant mass flow rate in expansion valve ( $kg s^{-1}$ )
$\dot{m}_{water}$	Water mass flow rate ( $kg s^{-1}$ )
$P_1$	Junction pressure at evaporator outlet ( $kPa$ )

$P_2$	Junction pressure at condenser inlet ( $kP_a$ )
$P_3$	Junction pressure at condenser outlet ( $kP_a$ )
$P_4$	Junction pressure at evaporator inlet ( $kP_a$ )
$P_{comp,out}$	Refrigerant pressure at compressor outlet ( $kP_a$ )
$P_{cond}$	Refrigerant pressure in condenser ( $kP_a$ )
$P_{cond}^0$	Initial refrigerant pressure in condenser ( $kP_a$ )
$P_{evap}$	Refrigerant pressure in evaporator ( $kP_a$ )
$P_{evap}^0$	Initial refrigerant pressure in evaporator ( $kP_a$ )
$(P_{ref,in})_{cond}$	Refrigerant pressure at condenser inlet ( $kP_a$ )
$(P_{ref,out})_{cond}$	Refrigerant pressure at condenser outlet ( $kP_a$ )
$(P_{ref,in})_{evap}$	Refrigerant pressure at evaporator inlet ( $kP_a$ )
$(P_{ref,out})_{evap}$	Refrigerant pressure at evaporator outlet ( $kP_a$ )
$P_{txv,in}$	Refrigerant pressure at expansion valve inlet ( $kP_a$ )
$P_{txv,out}$	Refrigerant pressure at expansion valve outlet ( $kP_a$ )
$Q_{air,fresh}$	Fresh air load ( $kw$ )
$Q_{air,room}$	Room air load ( $kw$ )
$Q_{cond}$	Heat rejection in condenser ( $kw$ )
$Q_{cond,2ph}$	Heat absorption in condenser two-phase zone ( $kw$ )
$Q_{cond,sph}$	Heat absorption in condenser superheat zone ( $kw$ )
$Q_{cond,sub}$	Heat absorption in condenser subcooled zone ( $kw$ )
$Q_{evap}$	Heat absorption in evaporator ( $kw$ )
$Q_{evap,2ph}$	Heat absorption in evaporator two-phase zone ( $kw$ )

$Q_{evap,sph}$	Heat absorption in evaporator superheat zone ( $kw$ )
$Q_{ref,i}$	Heat rejected by refrigerant in condenser ( $kw$ )
$Q_{water,i}$	Heat absorbed by water in condenser ( $kw$ )
$Q_{water,in}$	Inlet heat of water ( $kw$ )
$Q_{water,out}$	Outlet heat of water ( $kw$ )
$RPM_{comp}$	Rotational speed of compressor ( $rpm$ )
$t$	Final time ( $s$ )
$t^0$	Initial time ( $s$ )
$T_{air,fresh}$	Fresh air temperature ( $^{\circ}C$ )
$T_{air,out}$	Outdoor air temperature ( $^{\circ}C$ )
$T_{air,room}$	Room air temperature ( $^{\circ}C$ )
$T_{air,supply}$	Supply air temperature ( $^{\circ}C$ )
$T_{c,n}$	Refrigerant temperature in $n^{th}$ -control volume of condenser ( $^{\circ}C$ )
$T_{cond,ref,2ph}$	Refrigerant temperature in condenser two-phase zone ( $^{\circ}C$ )
$T_{cond,ref,sph}$	Refrigerant temperature in condenser superheat zone ( $^{\circ}C$ )
$T_{cond,ref,sub}$	Refrigerant temperature in condenser subcooled zone ( $^{\circ}C$ )
$T_{cond,wall,2ph}$	Wall temperature in condenser two-phase zone ( $^{\circ}C$ )
$T_{cond,wall,sph}$	Wall temperature in condenser superheat zone ( $^{\circ}C$ )
$T_{cond,wall,sub}$	Wall temperature in condenser subcooled zone ( $^{\circ}C$ )
$T_{cond,water,in}$	Water temperature at condenser inlet ( $^{\circ}C$ )
$T_{evap,ref}$	Refrigerant temperature in evaporator ( $^{\circ}C$ )
$T_{evap,ref,2ph}$	Refrigerant temperature in evaporator two-phase zone ( $^{\circ}C$ )

$T_{evap,ref,sph}$	Refrigerant temperature in evaporator superheat zone (°C)
$T_{evap,wall}$	Wall temperature in evaporator (°C)
$T_{evap,wall,2ph}$	Wall temperature in evaporator two-phase zone (°C)
$T_{evap,water,in}$	Water temperature at evaporator inlet (°C)
$T_{evap,wall,sph}$	Wall temperature in evaporator superheat zone (°C)
$T_{hx,dry}$	Air temperature at heat exchanger's dry zone (°C)
$T_{hx,wall}$	Wall temperature at heat exchanger (°C)
$(T_k)_{cond}$	Refrigerant temperature in $k^{th}$ -control volume of condenser (°C)
$(T_{ref,in})_{cond}$	Refrigerant temperature at condenser inlet (°C)
$(T_{ref,out})_{cond}$	Refrigerant temperature at condenser outlet (°C)
$(T_{ref,in})_{evap}$	Refrigerant temperature at evaporator inlet (°C)
$(T_{ref,out})_{evap}$	Refrigerant temperature at evaporator outlet (°C)
$T_{Sh,operating}$	Refrigerant operating superheat (°C)
$T_{Sh,static}$	Refrigerant static superheat (°C)
$T_{wall,c,n}$	Wall temperature in $n^{th}$ -control volume of condenser (°C)
$(T_{wall,k})_{cond}$	Wall temperature in $k^{th}$ -control volume of condenser (°C)
$(T_{wall,k}^0)_{cond}$	Initial wall temperature in $k^{th}$ -control volume of condenser (°C)
$T_{water,in}$	Inlet water temperature (°C)
$(T_{water,in})_{cond}$	Water temperature at condenser inlet (°C)
$(T_{water,in})_{evap}$	Water temperature at evaporator inlet (°C)
$T_{water,out}$	Outlet water temperature (°C)



$(T_{water,out})_{cond}$	Water temperature at condenser outlet ( $^{\circ}\text{C}$ )
$(T_{water,out})_{evap}$	Water temperature at evaporator outlet ( $^{\circ}\text{C}$ )
$u$	Axial velocity ( $m\ s^{-1}$ )
$U_{cond,water}$	Heat transfer coefficient of water in condenser ( $kw\ m^{-2}\ ^{\circ}\text{C}^{-1}$ )
$(UA)_{cond}$	Overall heat transfer coefficient in condenser ( $kw\ ^{\circ}\text{C}^{-1}$ )
$(UA)_{evap}$	Overall heat transfer coefficient in condenser ( $kw\ ^{\circ}\text{C}^{-1}$ )
$V_{air,fresh}$	Fresh air volume ( $m^3$ )
$V_{air,room}$	Room air volume ( $m^3$ )
$\dot{V}_{air,room}$	Air flow rate in room ( $m^3\ s^{-1}$ )
$V_{air,supply}$	Supply air volume ( $m^3$ )
$\dot{V}_{air,supply}$	Flow rate of supply air ( $m^3\ s^{-1}$ )
$V_{c,n}$	Internal volume of $n^{th}$ -control volume in condenser ( $m^3$ )
$V_{hx,dry}$	Air volume at heat exchanger's dry zone ( $m^3$ )
$V_{hx,wet}$	Air volume at heat exchanger's wet zone ( $m^3$ )
$V_{ref}$	Refrigerant speed ( $m\ s^{-1}$ )
$\dot{V}_{water}$	Water flow rate ( $m^3\ s^{-1}$ )
$W_{air,room}$	Room air's moisture content ( $kg\ kg^{-1}\ dry\ air$ )
$W_{air,supply}$	Supply air's moisture content ( $kg\ kg^{-1}\ dry\ air$ )
$\vec{x}_s$	Output for steady state modelling
$\alpha_{cond,2ph}$	Heat transfer coefficient in condenser two-phase zone ( $kw\ m^{-2}\ ^{\circ}\text{C}^{-1}$ )
$\alpha_{cond,out}$	Heat transfer coefficient at condenser outer surface ( $kw\ m^{-2}\ ^{\circ}\text{C}^{-1}$ )
$\alpha_{cond,sph}$	Heat transfer coefficient in condenser superheat zone ( $kw\ m^{-2}\ ^{\circ}\text{C}^{-1}$ )

$\alpha_{cond,sub}$	Heat transfer coefficient in condenser subcooled zone ( $kw m^{-2}^{\circ}C^{-1}$ )
$\alpha_{c,n}$	Heat transfer coefficient in $n^{th}$ -control volume of condenser ( $kw m^{-2}^{\circ}C^{-1}$ )
$\alpha_{evap}$	Heat transfer coefficient in evaporator ( $kw m^{-2}^{\circ}C^{-1}$ )
$\alpha_{evap,2ph}$	Heat transfer coefficient in evaporator two-phase zone ( $kw m^{-2}^{\circ}C^{-1}$ )
$\alpha_{evap,out}$	Heat transfer coefficient at evaporator outer surface ( $kw m^{-2}^{\circ}C^{-1}$ )
$\alpha_{evap,sph}$	Heat transfer coefficient in evaporator superheat zone ( $kw m^{-2}^{\circ}C^{-1}$ )
$\alpha_{hx,dry}$	Heat transfer coefficient at heat exchanger's dry zone ( $kw m^{-2}^{\circ}C^{-1}$ )
$\alpha_{hx,wet}$	Heat transfer coefficient at heat exchanger's wet zone ( $kw m^{-2}^{\circ}C^{-1}$ )
$\Delta t$	Time step (s)
$\delta Q_{evap}$	Small heat absorbed in evaporator ( $kw$ )
$\bar{V}_{cond}$	Void fraction in condenser
$\bar{V}_{evap}$	Void fraction in evaporator
$\eta_{cond,fin}$	Effectiveness of condenser fins
$\eta_{isen}$	Isentropic efficiency of compressor
$\eta_{vol}$	Volumetric efficiency of compressor
$\rho_{air}$	Air density ( $kg m^{-3}$ )
$\rho_{c,n}$	Refrigerant density in $n^{th}$ -control volume of condenser ( $kg m^{-3}$ )
$\rho_{comp,in}$	Density of refrigerant at compressor inlet ( $kg m^{-3}$ )
$\rho_{cond,2ph}$	Density of two-phase refrigerant in condenser ( $kg m^{-3}$ )
$\rho_{cond,gas}$	Density of refrigerant gas in condenser ( $kg m^{-3}$ )
$\rho_{cond,liq}$	Density of refrigerant liquid in condenser ( $kg m^{-3}$ )
$\rho_{cond,sph}$	Density of superheated refrigerant in condenser ( $kg m^{-3}$ )

$\rho_{cond,sub}$	Density of subcooled refrigerant in condenser ( $kg\ m^{-3}$ )
$\rho_{evap,2ph}$	Density of two-phase refrigerant in evaporator ( $kg\ m^{-3}$ )
$\rho_{evap,gas}$	Density of refrigerant gas in evaporator ( $kg\ m^{-3}$ )
$\rho_{evap,liq}$	Density of refrigerant liquid in evaporator ( $kg\ m^{-3}$ )
$\rho_{evap,sph}$	Density of superheated refrigerant in evaporator ( $kg\ m^{-3}$ )
$\rho_{txv,in}$	Refrigerant density at expansion valve inlet ( $kg\ m^{-3}$ )
$\rho_{water}$	Water density ( $kg\ m^{-3}$ )
$\tau$	Thermal time (s)

# TABLE OF CONTENTS

<b>CHAPTER 1 INTRODUCTION .....</b>	<b>1</b>
1.1. PROBLEM STATEMENT .....	1
1.1.1. Context of the problem .....	3
1.1.2. Research gap.....	4
1.2. RESEARCH OBJECTIVE AND QUESTIONS.....	5
1.3. APPROACH.....	6
1.4. RESEARCH GOALS.....	6
1.5. RESEARCH CONTRIBUTION .....	6
1.6. RESEARCH OUTPUTS .....	6
1.7. OVERVIEW OF STUDY .....	7
<b>CHAPTER 2 LITERATURE REVIEW .....</b>	<b>9</b>
2.1. INTRODUCTION.....	9
2.2. MATHEMATICAL MODELLING.....	10
2.3. CONVENTIONAL NONLINEAR STRATEGIES .....	12
2.4. ENERGY SAVING METHODS .....	16
2.5. INTELLIGENT CONTROL STRATEGIES .....	17
2.6. COMPRESSOR MODELLING.....	19

2.7.	EXPANSION VALVE MODELLING .....	21
<b>CHAPTER 3 MODELLING OF THE REFRIGERANT DYNAMICS.....</b>		<b>24</b>
3.1.	INTRODUCTION.....	24
3.2.	LITERATURE REVIEW .....	25
3.2.1.	Steady state modelling .....	25
3.2.2.	Transient state modelling.....	29
3.3.	STEADY STATE MODELLING .....	33
3.3.1.	Compressor modelling.....	35
3.3.2.	Condenser modelling .....	36
3.3.3.	Expansion valve modelling.....	38
3.3.4.	Solution of the steady state modelling.....	39
3.3.5.	Derivation of the steady state modelling matrix .....	39
3.3.6.	Steady state modelling matrix .....	40
3.4.	TRANSIENT STATE MODELLING .....	41
3.4.1.	Condenser modelling .....	41
3.4.2.	Discretization of the modelling equations of the condenser .....	46
3.5.	EXPERIMENTAL INVESTIGATION OF A VC SYSTEM .....	52
3.6.	RESULTS AND DISCUSSION .....	56
3.6.1.	Steady state modelling.....	56
3.6.2.	Transient state modelling.....	61

3.7.	CONCLUSION .....	66
<b>CHAPTER 4 CONTROL-ORIENTED MODELLING OF THE REFRIGERANT DYNAMICS.....</b>		<b>69</b>
4.1.	INTRODUCTION.....	69
4.2.	LITERATURE REVIEW .....	71
4.3.	CONTROL – ORIENTED MODELLING OF THE HEAT EXCHANGERS.....	73
4.3.1.	Two – phase zone of the evaporator .....	75
4.3.2.	Superheat zone of the evaporator .....	77
4.3.3.	Superheat zone of the condenser .....	79
4.3.4.	Two – phase zone of the condenser .....	81
4.3.5.	Subcool zone of the condenser.....	83
4.4.	STATE SPACE FORMULATION ON THE VC SYSTEM .....	84
4.5.	MPC IMPLEMENTATION ON THE VC SYSTEM .....	88
4.6.	RESULTS AND DISCUSSION .....	91
4.7.	CONCLUSION .....	100
<b>CHAPTER 5 CONTROL-ORIENTED MODELLING OF THE INDOOR AIR CONDITIONS.....</b>		<b>102</b>
5.1.	INTRODUCTION.....	102
5.2.	LITERATURE REVIEW .....	104
5.3.	CHILLER – FCU SETUP .....	107
5.4.	SUB LAYER PID .....	108
5.4.1.	Primary heat exchanger modelling .....	108

5.4.2. Room modelling .....	110
5.4.3. Plant modelling .....	111
5.4.4. PID implementation on the primary heat exchanger .....	112
5.5. UPPER LAYER MPC .....	113
5.5.1. Dynamic modelling.....	113
5.5.2. State space formulation on the VCAC system .....	116
5.5.3. MPC implementation on the VCAC system .....	118
5.6. RESULTS AND DISCUSSION .....	120
5.6.1. Sub layer PID .....	120
5.6.2. Upper layer MPC .....	122
5.6.2.1. Set point tracking assessment .....	125
5.6.2.2. Disturbance rejection assessment .....	127
5.7. CONCLUSION .....	129
<b>CHAPTER 6 CONCLUSION AND FUTURE WORK .....</b>	<b>131</b>
6.1. INTRODUCTION.....	131
6.2. CONCLUSION .....	131
6.3. FUTURE WORK .....	134
<b>REFERENCES .....</b>	<b>136</b>
<b>ADDENDUM .....</b>	<b>178</b>
A.1. SIMULINK MODEL OF A VC SYSTEM .....	178
A.2. HEAT TRANSFER CORRELATIONS .....	178

A.3.	DERIVATION OF DISCRETIZED EQUATIONS .....	179
A.4.	MODEL TRANSFORMATION FROM PREDICTIVE TO CONTROL-ORIENTED .....	184
A.4.1.	Evaporator modelling .....	185
A.4.2.	Condenser modelling .....	189
A.4.3.	Derivation of steady state equations .....	189



# LIST OF FIGURES

Figure 3.1 <i>Conventional VC system</i> .....	34
Figure 3.2 <i>Control volume of condenser – 3 control volumes</i> .....	42
Figure 3.3 <i>Control volume of condenser – 1 control volume</i> .....	43
Figure 3.4 <i>Experimental setup</i> .....	53
Figure 3.5 <i>p-h diagram of the VC cycle</i> .....	53
Figure 3.6 <i>Temperature curves of the refrigerant</i> .....	57
Figure 3.7 <i>Temperature curves of water</i> .....	57
Figure 3.8 <i>Heat curves of the refrigerant</i> .....	58
Figure 3.9 <i>Heat curves of water</i> .....	58
Figure 3.10 <i>Pressure curves of the refrigerant</i> .....	59
Figure 3.11 <i>Enthalpy curves of the refrigerant</i> .....	59
Figure 3.12 <i>Refrigerant density in condenser</i> .....	62
Figure 3.13 <i>Refrigerant density in evaporator</i> .....	62
Figure 3.14 <i>Refrigerant temperature in condenser</i> .....	62
Figure 3.15 <i>Refrigerant temperature in evaporator</i> .....	62
Figure 3.16 <i>Refrigerant enthalpy in condenser</i> .....	63
Figure 3.17 <i>Refrigerant enthalpy in evaporator</i> .....	63
Figure 3.18 <i>Refrigerant pressure in condenser and evaporator</i> .....	65
Figure 4.1 <i>Evaporator model with two-phase and superheat zones</i> .....	74
Figure 4.2 <i>Condenser model with superheat, two-phase and subcool zones</i> .....	75
Figure 4.3 <i>Computed variables on Simulink</i> .....	91

Figure 4.4 <i>MPC model</i> .....	92
Figure 4.5 <i>Simulink models of the VC components</i> .....	92
Figure 4.6 <i>System responses to disturbances</i> .....	93
Figure 4.7 <i>Coupled reference tracking</i> .....	96
Figure 5.1 <i>Chiller-FCU Setup</i> .....	108
Figure 5.2 <i>Block diagram of the open loop plant</i> .....	112
Figure 5.3 <i>PID block diagram</i> .....	113
Figure 5.4 <i>Open loop's response</i> .....	121
Figure 5.5 <i>Close loop's response</i> .....	121
Figure 5.6 <i>MPC block diagram</i> .....	124
Figure 5.7 <i>Temperature set point tracking</i> .....	126
Figure 5.8 <i>System responses to load variation</i> .....	128

# LIST OF TABLES

Table 3.1 <i>Dynamic models of VC systems</i> .....	33
Table 3.2 <i>Description of the governing parameters</i> .....	35
Table 3.3 <i>Steady state modelling equations of the evaporator</i> .....	37
Table 3.4 <i>Refrigerant conditions</i> .....	46
Table 3.5 <i>Transient state modelling equations of the evaporator</i> .....	52
Table 3.6 <i>Steady state parameters [145]</i> .....	56
Table 3.7 <i>Transient state parameters [145]</i> .....	61
Table 4.1 <i>Components of the <b>D1</b> Matrix</i> .....	85
Table 4.2 <i>Components of the <b>F1</b> matrix</i> .....	86
Table 4.3 <i>Integrated parameters</i> .....	94
Table 5.1 <i>Parameters of the plant model</i> .....	111
Table 5.2 <i>Components of the <b>D2</b> Matrix</i> .....	116
Table 5.3 <i>Components of the <b>F2</b> matrix</i> .....	117
Table 5.4 <i>Ziegler-Nichols parameters and gains</i> .....	121
Table 5.5 <i>Plant performance indicators</i> .....	122
Table 5.6 <i>MPC parameters</i> .....	123

# CHAPTER 1 INTRODUCTION

## 1.1. PROBLEM STATEMENT

Energy efficiency in buildings has attracted a lot of attention over the years with increasing energy consumption of buildings globally due to population growth and improving life conditions. Over 10% of the world expenditures is allocated to energy demand and it is estimated that over 80% of the global energy production is fossil. However, renewable energy production such as solar and wind is estimated to grow every year by 20% unlike fossil production which observes a slow growth. The remaining 20% of global energy production is dedicated to electricity. Among the energy source used in buildings, electricity is the largest, followed by natural gas then petroleum. In recent years, energy consumption in buildings and in particular electricity has increased with growing demand.

Air conditioning (AC) systems are by far the appliances with the highest energy consumption in buildings with an estimated 50% of total energy consumption in buildings [1]. The world manufacturers of AC systems are working towards innovating more sophisticated and energy efficient systems for air cooling or heating. Moreover, energy issue is turning to be critical to address environmental problem as one might have less significant impact on environment by reducing energy consumption. The demand for AC systems is significantly growing in developing countries with improving life conditions of the population. Adoption of AC systems in household and service sectors raises the question regarding energy consumption and greenhouse gas (GHG) emissions.

The energy consumption of AC systems depends strongly on their design and the selection of the appropriate equipment line-up. Operating time and maintenance are also factors defining the energy consumption of AC systems. Available data disclose the high amount of energy consumed by AC systems and the relevance to address this issue. AC systems' main purpose is to maintain temperature and humidity within a comfort range. Therefore, AC systems could be used to reduce or increase temperature depending on either hot or cold weather. The process of AC systems is associated with integrated VC systems that govern the fluid dynamics.

Heating, ventilation and air conditioning (HVAC) systems remain complicated to understand and this contributes to enable inefficient energy usage. The possibility to improve the efficiency of AC systems remains important. The energy efficiency ratio (*EER*) which is a dimensionless parameter measuring the performance of AC systems operating in cooling mode is the ratio of the cooling output energy produced by the AC system to its electrical input energy. *EER* could be expressed as follows:

$$EER = \frac{\dot{Q}_{cooling-produced} [kwh]}{\dot{W}_{input} [kwh]} \quad (1.1)$$

$\dot{Q}_{cooling-produced}$  Negative heat production (*kwh*)

$\dot{W}_{input}$  Input work (*kwh*)

*EER* of AC systems could also be evaluated during a specific cooling time setting during which a determined power has been consumed by the system. This evaluation of efficiency is referred to as seasonal energy efficiency ratio (*SEER*).

In Europe, we often refer to (*SEER*) as European seasonal efficiency ratio (*ESEER*) and as integrated energy efficiency ratio (*IEER*) in the United States. In practice, *EER* values disclosed on technical manual books of AC systems are provided based on specific laboratory conditions. It appears that on a real on-site installation the actual value of *EER* would be lower than the laboratory value due to varying operating conditions in real operating conditions. This difference gives room for design improvement of AC systems to the point where the gap of *EER* values between laboratories versus on-sites gets bridged to the best possible extent.

The counterpart of *EER* is the coefficient of performance (*COP*) which is the ratio of the heating output energy produced by a space heating heat pump system to its electrical input energy. In a simple way, the *COP* could be defined as the efficiency parameter of a space heating heat pump system in heating mode. *COP* could be expressed as follows:

$$COP = \frac{\dot{Q}_{\text{heating-produced}} [kwh]}{\dot{W}_{\text{input}} [kwh]} \quad (1.2)$$

$\dot{Q}_{\text{heating-produced}}$  Positive heat production (*kwh*)

### **1.1.1. Context of the problem**

Improvement of the energy efficiency of AC systems has a direct impact on reducing the energy consumption and GHG emissions of buildings. Enhancement of AC systems' energy efficiency has attracted a lot of attention among researchers, manufacturers, governments and non-governmental organizations (NGO's). Research to improve the energy efficiency of AC is performed around the world. For instance, some research focuses on developing advanced control strategies to optimize the operations of AC systems whilst some other focuses on the isolation of

the building envelopes. In this work, attention is given to control strategies adopted to reduce the energy consumption of AC systems. Literatures on advanced control strategies for optimal energy consumption of AC systems are presented in the literature review section.

### **1.1.2. Research gap**

The research gaps in this work were identified after completing the review of a significant number of published literatures and the subsequent sections summarize the identified gaps.

Implementation of performant control strategies on AC systems for control of the fluid dynamics and indoor air conditions usually requires developing comprehensive mathematical models through which the controllers could be developed. However, the mathematical models found in the literatures are not very easy to adopt for control purposes outside of the scope of work on which they were developed. This is mainly because various steps to determine the model outputs are not usually fully disclosed or more often tedious to reproduce.

Additionally, the control strategies adopted in the literature for control of the fluid dynamics in VC systems do not discuss the simultaneous regulation of superheat and capacity on one hand whilst considering the existence of coupling effects among superheat and capacity on the other hand, which has a direct impact on the system's energy efficiency. Furthermore, although existing in the literatures, nonlinear multivariable controllers of indoor air temperature, humidity and CO<sub>2</sub> level considering the existing coupling effects may require improvement.

Firstly, in terms of CO<sub>2</sub> level control with fresh air intake without creation of imbalanced loads that could alter energy saving with increasing compressor and fans' speeds to overcome the imbalance. Secondly, in terms of the performance of the multivariable controller for indoor air

temperature, humidity and CO<sub>2</sub> level. With adequate control of CO<sub>2</sub> level, one could enhance the overall performance of the controller with less energy requirement for the compressor and fans.

## **1.2. RESEARCH OBJECTIVE AND QUESTIONS**

This work aims to use mathematical, numerical and experimental approaches [2, 3] to develop the following:

- Steady and transient state models to capture the fluid dynamics in VC systems so that the refrigerant pressure, temperature and enthalpy could be predicted during steady and transient operating conditions.
- A control-oriented model that considers phase changes in the condenser and evaporator of VC systems so that the refrigerant dynamics could be captured with more accuracy to enable MPC implementation for simultaneous superheat and capacity control.
- A hybrid controller with PID combined with MPC to control simultaneously indoor temperature, humidity and CO<sub>2</sub> level whilst carefully maintaining the temperature of fresh air intake within settings to prevent from imbalanced loads.

The following questions should be addressed to reach the aforementioned objectives:

- How to develop comprehensive mathematical models that could predict the steady and transient behaviors of the fluid in VC systems whilst remaining easy to reproduce or adopt on other similar problems?



- How to migrate from predictive to control-oriented models enabling the multivariable control of the fluid dynamics in VC systems whilst considering the coupling effect between inter-connected variables?
- How to combine MPC with a PID control loop to control simultaneously the indoor air conditions to maintain satisfactory indoor air quality (IAQ) without necessarily increasing energy consumption?

### **1.3. APPROACH**

Mathematical formulations are adopted and integrated in this work, then transformed using adequate techniques to obtain equations that could be solved numerically then validated with experimental data to end up with the interpretation of the results.

### **1.4. RESEARCH GOALS**

The ultimate goals of this research work are to contribute in the development of energy efficient HVAC systems required to reduce carbon emissions so that net zero targets could be achieved in the built environment sector.

### **1.5. RESEARCH CONTRIBUTION**

Out of this work, three journal articles have been published and a fourth one was submitted for publication in peer reviewed international journals along with one presentation during an Institute of Electrical and Electronics Engineers (IEEE) conference. Article and conference details are listed in the subsequent section.

### **1.6. RESEARCH OUTPUTS**

[A1] C. Sanama, X. Xia, “Transient state modelling and experimental investigation of the thermal behavior of a vapor compression system,” *Mathematical Problems in Engineering*, vol. 2021, pp. 1-16, Paper ID 9941451, 2021.

[A2] C. Sanama, X. Xia, “Modelling and experimental investigation of a vapor compression system under steady state regime,” *International Journal of Mechanical Engineering and Robotics Research*, vol. 11, pp. 114-122, 2022.

[A3] C. Sanama, X. Xia, M. Nguepnang, “PID-MPC implementation on a chiller-fan coil unit,” *Journal of Mathematics*, vol. 2022, pp. 1-13, Paper ID 8405361, 2022.

[A4] C. Sanama, X. Xia, “Control-oriented modelling for multivariable control of refrigerant dynamics in vapor compression systems,” submitted to *Advances in Mathematical Physics*, (under review).

[C1] C. Sanama, “Steady state modelling and experimental investigation of the thermal behavior of a vapor compression system,” *IEEE 12<sup>th</sup> International Conference on Mechanical and Intelligent Manufacturing Technologies*, Paper ID MT069, Cape Town (Virtual), 2021.

## **1.7. OVERVIEW OF STUDY**

This thesis is divided in 6 chapters as follows:

- Chapter 1 introduces the background of the research work, the research gap, the scope and objectives.
- Chapter 2 presents the preliminary literature study on mathematical modelling and control strategies of VC systems.
- Chapter 3 introduces the mathematical modelling of the refrigerant dynamics in VC systems.

- Chapter 4 presents the control-oriented modelling for multivariable control of the refrigerant dynamics in VC systems.
- Chapter 5 introduces the control-oriented model for the control of indoor air conditions with integrated vapor compression air-conditioning (VCAC) systems.
- Chapter 6 presents the conclusion and future work.
- A complete list of references is provided at the end of this work.
- Addendum section is provided for additional information.

## CHAPTER 2 LITERATURE REVIEW

### 2.1. INTRODUCTION

As mentioned, energy consumption in buildings is mainly driven by AC systems with over 50% share of the total energy consumed in buildings. Therefore, implementation of adequate measures such as performant controllers on AC systems might influence significantly on the overall energy consumption of buildings. Controlling and monitoring energy consumption of buildings is paramount for energy efficiency and reduction of GHG emissions. Applicable control strategies on AC systems could be classified in two categories namely conventional nonlinear and intelligent control strategies. Nonlinear and intelligent control schemes could be coupled to energy saving methods to achieve higher performances. Mathematical models are usually required to describe the systems through which a controller is implemented therefore, the subsequent section will also present the relevant literatures of mathematical modelling adopted on AC systems for prediction of parameters and for control purposes.

The subsequent sections of this chapter are listed as follows. In section 2.2. the literatures of the published mathematical models of VC systems are reviewed. The methods for conventional nonlinear control, the energy savings and the intelligent control are respectively reviewed in section 2.3, section 2.4 and section 2.5. The literature surveys on the compressor modelling are presented in section 2.6. Finally, the literatures on the expansion valve models are reviewed in section 2.7.

## **2.2. MATHEMATICAL MODELLING**

AC systems are required to be energy efficient to reduce their energy consumption. Measures such as optimization of system parameters are frequently undertaken to achieve energy saving. Mathematical equations that integrate the conservation of mass and energy conservation on every component of an AC system are required to solve optimization problems. Component modelling might be very complex at times due to the uncertainty of the operating conditions that a system could undergo. [4], have presented a mathematical modelling of the components of a fan-coil system. They have also detailed the model implementation with the simulation package Matlab-Simulink. Their model development was under the assumption that conservation of mass and energy occurs on every component. The model was used to compare the effect of the ventilation rate of external air on the psychrometric state of the room air with the temperature of the cooling coil. However, their work was limited to a secondary system modelling and did not include the primary system modelling so that a control strategy to ensure energy saving whilst keeping thermal comfort could be established.

The earliest HVAC systems modelling methods were namely, white box model, black box model and grey box model. Black box models sometimes called experimental or empirical models are modelling methods that take roots from acquired data of the process under investigation. Black box models capture relevant trends of AC systems without any knowledge of their internal process by simply analyzing inputs and outputs. Another advantage of black box modelling is that it could be adopted for prediction of the system's dynamics. Grey box schemes are combination of black and white box schemes as they merge data process and analytical structure to establish the models of processes under investigation. White box models sometimes called the mathematical or physical

models are adopted due to their simplicity to investigate a system despite its complexity compared to the two other modelling methods [5].

White box models could be divided in lumped and distributed parameter models depending on the complexity of the system under investigation. Lumped parameter models are described by ordinary differential equations due to their small size hence the elements of the models are represented at a unique point in space so that spatial derivatives terms of the state parameters could be neglected or averaged and only time derivatives terms might be considered.

In contrast, models with distributed parameters are described by partial differential equations (PDE's) because the elements of the models are distributed in space with their physical quantities supposedly changing with time and space. Models with lumped parameters require less computational time than their distributed parameters counterpart since they lead to systems of first order ordinary differential equations easy to solve whilst, much effort is required in distributed methods to compute the spatial terms and to adjust with the computational instabilities.

The signal processing of AC systems could be represented by white box models through the conservation law of mass and energy occurring on every component of the system. The conservation equations enable to represent on a mathematical form, the relationship between the system's inputs and outputs. For instance, the mathematical relationship between system input and output could serve for investigation of the change of indoor humidity and temperature. Mathematical models representing the conservation law occurring on each component usually lead to complex nonlinear equations. For simplicity, mathematical models could be divided in interfacing sub-models on which heat exchange and fluid momentum occurs [6]. Resulting sub-models lead to differential equations whose frequency domain could be described by transfer

functions. The Progress made in software and hardware development has removed some of the barriers to determine the solution of the nonlinear equations resulting from the mathematical models of systems.

Recent works on VC systems' modelling cover topics of nonlinear reduced order models and methodology to retrieve fluid properties for faster simulation [7-15]. These works reformulate the dynamic models of heat exchangers and integrate them with quasi-static models of expansion valve and compressor to form the complete reduced order models.

The simulation results indicated that reduced order models could predict the fluid dynamics faster than conventional models developed from finite volume schemes with minimum errors. Reduced order models could provide satisfactory performances for AC system modelling and they have been suggested earlier by authors such as [16-20].

Conventional AC system models are developed based on first principles and are usually adopted for prediction of the fluid dynamics along the VC cycle of systems. However, for combined prediction and control purposes, modelling techniques of VC systems have been developed by [21-25] to capture the fluid dynamics whilst also enabling the implementation of controllers with satisfactory performances in terms of robustness and energy savings. These modelling techniques are based on state space formulations of the fluid dynamics enabling the implementation of nonlinear multivariable controllers on the control-oriented models whilst also capturing the fluid's thermophysical transformations.

### **2.3. CONVENTIONAL NONLINEAR STRATEGIES**

Optimal control strategy on AC systems is used to achieve a significant energy saving and the best thermal comfort by providing effective system regulation. The aim of optimal control strategy implemented on AC systems is to minimize energy input function governed by the operating conditions whilst maintaining indoor comfort. The energy input function could also refer to a cost or objective function. The interaction of the governing parameters of an energy input function could be monitored through the implementation of an optimal control strategy. A mathematical model, a specified performance index and a set of boundary conditions as well as a listing of the uncontrolled parameters could formulate an optimal control strategy. [26], proposed an empirical model for optimal control of a large chilled water unit. They described an optimal operation that highlighted 10% of energy saving when the empirical model was used with a cooling system of a residential unit.

[27], used linear Quadratic Gaussian (LQG) strategy for indoor humidity and temperature control of a direct expansion (DX) AC system undergoing simultaneous variation of the compressor and supply fan speeds. The indoor temperature and humidity were effectively maintained at their set values despite the disturbance caused by the simultaneous speed variation of the compressor and supply fan [27]. [28], to improve the superheat control, disturbance rejection caused by sudden additional heat load and set value tracking, offered a linear model strategy. This model was solely implemented for a particular operating condition and could not be extended for wide operating conditions.

Unlike optimal control strategy that assumes the parameters to be constant within a specific range, adaptive control strategy of AC systems enables to take into consideration the variations of the parameters and even to monitor the non-measurable disturbances [29]. Therefore, adaptive control



strategy enables to monitor the nonlinear behavior of AC systems and the slow transient variation of their parameters. Adaptive control strategy enables the measurement of a specific performance index, which could be compared with a benchmark performance index to allow any adjustment to maintain the performance index within range. Recursive least squares (RLS) [30], is reported to be an effective adaptive control algorithm for controlling HVAC systems in buildings. On the other hands, [31] adopted novel adaptive back-stepping control method for HVAC system. Lyapunov stability was adopted and the control strategy achieved energy saving as well as optimal control [31].

Authors described adaptive control strategy as a nonlinear control scheme in which dynamic variations led by stochastic disturbances could occur in normal running operations of the system [32, 33]. Adaptive control strategy could be considered as a twofold feedback controller with one feedback for signal variations and the other one for changing parameters. [34], proposed an adaptive optimal control strategy for cooling and heating sources of building. They developed a function transforming a constrained optimization into an unconstrained optimization and achieved 7% energy saving using an optimal control.

The operating trends of AC systems are usually nonlinear and transient. AC systems are designed to run within a wide range of operating conditions. Nonlinear operating trends contribute in energy saving as the system could self-regulate to run faster or slower depending on the cooling or heating requirement. Transient trends enable the system to adjust in time their set values to maintain thermal comfort. Wide operating ranges allow systems to run efficiently under various weather conditions from low to high temperatures. Therefore, nonlinear control strategies are designed to regulate nonlinear and time-varying AC systems under wide operating ranges.

[35], investigated multi-input and multi-output (MIMO) nonlinear control models by comparing feedback linearization and gain scheduling control methods on air handling unit (AHU). The aim of this investigation was to lower energy consumption and operating cost whilst ensuring satisfactory indoor comfort [35]. Less oscillation and subsequently less energy consumption [35] are achieved under gain scheduling control implementation by using the positions of the valves as input control responses. Using the feedback linearization control method led to swift time responses of the temperature and humidity ratio tracking even though this was associated with supplementary overshoots [35].

Model predictive control (MPC) was experimented by [36] to control an AC system equipped with an outdoor air processing system. MPC performances were compared with the ones of a conventional feedback controller of a building management system (BMS). MPC achieved 20% more in terms of energy savings compared to the feedback controller whilst also improving significantly the thermal indoor conditions. [37], developed and experimented an MPC strategy to control HVAC systems. The results demonstrated high performances to optimize multimode operating conditions of HVAC systems as MPC adjusted the system's operating modes to achieve optimal control of the thermal indoor conditions.

[38], to integrate indoor conditions of a building with weather and occupancy data so that the overall energy consumed by the building could be minimal, adopted MPC. The results showed that over 18% of energy saving was achieved by controlling the HVAC systems with MPC at different temperature settings. Similar studies with MPC adoption for thermal control of indoor conditions were suggested by [39-46].

[47], to overcome the challenges associated with MPC implementation to control the thermal conditions in buildings, suggested state space formulation. Indoor air humidity and temperature as well as predicted mean vote (PMV) were integrated in the state space model to formulate an optimization problem with multi-objectives that resulted with a performance of over 19% in energy savings. [48], to improve indoor thermal comfort in a bioclimatic building, adopted an upper layer MPC and a sub layer PID for control of HVAC systems. The results demonstrated that in the presence of disturbances, thermal comfort was still maintained within range and 53% of energy savings was achieved.

#### **2.4. ENERGY SAVING METHODS**

Experimental study was performed by [49] on the impact of forced downtime method on AC's energy usage with unclear down time period. [49], suggested a method to decide forced thermo-off time based on the humidity and temperature forecast of the current day [50]. A centralized controller was sending to all individual remote controllers of air conditioners a forced thermo-off command and this resulted with an energy saving estimated within 7% to 27% in a campus of a selected university in 2007's summer.

[51], proposed an energy saving control method to reduce the power consumption of a room air conditioner. Their results showed that under the condition of the proposed control logic, the room air conditioner can save up to 3% of its energy consumption. Moreover, for a set temperature for cooling in summer of 27°C and heating in winter of 23°C, over 18.7% and 23.8% of energy consumption can be saved respectively. A survey result showed that the aforementioned set temperatures for cooling and heating are acceptable for occupants [51]. To complete their work, [51], combined their proposed energy saving control logic with a room model for simulating the

one-minute interval air temperature performance. This simulation led in determining the energy consumption of a room air conditioner and the optimal parameter setting for control. This resulted with an energy saving of 28.9% compared to the normal operation of the air conditioner.

Moreover, [52] proposed an energy-efficient control method enabling to lower the energy consumption of a centralized air conditioner equipped with variable speed pumps. An independent humidity and temperature control method was suggested by [53] to achieve AC's energy saving. The results of their strategy provided an improved COP of the air conditioner coupled with acceptable indoor conditions even in very humid and hot weather conditions. [54], used a genetic algorithm to analyze the optimal control strategy of an air conditioning system. They concluded that, varying the rate of fresh air supply and the supply air temperature saved 11% on energy cost. [55], offered an energy consumption model for an AC installed in a South Africa located data center. The energy consumption of the air conditioner was evaluated at different set temperature points. The accuracy of their proposed model was verified by comparing the energy consumption data obtained from their model with the measured energy consumption data of the data center. The root-mean-square-error (RMSE) of 11.5% was found between their simulated data and the measured data.

## **2.5. INTELLIGENT CONTROL STRATEGIES**

Fuzzy logic control (FLC) strategy for HVAC system is a control scheme based on a logic that does not require true or false response but rather relies on human reasoning to control uncertain systems [56-59]. Fuzzy logic applies simplistic mathematical concepts for controlling a system by treating analog type of input variables as logical values that might vary between 0 and 1. The input

variables in the fuzzy method are mapped by fuzzy membership functions and each input variable has a defined truth value; this process is referred to as fuzzification.

The applicable rules to each input variable are specified by using their respective membership function along with their truth values in order to determine the output; this process is referred to as fuzzy inference action. The applicable rule to each input variable leads to a result that in turn is mapped by an output membership function into a crisp or exact answer of the system to be used for control purpose or decision making; this process is referred to as defuzzification. [60], proposed a lateral and lateral-amplitude (LA) tuning fuzzy control strategies to improve the performance of fuzzy logic control on HVAC systems. [61], reported that adaptive fuzzy proportional derivative (PD) control strategy contributes on the improvement of the energy saving of a building by steering clear of oscillations and overshoots.

Genetic algorithm (GA) control scheme is used in order to find high-grade results in system's optimization based on Darwin's mechanism such as crossover, mutation and selection [62]. [63], adopted genetic tuning method (GTM) to determine the optimal parameters of FLC on an HVAC system. Fewer rules in expert knowledge were made possible and led to a simple automatic GA tuning process to control the HVAC system hence, satisfactory indoor conditions and energy performance were reached. Reports showed that, GA tuning method leading to the determination of optimal control parameters enables satisfactory performance of an HVAC system. GA tuning approach was also reported to yield to better system performance than the conventional Ziegler-Nichols tuning approach [62]. Optimal solution finding with GA was also proven more effective than conventional algorithms by [64] and [65]. However, the processing time to obtain optimal results must be reduced to improve the efficiency and robustness of the GA scheme [62]. Neural

network control strategy consists in interconnecting multiple neurons composed of inputs in parallel to form a layer network in order to control a system.

Some system could be identified as one-layer or as multiple layers of neurons network. In the case of a neuron network system of multiple layers, one has to consider the output of the first layer as the input of the following layer and so on. Therefore, the output layer is to be the layer whose output is the network output and the remaining layers are labeled as hidden layers. The network output of the neuron system is calculated from the set inputs, transfer function and weighing matrix.

Neural network control strategy enables to control complex systems that conventional control schemes cannot [66] and its parallel architecture allows the control process not to interrupt an undertaking in case of failure. Neural network control algorithms and architectures are established based on an understanding of a neurobiological operating system [67]; that means by mimicking the behavioral traits of a human brain [68]. [69], reported that neural network has become an adequate controller for uncertain nonlinear systems since significant progress has been made in adaptive as well as non-adaptive neural control to address the issues of stability, robustness and performance relevant to neural control [70]. Neural control schemes are mostly employed for nonlinear control systems even though they could also be applied to linear control systems [70].

## **2.6. COMPRESSOR MODELLING**

[71], introduced a comprehensive model of a spool compressor. Spool compressors provided new mechanism of gas compression using easy to manufacture parts. Analytical derivations were provided then, crank shaft power, volumetric efficiency and discharge temperature were predicted with the comprehensive spool compressor model. [72, 73], described spool compressors'

mechanism as similar to sliding vane compressors with only few differences such as the constrained vane with an eccentric cam, the rotor with rotating endplates and the dynamic sealing to prevent from leakage. More details on spool compressors are provided in [74, 75].

[76], studied turbulent refrigerant flow through reciprocating compressors' valves for prediction of pressure gradient using a finite volume scheme. Numerical results of the front disc pressure were in agreement with experiments at different settings of the valves' position. Reciprocating and centrifugal compressors are the most adopted in AC applications as a result of in-depth design and manufacturing knowledge of these components [77-79], with the former used for smaller capacity, the second for larger capacity. Increasing demand for energy efficient systems has taken up interest in developing recent compressor models such as comprehensive models that rely on conservation of mass and energy similar to [80]. Adoption of comprehensive compressor modelling was reported by [81-86].

[87], proposed a numerical approach for performance evaluation and dynamic behavior's investigation of a linear compressor. The results of the numerical model were discussed by [88] as the motor reached up to 90% efficiency at maximum operating frequency. [89], adopted a numerical method validated with experiments for a thermal evaluation of a linear compressor. Mathematical modelling and experimental investigation of linear compressors were suggested for performance evaluation of refrigeration systems with the results showing that COP varied by 3% within the operating frequency range [90] and 18.6% higher COP could be reached compared to reciprocating compressors [91]. Additional literatures on mathematical and numerical modelling of linear compressor with experimental validation could be found in [92-94].

[95], considered the conservation of angular momentum between torques (braking and driving) to offer a simple compressor model to predict discharge temperature and crank shaft work at specific mass flow rate setting. [96], developed a numerical model of VC system using linear compressor. The model was simulated with Matlab-Simulink and validated with an experimental prototype compressor using R1234yf refrigerant with the predicted results namely, mass flow rate, crank shaft power and compressor stroke falling within  $\pm 10\%$  error range.

[97], reviewed the key parameters influencing the performances of reciprocating compressors in AC systems such with emphasis on suction and discharge valves as the dynamic behavior of these components is predominant in design stage [98] and influences performances significantly [99]. Suction and discharge valves are required for refrigerant flow control [100-102], through the compressor to enhance the fluid's distribution and dynamics. [103], listed four key parameters to consider at design stage of compressor valves as the valve's dynamic response, pressure drop, backflow and mass flow rate intake.

## **2.7. EXPANSION VALVE MODELLING**

[104], suggested a steady state model for thermostatic expansion valves (TXV's) that required valve and bulb's geometric data. Unfortunately, this model showed some limitations during simulation of complete VC systems. Under damping and hunting due to TXV's were discussed using the established models. [105], presented a steady state model for simulation of TXV's. The model was established under simplified assumptions to offer simple and comprehensive correlations of TXV's. [106], compared the performances of nonlinear and linear TXV's using mathematical models supported by experiments. The adoption of nonlinear TXV's was suitable to



prevent from hunting. Linear TXV's on the other hand, were suitable for dynamic operating conditions but unsuitable to prevent from hunting.

[107], compared TXV performances with electronic expansion valve's (EEV's). During compressor startup, EEV demonstrated faster responses compared to TXV but in steady operating regime both valves provided similar performances. Similarly, [108], compared performances of EEV's versus TXV's. EEV's enhanced better energy saving performances compared to TXV's due to advantageous operating conditions as less condensing pressure was required by air cool condensers. [109-111] also reported the constraints and limitations of adopting TXV's instead of EEV's to operate VC systems at low condensing pressure to enhance overall performance of the system. TXV's enable stable superheat control but could manifest limitations to maintain superheat within settings [112]. Comprehensive literatures on EEV could be found in [113]. Despite better performances demonstrated by EEV's, TXV's remain widely adopted in applications using VC systems such as light AC and food refrigeration systems [114].

[109], proposed to maintain significant pressure difference between TXV's outlet and inlet to maintain desired refrigerant dynamic flow using linear TXV's correlation similar to [115]. Flow modelling through TXV's bleed port was suggested by [116, 117] to rapidly level out refrigerant pressure within the condenser and evaporator prior to compressor startup. The model results were validated and converged with experiments. [118], defined TXV as valve whose main function is to maintain refrigerant superheat within range to prevent the compressor from flooding, that was patented by [119].

Steady and transient states modelling of TXV's were suggested by [120]. Derivations of the models were provided and validated with experimental data. The models were also simulated in

complete VC systems using the software developed by [121, 122]. [123], evaluated the performances of 4 gray box TXV models. Each model was based on the equation of [124] and validated with experiments for mass flow rate prediction required for modelling of a complete VC system [125]. Models' validation was satisfactory in general with error below 10% due to the limitations in evaluating two-phase's refrigerant states and diaphragm force. Available TXV's models in the literatures could be found in [126-131].

# CHAPTER 3 MODELLING OF THE REFRIGERANT DYNAMICS

## 3.1. INTRODUCTION

Modelling of VC systems consists in investigating the variation of the governing parameters of the refrigerant dynamics such as pressure, enthalpy and temperature. Manufacturers of VC systems are working towards innovating more energy efficient systems to provide convenient indoor air cooling or heating without trading off efficiency and comfort requirements. Prediction of the refrigerant dynamics in VC systems is fundamental for innovation as this enables to develop comprehensive models eventually adopted for control and equipment design as well as for fault detection.

The aim of this chapter is to use mathematical methods supported with experiments to develop comprehensive models predicting the refrigerant dynamics in VC systems to determine optimal parameters in steady and transient operating conditions. These parameters could be adopted for refrigerant dynamics control such as superheat and capacity regulation as well as for indoor air control such as temperature, humidity and CO<sub>2</sub> level regulation.

The following sections address the aforementioned problem with existing equations to provide detailed modelling schemes supported with experiments. This work contributes in providing two mathematical models to track the refrigerant dynamics in VC systems. The first model is a steady state model where the refrigerant conditions are determined when the VC system reaches its steady operating conditions. The outputs of this model are particularly useful to integrate on nonlinear

controllers for linearization around a steady operating point for reference tracking. The second model is a transient state model with the prediction of the refrigerant conditions during transient operating conditions such as startup and shutdown. This model's outputs are particularly useful for optimal design of VC systems for performance improvement related to energy consumption during startup.

The subsequent sections of this chapter are listed as follows. In section 3.2., the literature study on predictive models of the refrigerant dynamics is presented. Predictive modelling in steady and transient states are discussed respectively in section 3.3 and section 3.4. The experimental investigation to validate the steady and transient state models is presented in section 3.5. The results and discussion will be elaborated in section 3.6., followed by the conclusion in section 3.7.

## **3.2. LITERATURE REVIEW**

### **3.2.1. Steady state modelling**

An early steady state heat pump model was proposed by [132] for system's performance simulation. The model was subdivided in four components namely the condenser, thermostatic expansion valve, evaporator and compressor. The condenser model was subdivided in de-superheater, condenser and sub-cooler zones whilst the evaporator was subdivided in evaporating and superheating zones. The simulation results of the four model components were obtained with a FORTRAN subroutine.

A model predicting the component behavior in steady state regime of a refrigerating air-to-air system was suggested by [133]. The evaporator and condenser models were derived from first principles along with empirical values. The compressor model was a hermetic type of compressor

that evaluated the amount of heat absorbed and lost by the circulating fluid as well as the suction and discharge pressures. [134], modified the model of [133] by incorporating a capillary expansion and a simpler compressor model. Their model was adopted for analytical assessment of varying performance of the system due to component changes in heat pump system. FORTRAN subroutine was adopted for simulation of the condenser and evaporator. Later on, improvement of the aforementioned model was proposed by [135] who enabled a simpler simulation of cooling operation, sub-cooling, superheating and pressure drop as well as an improvement in the convergence of simulation results.

Steady state modelling of air-to-air heat pump systems was performed by [136] using three FORTRAN simulation codes. The first code could simulate various cycle arrangements of heat-pump to describe performance. The second code was used for evaluation of specific operating conditions of heat pump. The third code was used for simulation of heat pump operations.

[137], has described a more detailed steady state modelling of heat pump system presenting the modelling principles with their benefits for simulation of an air-to-air heat pump system. The evaporator and condenser modelling were similar in the sense that identical assumptions such as the refrigerant stream heat transfer occurs only in the two-phase zone and the uniformity of overall heat transfer coefficient along the heat exchangers. The evaporator model was subdivided in two heat transfer zones of the refrigerant stream whilst the condenser was subdivided in three zones. For both heat exchangers, pressure drop and heat transfer effects were correlated in each zone. The compressor on the other hand was modelled with manufacturer's data and performance curves.

[138], conducted steady state modelling of heat exchangers proposing a logarithmic mean temperature difference (LMTD) technique to evaluate the rate of heat transfer between the

circulating fluid and the heat exchanger shell. Unfortunately, their approach lacked accuracy in situations where the circulating fluid is changing phase. [139], has established a model similar to [135] that enabled the performance simulation of air-to-air heat pump systems. A limited amount of experimental data was used to validate this model and the compressor model was a map-based model developed with available manufacturer's data [140].

Zone model to evaluate the performance of an air-cooled condenser was suggested by [141] who subdivided the condenser in de-superheating, condensing and sub-cooling zones. This method led to a set of non-linear equations resulting from the energy balance analysis in each zone for both the refrigerant and air streams as well as the effectiveness equation. The numerical results of the simulation were converging with experimental data.

[142], investigated the steady state behavior of a VC system with numerical approach using C++ code. System equilibrium was numerically tracked by using input parameters so that stable outputs could be obtained by assuming the convergence of the refrigerant mass flow rate and the energy balance through the evaporator [142]. [143], attempted to build a generic steady state model of fin and tube heat exchangers that could simulate any configuration of refrigerant circuits as well as evaluate the refrigerant distribution in the circuit and the rate of heat conduction through fins. The steady state model was constructed on the basis of graph theory and a novel algorithm for computation called alternative iteration method was introduced to calculate separately the energy and momentum equations in order to reduce the simulation time of the model. The comparison of the modelling and experimental results of this investigation showed a  $\pm 10\%$  error range.

[144], has reviewed the available simulation technique for VC systems such as the model-based techniques and evaluation of thermodynamics properties of the refrigerant. Innovative simulation

techniques such as knowledge engineering methods and computational methods for nanofluids were also presented [144]. A novel simulation method of steady state modelling was offered by [145] to improve the robustness, speediness and accuracy of the simulation of ordinary as well as complex vapor compression systems. The modelling method adopted was a component-based algorithm similar to [146]. This work led to more advanced means to determine the initial guess value for steady state modelling and the component evaluation time was reduced by about 40% whilst improvement on the robustness of the algorithm for solution tracking was achieved at 50%.

[147], suggested a steady state model based on first principles and empirical equations for variable speed VC systems operating with R134a refrigerant. The model used input parameters to evaluate the condensing and evaporating pressures as well as the temperature of the secondary stream at condenser and evaporator outlets. The model predicted the performance of a chiller system with an error below  $\pm 10\%$  [147].

Thermal as well as performance simulation of refrigeration and AC systems of a service vehicle was developed by [148] using steady state mathematical modelling of VC system. The model results were verified with experimental and field data. The model was adopted for performance assessment and acceptable results were used to implement a controller scheme to achieve optimized system performance. Significant improvement of the system COP was noted under optimal control.

[149], presented a simulation method for complex configuration of VC systems. The simulation was developed from a component-based approach in which the components of the VC system were treated as black box and connected to one another through junctions and ports. The simulation was validated with experimental results with an error below  $\pm 10\%$  [149]. [150], introduced a semi-

analytical model of heat pump system used for water heating. The model evaluated the system performance without any detailed geometry of the components [150]. The model was particularly useful in the sense that subcomponent models such as accumulator model were considered during simulation and the performance results of the model were in agreement with experiments [150].

[151], presented a regression-based modelling technique for emerging AC systems. The performance curves of the model were obtained from the system outputs or experimental data and were used for energy simulation of a building. The regression-based modelling could be adopted as an alternative modelling technique for emerging AC systems. [152], developed a model for performance simulation of a membrane-based VC system. This type of VC system has attracted a lot of attention in the research community as it could be an alternative for more environment friendly system of indoor air cooling. The performance simulation was performed with an initial state point model [153] and better results in terms of energy saving compared to commercial system were found.

### **3.2.2. Transient state modelling**

By converting two-phase flow zones in heat exchangers with lumped parameters for solution tracking, [154], suggested early heat exchangers' transient state models that used a mean void fraction approach. [155], introduced a transient state model of AC systems using the heat exchangers' moving boundary approach. Mass transfer was assumed to occur internally and heat transfer externally in the two-phase heat exchangers' zones. Despite the model's simplicity and reliance on a formulation of quasi-steady states, significant transient states had been foreseen with a satisfactory level of accuracy. The formulation of the lumped parameters used dynamic continuity, momentum, and energy equations. All components' time-dependent model equations



aside from the expansion valve were derived and numerically solved using the Euler method. For the components other than the expansion valve, numerical solution using the Euler method was used to derive and solve the transient models. The conditions of the refrigerant at each component outlet were validated with experimental data during startup operation for approximately 6 minutes.

[157, 158], suggested early models with heat exchangers' distributed parameters to represent analytically the dynamic behavior of VC systems. The secondary fluid, refrigerant, and heat exchanger wall were the three components that made up the heat exchanger model. Utilizing time-dependent PDE's derived from the conservation of mass and energy, the three elements were defined. To divide the heat exchangers and perform spatial and time-varying integrations to satisfy the conservation equations for any grid space and time step, small control volumes were adopted. [157, 158], assumed a uniform flow in the heat exchangers but the predictions of the mass distribution were weak. Improved predictions of the pressure in heat exchangers were suggested by [159], using interacting mass and energy balance. Additional literatures on transient state modelling could be found in [160].

Distributed parameters were adopted by [161], for investigation of the transient state behavior of an evaporator. Homogeneous gas and liquid mixture was assumed for the flow through the evaporator. The discretization of the conservation equations with the finite difference scheme was adopted and solved with a Gaussian elimination method. Temperature and pressure were determined numerically using the distributed model without validation with experimental data. Investigation of the heat exchanger zones namely, two-phase, liquid and vapor were suggested by [162] using lumped parameters. For each zone, the corresponding governing equations were derived based on the conservation law which led to 12 lumped parameters. An evaporator

simulation was suggested by [163], based on the 12 aforementioned lumped parameters, using the moving boundary approach and under wide operating ranges. Although the model provided insightful transient state prediction, it was not integrated in a complete VC system.

Moving boundary scheme was also adopted by [164], for advanced development of switched heat exchanger models with dynamic and nonlinear characteristics. The robustness of the model was tested and demonstrated experimentally using chiller systems. The results of the models were predicted with accuracy and the models' robustness was satisfactory for different settings. The possibility to adopt switched heat exchanger models for performance improvement of a controller was revealed by [165], following the simulation of a dynamic system with on/off cycles through Simulink with experimental verification of the results. Numerical investigation of VC systems' transient states was suggested by [166], transient momentum equations considering pressure drop were compared with steady state equations and the results of the numerical analysis were satisfactory.

Numerical investigation of the transient states of a VC system during start-up operation of the compressor was reported by [167]. Thermal equilibrium was assumed for simulation and it was found that discharge and suction dynamics were the most affected during the start-up operation of the compressor. Literatures on transient state models were reviewed by [168], and concluded that model-based approaches could be categorized in lumped parameters, moving boundary and finite volume methods that required experimental validation as their benefits were evaluated by [169]. [170], developed a dynamic model of a condensing boiler using a finite volume scheme in order to avoid static nonlinear efficiency curves and account for a proportion of transient wet and dry

heat transfer. For the purpose of tracking the energy efficiency of a gas-powered water heater, [170], adopted this model.

Satisfactory modelling results with moving boundary and finite volume approaches were reported by [171, 172] as accuracy was reached under stretched conditions [171], with the two schemes demonstrating similar level of precision as rapid solution tracking was achievable through the moving boundary method whilst flexibility was imputable to the finite volume approach [172]. Transient state modelling with on-off cycles of a VC system was reported by [173], for performance evaluation using a compressor modelling method similar to [174]. Satisfactory results were achieved and validated with experimental data.

Additional existing modelling techniques of VC systems classified as quasi-steady models [175, 176], lumped models [177-180], distributed models [181-192], moving boundaries models [193-199] and lumped or distributed moving boundaries models [200-202] are reported in Table 3.1 following the work of [203, 204].

Table 3.1 Dynamic models of VC systems

Scheme	Author	Year
Quasi-steady	Murphy and Goldschmidt [175]	1985
	Browne and Bansal [176]	2002
Lumped	Melo, Ferreira, Pereira and Negrao [177]	1988
	Vargas and Parise [178]	1995
	Nunes, Castro, Machado and Koury [179]	2016
	Li, Chu, Xu, Yang, Ji, Ni, Bao and Wang [180]	2017
Distributed	Sami, Duong, Mercadier and Galanis [181]	1987
	MacArthur and Grald [182]	1989
	Chen and Lin [183]	1991
	Judge and Radermacher [184]	1997
	Rossi and Braun [185]	1999
	Koury, Machado and Ismail [186]	2001
	Schiavo and Casella [187]	2007
	Hermes and Melo [188]	2009
	Koury, Faria, Nunes, Ismail and Machado [189]	2013
	Berger, Posch, Heimel, Almbauer, Eichinger and Stupnik [190]	2015
Wu, Gagnière, Couenne, Hamroun, Latour and Jallut [191]	2015	
Laughman, Qiao, Aute and Radermacher [192]	2015	
Moving boundaries	Janssen, de Wit and Kuijpers [193]	1992
	He, Liu and Asada [194]	1994
	Zhang and Zhang [195]	2006
	Schurt, Hermes and Neto [196]	2009
	Li and Alleyne [197]	2010
	Esbri, Millian, Mota-Babiloni, Moles and Verdu [198]	2015
Yang and Ordonez [199]	2018	
Lumped or distributed moving boundaries	Bendapudi, Braun and Groll [200]	2008
	Liang, Shao, Tian and Yang [201]	2010
	Rodriguez and Rasmussen [202]	2017

### 3.3. STEADY STATE MODELLING

A typical VC system is shown in Fig. 3.1 along with its steady state parameters for each component:

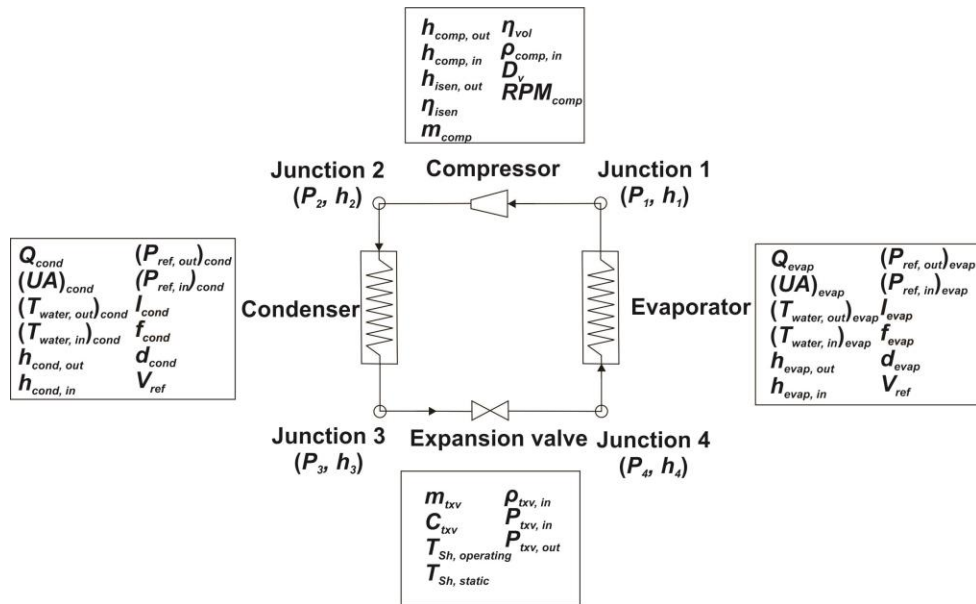


Figure 3.1 Conventional VC system

The compressor is adopted to increase the pressure of the refrigerant that is circulated. Rising pressure adds more heat to the refrigerant and the condenser is used to remove that heat to reject it to the surrounding environment. To control the refrigerant flow, an expansion valve is placed downstream of the condenser to reduce the refrigerant pressure and control the refrigerant mass flow fed into the evaporator whose purpose is to absorb heat from the surrounding environment to provide cooling effect. The components are connected to one another through the junctions [145]. The VC system adopted here is a water cooled VC system.

The governing parameters of a VC system are described in Table 3.2 as follows:

Table 3.2 Description of the governing parameters

Structure	Elements	Description
Junction	Pressure and enthalpy	<ul style="list-style-type: none"> <li>○ Specification of the refrigerant state</li> <li>○ Refrigerant state input to compute output</li> </ul>
	Dependent parameters	<ul style="list-style-type: none"> <li>○ Parameters that are calculated explicitly from the governing equation of each component</li> <li>○ These parameters do not form the unknowns of the system to be solved</li> </ul>
Parameters	Independent parameters	<ul style="list-style-type: none"> <li>○ Physical parameters to be determined by the system solver</li> <li>○ They are established parameters that can be found in the library</li> </ul>
	Transient parameters	<ul style="list-style-type: none"> <li>○ Parameters that change with time and are usually used in transient analysis</li> <li>○ Parameters requiring an initial value in order to be simulated by the system solver</li> </ul>

### 3.3.1. Compressor modelling

The following equations apply to the compressor's outlet condition and refrigerant mass flow rate:

$$h_{comp,out} = h_{comp,in} + \frac{h_{isen,out} - h_{comp,in}}{\eta_{isen}} \quad (3.1)$$

$$m_{comp} = \eta_{vol} \rho_{comp,in} D_v \frac{RPM_{comp}}{60} \quad (3.2)$$

$h_{comp,out}$  Refrigerant enthalpy at compressor outlet ( $kJ kg^{-1}$ )

$h_{comp,in}$  Refrigerant enthalpy at compressor inlet ( $kJ kg^{-1}$ )

$h_{isen,out}$	Refrigerant isentropic enthalpy at compressor outlet ( $kJ\ kg^{-1}$ )
$m_{comp}$	Refrigerant mass flow rate in compressor ( $kg\ s^{-1}$ )
$\eta_{vol}$	Volumetric efficiency of compressor
$\rho_{comp,in}$	Density of refrigerant at compressor inlet ( $kg\ m^{-3}$ )
$D_v$	Displacement volume of compressor ( $m^3\ s^{-1}$ )
$RPM_{comp}$	Rotational speed of compressor ( $rpm$ )

### 3.3.2. Condenser modelling

The heat rejected by the condenser could be evaluated as follows:

$$Q_{cond} = (UA)_{cond} [(T_{water,out})_{cond} - (T_{water,in})_{cond}] \quad (3.3)$$

$Q_{cond}$	Heat rejection in condenser ( $kw$ )
$(UA)_{cond}$	Overall heat transfer coefficient in condenser ( $kw\ ^\circ C^{-1}$ )
$(T_{water,out})_{cond}$	Water temperature at condenser outlet ( $^\circ C$ )
$(T_{water,in})_{cond}$	Water temperature at condenser inlet ( $^\circ C$ )

The refrigerant's outlet enthalpy through the condenser could be calculated as follows:

$$h_{cond,out} = h_{cond,in} - \frac{Q_{cond}}{m_{comp}} \quad (3.4)$$

$h_{cond,out}$	Refrigerant enthalpy at condenser outlet ( $kJ\ kg^{-1}$ )
$h_{cond,in}$	Refrigerant enthalpy at condenser inlet ( $kJ\ kg^{-1}$ )

The refrigerant outlet pressure could be expressed as follows:

$$(P_{ref,out})_{cond} = (P_{ref,in})_{cond} - f_{cond} \frac{2l_{cond}}{\pi d_{cond}^3} m_{comp} V_{ref} \quad (3.5)$$

$(P_{ref,out})_{cond}$	Refrigerant pressure at condenser outlet ( $kP_a$ )
$(P_{ref,in})_{cond}$	Refrigerant pressure at condenser inlet ( $kP_a$ )
$f_{cond}$	Friction factor in condenser
$l_{cond}$	Condenser length ( $m$ )
$d_{cond}$	Inner diameter of condenser ( $m$ )
$V_{ref}$	Refrigerant speed ( $m s^{-1}$ )

Let's recall that the evaporator's thermal behavior is similar to the condenser behavior, but in the reverse way, so its modelling equations are shown in Table 3.3 as follows:

**Table 3.3** Steady state modelling equations of the evaporator

Parameter	Model	Components
Rate of heat absorption	$Q_{evap} = -(UA)_{evap} [(T_{water,out})_{evap} - (T_{water,in})_{evap}]$	<ul style="list-style-type: none"> <li><math>Q_{evap}</math> is the rate of heat absorption of the evaporator from the surrounding air stream to the refrigerant in (<math>kwh</math>)</li> <li><math>(UA)_{evap}</math> is the overall heat transfer coefficient of the evaporator in (<math>kW/^\circ C</math>)</li> </ul>
Evaporator outlet enthalpy	$h_{evap,out} = h_{evap,in} - \frac{Q_{evap}}{m_{txv}}$	<ul style="list-style-type: none"> <li><math>h_{evap,out}</math> is the outlet enthalpy of the refrigerant in (<math>kJ/kg</math>)</li> <li><math>h_{evap,in}</math> is the inlet enthalpy of the refrigerant in (<math>kJ/kg</math>)</li> </ul>



Frictional pressure drop & evaporator outlet pressure	$\Delta P_{evap,ref}$ $= f_{evap} \frac{2l_{evap}}{\pi d_{evap} (\rho_{ref,in})_{evap}} m_{txv}^2$ $= (P_{ref,in})_{evap} - (P_{ref,out})_{evap}$	<ul style="list-style-type: none"> <li>○ <math>\Delta P_{evap,ref}</math> is the refrigerant frictional pressure drop along the evaporator in (<math>kPa</math>)</li> <li>○ <math>(P_{ref,out})_{evap}</math> is the evaporator outlet pressure of the refrigerant in (<math>kPa</math>)</li> <li>○ <math>f_{evap}</math> is the friction factor in the evaporator tube</li> </ul>
---	---	--

### 3.3.3. Expansion valve modelling

The following equation could be used to determine the refrigerant mass flow rate at the thermostatic expansion valve:

$$m_{txv} = C_{txv} (T_{Sh,operating} - T_{Sh,static}) \sqrt{\rho_{txv,in} (P_{txv,in} - P_{txv,out})} \quad (3.6)$$

$m_{txv}$	Refrigerant mass flow rate in expansion valve ( $kg\ s^{-1}$ )
$C_{txv}$	Valve flow coefficient
$T_{Sh,operating}$	Refrigerant operating superheat ( $^{\circ}C$ )
$T_{Sh,static}$	Refrigerant static superheat ( $^{\circ}C$ )
$\rho_{txv,in}$	Refrigerant density at expansion valve inlet ( $kg\ m^{-3}$ )
$P_{txv,in}$	Refrigerant pressure at expansion valve inlet ( $kPa$ )
$P_{txv,out}$	Refrigerant pressure at expansion valve outlet ( $kPa$ )

The system's refrigerant mass flow rate is balanced at steady state and defined as follows:

$$m_{txv} = m_{comp} \quad (3.7)$$

Therefore, the refrigerant outlet pressure at the expansion valve is expressed as follows:

$$P_{txv,out} = P_{txv,in} - \frac{m_{comp}^2}{\rho_{txv,in} [c_{txv}(T_{Sh,operating} - T_{Sh,static})]^2} \quad (3.8)$$

### 3.3.4. Solution of the steady state modelling

In this work pressure and enthalpy are determined to evaluate the refrigerant state at each junction. The inlet conditions are set at the inlet of each component whilst the outlet conditions have to be determined at the outlet.

### 3.3.5. Derivation of the steady state modelling matrix

The refrigerant condition (enthalpy and pressure) must be determined at each junction (Fig. 3.1).

The unknown vector could be written as follows:

$$\vec{x}_s = [P_1; P_2; P_3; P_4; h_1; h_2; h_3; h_4]^T \quad (3.9)$$

The solution of the system modelling should verify the following residual system of conservation equations at each junction:

$$\begin{bmatrix} (P_{ref,out})_{evap} \\ P_{comp,out} \\ (P_{ref,out})_{cond} \\ P_{txv,out} \\ h_{evap,out} \\ h_{comp,out} \\ h_{cond,out} \\ h_{txv,out} \end{bmatrix} = \begin{bmatrix} P_1 \\ P_2 \\ P_3 \\ P_4 \\ h_1 \\ h_2 \\ h_3 \\ h_4 \end{bmatrix} \quad (3.10)$$

The enthalpy and pressure at each junction could be used to express the outlet refrigerant conditions as follows:

$$\left\{ \begin{array}{l} (P_{ref,out})_{evap} = P_4 - f_{evap} \frac{2l_{evap}}{\pi d_{evap}^3} m_{comp} V_{ref} \\ P_{comp,out} = P_2 \\ P_{txv,out} = P_3 - \frac{m_{comp}^2}{\rho_{txv,in} [C_{txv}(T_{Sh,operating} - T_{Sh,static})]^2} \\ (P_{ref,out})_{cond} = P_2 - f_{cond} \frac{2l_{cond}}{\pi d_{cond}^3} m_{comp} V_{ref} \\ h_{evap,out} = h_4 + \frac{Q_{evap}}{m_{comp}} \\ h_{comp,out} = h_1 + \frac{h_{isen,out} - h_1}{\eta_{isen}} \\ h_{cond,out} = h_2 - \frac{Q_{cond}}{m_{comp}} \\ h_{txv,out} = h_4 \end{array} \right. \quad (3.11)$$

$h_{txv,out}$  Refrigerant enthalpy at expansion valve outlet ( $kJ kg^{-1}$ )

### 3.3.6. Steady state modelling matrix

To determine the modelling outputs, the refrigerant pressure at the compressor outlet and the outlet enthalpy at the expansion valve must be set. Substituting and re-arranging (3.11) into (3.10) leads to:

$$\begin{bmatrix} -1 & 0 & 0 & 1 & 0 & 0 & 0 & 0 \\ 0 & 1 & 0 & 0 & 0 & 0 & 0 & 0 \\ 0 & 1 & -1 & 0 & 0 & 0 & 0 & 0 \\ 0 & 0 & 1 & -1 & 0 & 0 & 0 & 0 \\ 0 & 0 & 0 & 0 & -1 & 0 & 0 & 1 \\ 0 & 0 & 0 & 0 & (\eta_{isen} - 1) & -\eta_{isen} & 0 & 0 \\ 0 & 0 & 0 & 0 & 0 & 1 & -1 & 0 \\ 0 & 0 & 0 & 0 & 0 & 0 & 0 & 1 \end{bmatrix} \begin{bmatrix} P_1 \\ P_2 \\ P_3 \\ P_4 \\ h_1 \\ h_2 \\ h_3 \\ h_4 \end{bmatrix}$$

$$= \frac{\begin{bmatrix} f_{evap} \frac{2l_{evap}}{\pi d_{evap}^3} m_{comp} V_{ref} \\ P_{comp,out} \\ f_{cond} \frac{2l_{cond}}{\pi d_{cond}^3} m_{comp} V_{ref} \\ m_{comp}^2 \end{bmatrix}}{\rho_{txv,in} [C_{txv} (T_{Sh,operating} - T_{Sh,static})]^2} \begin{bmatrix} -\frac{Q_{evap}}{m_{comp}} \\ -h_{isen,out} \\ \frac{Q_{cond}}{m_{comp}} \\ h_{txv,out} \end{bmatrix} \quad (3.12)$$

### 3.4. TRANSIENT STATE MODELLING

Fig.3.1 is adopted leaving out the steady state parameters to perform transient state modelling.

#### 3.4.1. Condenser modelling

The following equations could be used to define the conservation of the refrigerant's mass and energy within the condenser whilst disregarding the pressure loss:

$$\frac{\partial \rho}{\partial t} + \frac{\partial(\rho u)}{\partial x} = 0 \quad (3.13)$$

$$\frac{\partial(\rho h)}{\partial t} + \frac{\partial(\rho u h)}{\partial x} + \delta Q_{ref} = 0 \quad (3.14)$$

$\rho$	Refrigerant density ( $kg/m^3$ )
$u$	Velocity of the refrigerant ( $m/s$ )
$h$	Specific enthalpy of the refrigerant ( $kJ/kg$ )
$\delta Q_{ref}$	Infinitesimal heat transported by the refrigerant ( $kw/m^3$ )

For each control volume of the condenser shown in Fig. 3.2, the conservation equations could be discretized using a finite volume scheme as follows:

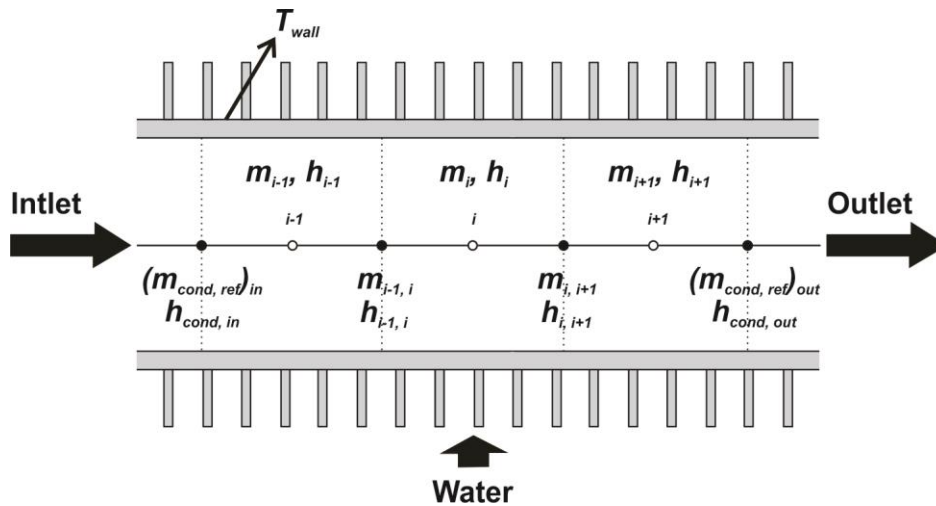


**Figure 3.2** Control volume of condenser – 3 control volumes

$(m_{cond,ref})_{in}$	Refrigerant mass flow rate at condenser inlet ( $kg/s$ )
$T_{wall}$	Temperature of the condenser wall ( $^{\circ}C$ )
$(m_{cond,ref})_{out}$	Refrigerant mass flow rate at condenser outlet ( $kg/s$ )

$h_{cond,in}$	Refrigerant enthalpy at condenser inlet ( $kJ/kg$ )
$m_{i-1,i}$	Refrigerant mass flow rate at $(i - 1, i)^{th}$ - Intermediary point ( $kg/s$ )
$m_{i,i+1}$	Refrigerant mass flow rate at $(i, i + 1)^{th}$ - Intermediary point ( $kg/s$ )
$h_{i-1,i}$	Refrigerant enthalpy at $(i - 1, i)^{th}$ - Intermediary point ( $kJ/kg$ )
$h_{i,i+1}$	Refrigerant enthalpy at $(i, i + 1)^{th}$ - Intermediary point ( $kJ/kg$ )
$m_{i-1}$	Refrigerant mass flow rate at $(i - 1)^{th}$ - control volume ( $kg/s$ )
$m_i$	Refrigerant mass flow rate at $i^{th}$ - control volume ( $kg/s$ )
$m_{i+1}$	Refrigerant mass flow rate at $(i + 1)^{th}$ - control volume ( $kg/s$ )
$h_{i-1}$	Refrigerant enthalpy in $(i - 1)^{th}$ -control volume ( $kJ/kg$ )
$h_i$	Refrigerant enthalpy in $i^{th}$ -control volume ( $kJ/kg$ )
$h_{i+1}$	Refrigerant enthalpy in $(i + 1)^{th}$ -control volume ( $kJ/kg$ )

Eq. (3.13) and (3.14) could be discretized assuming the inlet and outlet refrigerant conditions to be the boundaries as shown in Fig. 3.3 as follows:

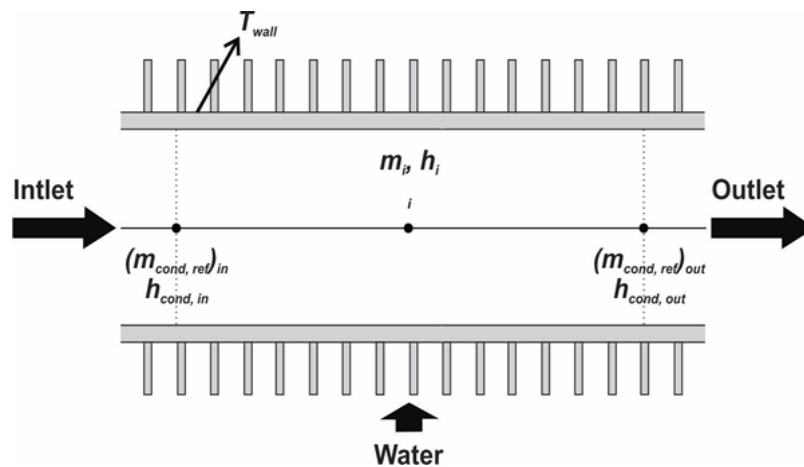


**Figure 3.3** Control volume of condenser – 1 control volume

$$\frac{\partial(\rho V)_i}{\partial t} - (m_{cond,ref})_{in} + (m_{cond,ref})_{out} = 0 \quad (3.15)$$

$$\frac{\partial(\rho h V)_i}{\partial t} - (m_{cond,ref})_{in} h_{cond,in} + (m_{cond,ref})_{out} h_{cond,out} + Q_{ref,i} = 0 \quad (3.16)$$

Decomposition of the derivative of  $\rho = f(P, h)$  using the chain rule for partial derivative resulted in the following arrangement of (3.15) and (3.16):

$$V_i \left[ \frac{\partial \rho_i}{\partial P} \Big|_{h,i} \frac{dP_{cond}}{dt} + \frac{\partial \rho_i}{\partial h_i} \Big|_P \frac{dh_i}{dt} \right] = (m_{cond,ref})_{in} - (m_{cond,ref})_{out} \quad (3.17)$$

$$\begin{aligned} V_i \left[ \left( h_i \frac{\partial \rho_i}{\partial P} \Big|_{h,i} - 1 \right) \frac{dP_{cond}}{dt} + \left( h_i \frac{\partial \rho_i}{\partial h_i} \Big|_P + \rho_i \right) \frac{dh_i}{dt} \right] \\ = (m_{cond,ref})_{in} h_{cond,in} - (m_{cond,ref})_{out} h_{cond,out} - Q_{ref,i} \end{aligned} \quad (3.18)$$

$V_i$	Internal volume of $i^{th}$ -control volume ( $m^3$ )
$h_i$	Refrigerant enthalpy in $i^{th}$ -control volume ( $kJ/kg$ )
$Q_{ref,i}$	Heat rejected by refrigerant in condenser ( $kw$ )
$\rho_i$	Refrigerant density in $i^{th}$ -control volume ( $kg/m^3$ )
$P_{cond}$	Refrigerant pressure in condenser ( $kPa$ )

Within the  $i^{th}$ -control volume, the heat transfer between the refrigerant and the condenser wall could be given as follows:

$$Q_{ref,i} = \alpha_i \frac{A_i}{N_{cells}} (T_i - T_{wall,i}) \quad (3.19)$$

$\alpha_i$	Heat transfer coefficient in the $i^{th}$ -control volume ( $kw/m^2\text{°C}$ )
$N_{cells}$	Number of cells of the condenser model
$A_i$	Internal surface of $i^{th}$ -control volume ( $m^2$ )
$T_i$	Refrigerant temperature in $i^{th}$ -control volume ( $\text{°C}$ )
$T_{wall,i}$	Wall temperature in $i^{th}$ -control volume ( $\text{°C}$ )

The temperature of the condenser wall varies over time during transient operation, and this variation could be evaluated as follows:

$$\frac{(MC)_{cond}}{N_{cells}} \frac{dT_{wall,i}}{dt} = Q_{ref,i} - Q_{water,i} \quad (3.20)$$

$$Q_{water,i} = U_{cond,water} \frac{A_{o,eff}}{N_{cells}} (T_{wall,i} - T_{water,in}) \quad (3.21)$$

$$A_{cond,eff} = A_{cond,tube} + \eta_{cond,fin} A_{cond,fin} \quad (3.22)$$

$(MC)_{cond}$	Thermal mass of condenser wall ( $kJ/\text{°C}$ )
$Q_{water,i}$	Heat absorbed by water in condenser ( $kw$ )
$U_{cond,water}$	Heat transfer coefficient of water in condenser ( $kw/m^2\text{°C}$ )
$A_{cond,eff}$	Effective outer surface of condenser ( $m^2$ )
$A_{cond,tube}$	Outer surface of condenser tubes ( $m^2$ )
$\eta_{cond,fin}$	Effectiveness of condenser fins
$A_{cond,fin}$	Surface of condenser fins ( $m^2$ )



The refrigerant conditions within each control volume in Fig. 3.2 could be presented in Table 3.4 as follows:

**Table 3.4 Refrigerant conditions**

Control volume			
Conditions	$i - 1$	$i$	$i + 1$
Inlet	○ $(m_{cond,ref})_{in}$	○ $m_{i-1,i}$	○ $m_{i,i+1}$
	○ $h_{cond,in}$	○ $h_{i-1,i}$	○ $h_{i,i+1}$
Centre	○ $m_{i-1}$	○ $m_i$	○ $m_{i+1}$
	○ $h_{i-1}$	○ $h_i$	○ $h_{i+1}$
Outlet	○ $m_{i-1,i}$	○ $m_{i,i+1}$	○ $(m_{cond,ref})_{out}$
	○ $h_{i-1,i}$	○ $h_{i,i+1}$	○ $h_{cond,out}$

### 3.4.2. Discretization of the modelling equations of the condenser

Eq. (3.17) and (3.18) from the condenser model in Fig. 3.2 could be discretized across the  $(i - 1)^{th}$ ,  $i^{th}$  and  $(i + 1)^{th}$  control volumes to produce the following set of equations:

$$\left\{ \begin{array}{l}
 (m_{cond,ref})_{in} h_{i-1} - m_{i-1,i} h_{i-1} - V_{i-1} \frac{dP_{cond}}{dt} + V_{i-1} \rho_{i-1} \frac{dh_{i-1}}{dt} + m_{i-1,i} h_{i-1,i} \\
 = (m_{cond,ref})_{in} h_{cond,in} - \alpha_{i-1} \frac{A_{i-1}}{N_{cells}} (T_{i-1} - T_{wall,i-1}) \\
 m_{i-1,i} h_i - m_{i,i+1} h_i - V_i \frac{dP_{cond}}{dt} + V_i \rho_i \frac{dh_i}{dt} - m_{i-1,i} h_{i-1,i} + m_{i,i+1} h_{i,i+1} \\
 = -\alpha_i \frac{A_i}{N_{cells}} (T_i - T_{wall,i}) \\
 m_{i,i+1} h_{i+1} - (m_{cond,ref})_{out} h_{i+1} - V_{i+1} \frac{dP_{cond}}{dt} + V_{i+1} \rho_{i+1} \frac{dh_{i+1}}{dt} - m_{i,i+1} h_{i,i+1} \\
 = -(m_{cond,ref})_{out} h_{cond,out} - \alpha_{i+1} \frac{A_{i+1}}{N_{cells}} (T_{i+1} - T_{wall,i+1})
 \end{array} \right. \quad (3.23)$$

$V_{i-1}$  Internal volume of  $(i - 1)^{th}$ -control volume ( $m^3$ )

$V_{i+1}$  Internal volume of  $(i + 1)^{th}$ -control volume ( $m^3$ )

$\rho_{i-1}$  Refrigerant density in  $(i - 1)^{th}$ -control volume ( $kg/m^3$ )

$\rho_{i+1}$	Refrigerant density in $(i + 1)^{th}$ -control volume ( $kg/m^3$ )
$\alpha_{i-1}$	Heat transfer coefficient in the $(i - 1)^{th}$ -control volume ( $kw/m^2\text{°C}$ )
$\alpha_{i+1}$	Heat transfer coefficient in the $(i + 1)^{th}$ -control volume ( $kw/m^2\text{°C}$ )
$A_{i-1}$	Internal surface of $(i - 1)^{th}$ -control volume ( $m^2$ )
$A_{i+1}$	Internal surface of $(i + 1)^{th}$ -control volume ( $m^2$ )
$T_{i-1}$	Refrigerant temperature in $(i - 1)^{th}$ -control volume ( $\text{°C}$ )
$T_{i+1}$	Refrigerant temperature in $(i + 1)^{th}$ -control volume ( $\text{°C}$ )
$T_{wall,i-1}$	Wall temperature in $(i - 1)^{th}$ -control volume ( $\text{°C}$ )
$T_{wall,i+1}$	Wall temperature in $(i + 1)^{th}$ -control volume ( $\text{°C}$ )

Eq. (3.23) could be arranged as follows:

$$\left\{ \begin{array}{l}
 (m_{cond,ref})_{in} h_{i-1} - V_{i-1} \frac{dP_{cond}}{dt} + V_{i-1} \rho_{i-1} \frac{dh_{i-1}}{dt} + m_{i-1,i} (h_{i-1,i} - h_{i-1}) \\
 = (m_{cond,ref})_{in} h_{cond,in} - \alpha_{i-1} \frac{A_{i-1}}{N_{cells}} (T_{i-1} - T_{wall,i-1}) \\
 m_{i-1,i} (h_i - h_{i-1,i}) - V_i \frac{dP_{cond}}{dt} + V_i \rho_i \frac{dh_i}{dt} + m_{i,i+1} (h_{i,i+1} - h_i) \\
 = -\alpha_i \frac{A_i}{N_{cells}} (T_i - T_{wall,i}) \\
 m_{i,i+1} (h_{i+1} - h_{i,i+1}) - (m_{cond,ref})_{out} h_{i+1} - V_{i+1} \frac{dP_{cond}}{dt} + V_{i+1} \rho_{i+1} \frac{dh_{i+1}}{dt} \\
 = -(m_{cond,ref})_{out} h_{cond,out} - \alpha_{i+1} \frac{A_{i+1}}{N_{cells}} (T_{i+1} - T_{wall,i+1})
 \end{array} \right. \quad (3.24)$$

Eq. (3.24) could be simplified by assuming that the enthalpy variation from a nodal point to an intermediary point (Fig. 3.2) is negligible enough to be taken into account in transient state modelling:

$$\left\{ \begin{aligned}
 & (m_{cond,ref})_{in} h_{i-1} - V_{i-1} \frac{dP_{cond}}{dt} + V_{i-1} \rho_{i-1} \frac{dh_{i-1}}{dt} \\
 = & (m_{cond,ref})_{in} h_{cond,in} - \alpha_{i-1} \frac{A_{i-1}}{N_{cells}} (T_{i-1} - T_{wall,i-1}) \\
 & - V_i \frac{dP_{cond}}{dt} + V_i \rho_i \frac{dh_i}{dt} \\
 = & -\alpha_i \frac{A_i}{N_{cells}} (T_i - T_{wall,i}) \\
 & - (m_{cond,ref})_{out} h_{i+1} - V_{i+1} \frac{dP_{cond}}{dt} + V_{i+1} \rho_{i+1} \frac{dh_{i+1}}{dt} \\
 = & - (m_{cond,ref})_{out} h_{cond,out} - \alpha_{i+1} \frac{A_{i+1}}{N_{cells}} (T_{i+1} - T_{wall,i+1})
 \end{aligned} \right. \quad (3.25)$$

The initial and final conditions of the pressure could be used to approximate the transient terms in (3.25) as follows:

$$\left\{ \begin{aligned}
 & -\frac{V_{i-1}}{\Delta t} P_{cond} + \left( \frac{V_{i-1} \rho_{i-1}}{\Delta t} + (m_{cond,ref})_{in} \right) h_{i-1} \\
 = & (m_{cond,ref})_{in} h_{cond,in} - \alpha_{i-1} \frac{A_{i-1}}{N_{cells}} (T_{i-1} - T_{wall,i-1}) - \frac{V_{i-1}}{\Delta t} P_{cond}^0 + \frac{V_{i-1} \rho_{i-1}}{\Delta t} h_{i-1}^0 \\
 & - \frac{V_i}{\Delta t} P_{cond} + \frac{V_i \rho_i}{\Delta t} h_i \\
 = & -\alpha_i \frac{A_i}{N_{cells}} (T_i - T_{wall,i}) - \frac{V_i}{\Delta t} P_{cond}^0 + \frac{V_i \rho_i}{\Delta t} h_i^0 \\
 & - \frac{V_{i+1}}{\Delta t} P_{cond} + \left( \frac{V_{i+1} \rho_{i+1}}{\Delta t} - (m_{cond,ref})_{out} \right) h_{i+1} \\
 = & - (m_{cond,ref})_{out} h_{cond,out} - \alpha_{i+1} \frac{A_{i+1}}{N_{cells}} (T_{i+1} - T_{wall,i+1}) - \frac{V_{i+1}}{\Delta t} P_{cond}^0 + \frac{V_{i+1} \rho_{i+1}}{\Delta t} h_{i+1}^0
 \end{aligned} \right. \quad (3.26)$$

$P_{cond}^0$	Refrigerant pressure in condenser ( $kPa$ )
$h_{i-1}^0$	Initial refrigerant enthalpy in $(i-1)^{th}$ -control volume ( $kJ/kg$ )
$h_i^0$	Initial refrigerant enthalpy in $i^{th}$ -control volume ( $kJ/kg$ )
$h_{i+1}^0$	Initial refrigerant enthalpy in $(i+1)^{th}$ -control volume ( $kJ/kg$ )

$$\Delta t = t - t^0 \quad (3.27)$$

$\Delta t$	Time step for solution tracking (s)
$t$	Final time (s)
$t^0$	Initial time (s)

A central difference scheme could be used to approximate the enthalpy at the condenser model's central node as follows:

$$h_i = \frac{h_{i-1} + h_{i+1}}{2} \quad (3.28)$$

Inserting (3.28) into (3.26), for transient state modeling, the set of equations that must be solved could be expressed as follows:

$$\left\{ \begin{array}{l} -\frac{V_{i-1}}{\Delta t} P_{cond} + \left( \frac{V_{i-1}\rho_{i-1}}{\Delta t} + (m_{cond,ref})_{in} \right) h_{i-1} \\ = (m_{cond,ref})_{in} h_{cond,in} - \alpha_{i-1} \frac{A_{i-1}}{N_{cells}} (T_{i-1} - T_{wall,i-1}) - \frac{V_{i-1}}{\Delta t} P_{cond}^0 + \frac{V_{i-1}\rho_{i-1}}{\Delta t} h_{i-1}^0 \\ -\frac{V_i}{\Delta t} P_{cond} + \frac{1}{2} \frac{V_i\rho_i}{\Delta t} h_{i-1} + \frac{1}{2} \frac{V_i\rho_i}{\Delta t} h_{i+1} \\ = -\alpha_i \frac{A_i}{N_{cells}} (T_i - T_{wall,i}) - \frac{V_i}{\Delta t} P_{cond}^0 + \frac{V_i\rho_i}{\Delta t} h_i^0 \\ -\frac{V_{i+1}}{\Delta t} P_{cond} + \left( \frac{V_{i+1}\rho_{i+1}}{\Delta t} - (m_{cond,ref})_{out} \right) h_{i+1} \\ = -(m_{cond,ref})_{out} h_{cond,out} - \alpha_{i+1} \frac{A_{i+1}}{N_{cells}} (T_{i+1} - T_{wall,i+1}) - \frac{V_{i+1}}{\Delta t} P_{cond}^0 + \frac{V_{i+1}\rho_{i+1}}{\Delta t} h_{i+1}^0 \end{array} \right. \quad (3.29)$$

In a matrix, (3.29) could be shown as follows:

$$\begin{aligned}
 & \begin{bmatrix} -\frac{V_{i-1}}{\Delta t} & \frac{V_{i-1}\rho_{i-1}}{\Delta t} + (m_{cond,ref})_{in} & 0 \\ -\frac{V_i}{\Delta t} & \frac{1}{2} \frac{V_i\rho_i}{\Delta t} & \frac{1}{2} \frac{V_i\rho_i}{\Delta t} \\ -\frac{V_{i+1}}{\Delta t} & 0 & \frac{V_{i+1}\rho_{i+1}}{\Delta t} - (m_{cond,ref})_{out} \end{bmatrix} \begin{bmatrix} P_{cond} \\ h_{i-1} \\ h_{i+1} \end{bmatrix} \\
 & = \begin{bmatrix} (m_{cond,ref})_{in} h_{cond,in} - \alpha_{i-1} \frac{A_{i-1}}{N_{cells}} (T_{i-1} - T_{wall,i-1}) - \frac{V_{i-1}}{\Delta t} P_{cond}^0 + \frac{V_{i-1}\rho_{i-1}}{\Delta t} h_{i-1}^0 \\ -\alpha_i \frac{A_i}{N_{cells}} (T_i - T_{wall,i}) - \frac{V_i}{\Delta t} P_{cond}^0 + \frac{V_i\rho_i}{\Delta t} h_i^0 \\ -(m_{cond,ref})_{out} h_{cond,out} - \alpha_{i+1} \frac{A_{i+1}}{N_{cells}} (T_{i+1} - T_{wall,i+1}) - \frac{V_{i+1}}{\Delta t} P_{cond}^0 + \frac{V_{i+1}\rho_{i+1}}{\Delta t} h_{i+1}^0 \end{bmatrix} \quad (3.30)
 \end{aligned}$$

The following could be done to extend (3.30) to n-control volumes:

$$\begin{aligned}
 & \begin{bmatrix} -\frac{V_{c,1}}{\Delta t} & \frac{V_{c,1}\rho_{c,1}}{\Delta t} + (m_{cond,ref})_{in} & 0 & 0 & 0 & 0 & 0 & 0 \\ \vdots & \vdots & \vdots & \vdots & \vdots & \vdots & \vdots & \vdots \\ -\frac{V_{i-1}}{\Delta t} & 0 & 0 & \frac{V_{i-1}\rho_{i-1}}{\Delta t} & 0 & 0 & 0 & 0 \\ -\frac{V_i}{\Delta t} & 0 & 0 & \frac{1}{2} \frac{V_i\rho_i}{\Delta t} & \frac{1}{2} \frac{V_i\rho_i}{\Delta t} & 0 & 0 & 0 \\ -\frac{V_{i+1}}{\Delta t} & 0 & 0 & 0 & \frac{V_{i+1}\rho_{i+1}}{\Delta t} & 0 & 0 & 0 \\ \vdots & \vdots & \vdots & \vdots & \vdots & \vdots & \vdots & \vdots \\ -\frac{V_{c,n-1}}{\Delta t} & 0 & 0 & 0 & 0 & \frac{V_{c,n-1}\rho_{c,n-1}}{\Delta t} & 0 & 0 \\ -\frac{V_{c,n}}{\Delta t} & 0 & 0 & 0 & 0 & 0 & \frac{V_{c,n}\rho_{c,n}}{\Delta t} - (m_{cond,ref})_{out} & 0 \end{bmatrix} \begin{bmatrix} P_{cond} \\ h_{c,1} \\ \vdots \\ h_{i-1} \\ h_{i+1} \\ \vdots \\ h_{c,n-1} \\ h_{c,n} \end{bmatrix} \\
 & = \begin{bmatrix} (m_{cond,ref})_{in} h_{cond,in} - \alpha_{c,1} \frac{A_{c,1}}{N_{cells}} (T_{c,1} - T_{wall,c,1}) - \frac{V_{c,1}}{\Delta t} P_{cond}^0 + \frac{V_{c,1}\rho_{c,1}}{\Delta t} h_{c,1}^0 \\ \vdots \\ -\alpha_{i-1} \frac{A_{i-1}}{N_{cells}} (T_{i-1} - T_{wall,i-1}) - \frac{V_{i-1}}{\Delta t} P_{cond}^0 + \frac{V_{i-1}\rho_{i-1}}{\Delta t} h_{i-1}^0 \\ -\alpha_i \frac{A_i}{N_{cells}} (T_i - T_{wall,i}) - \frac{V_i}{\Delta t} P_{cond}^0 + \frac{V_i\rho_i}{\Delta t} h_i^0 \\ -\alpha_{i+1} \frac{A_{i+1}}{N_{cells}} (T_{i+1} - T_{wall,i+1}) - \frac{V_{i+1}}{\Delta t} P_{cond}^0 + \frac{V_{i+1}\rho_{i+1}}{\Delta t} h_{i+1}^0 \\ \vdots \\ -\alpha_{c,n-1} \frac{A_{c,n-1}}{N_{cells}} (T_{c,n-1} - T_{wall,c,n-1}) - \frac{V_{c,n-1}}{\Delta t} P_{cond}^0 + \frac{V_{c,n-1}\rho_{c,n-1}}{\Delta t} h_{c,n-1}^0 \\ -(m_{cond,ref})_{out} h_{cond,out} - \alpha_{c,n} \frac{A_{c,n}}{N_{cells}} (T_{c,n} - T_{wall,c,n}) - \frac{V_{c,n}}{\Delta t} P_{cond}^0 + \frac{V_{c,n}\rho_{c,n}}{\Delta t} h_{c,n}^0 \end{bmatrix} \quad (3.31)
 \end{aligned}$$

The following definition could be used to describe the wall temperature in any control volume of the condenser model:

$$\begin{aligned}
 (T_{wall,k})_{cond} = & \frac{\alpha_k A_k}{\alpha_k A_k + A_{cond,eff} U_{cond,water} + \frac{(MC)_{cond}}{\Delta t}} (T_k)_{cond} \\
 & + \frac{A_{cond,eff} U_{cond,water}}{\alpha_k A_k + A_{cond,eff} U_{cond,water} + \frac{(MC)_{cond}}{\Delta t}} (T_{water,in})_{cond} \\
 & + \frac{\frac{(MC)_{cond}}{\Delta t}}{\alpha_k A_k + A_{cond,eff} U_{cond,water} + \frac{(MC)_{cond}}{\Delta t}} (T_{wall,k}^0)_{cond}
 \end{aligned} \quad (3.32)$$

$(T_{wall,k})_{cond}$	Wall temperature in $k^{th}$ -control volume ( $^{\circ}\text{C}$ )
$(T_{wall,k}^0)_{cond}$	Initial wall temperature in $k^{th}$ -control volume ( $^{\circ}\text{C}$ )
$(T_k)_{cond}$	Refrigerant temperature in $k^{th}$ -control volume ( $^{\circ}\text{C}$ )
$\alpha_k$	Heat transfer coefficient in the $k^{th}$ -control volume ( $\text{kw}/\text{m}^2\text{^{\circ}\text{C}}$ )
$A_k$	Internal surface of $k^{th}$ -control volume ( $\text{m}^2$ )

The definition of  $k$ , which stands for the control volume number, is as follows:

$$k = \{1; 2; \dots \dots \dots; n - 1; n\} \quad (3.33)$$

The equations for transient state modelling of the evaporator are presented in Table 3.5 as follows:

Table 3.5 Transient state modelling equations of the evaporator

Parameter	Model	Nomenclature
Energy conservation	$V_j \left[ \left( h_j \frac{\partial \rho_j}{\partial P} \Big _{h,j} - 1 \right) \frac{dP_{evap}}{dt} + \left( h_j \frac{\partial \rho_j}{\partial h_j} \Big _p + \rho_j \right) \frac{dh_j}{dt} \right]$ $= (m_{evap,ref})_{in} h_{evap,in}$ $- (m_{evap,ref})_{out} h_{evap,out}$ $- Q_{ref,j}$	<ul style="list-style-type: none"> <li>○ <math>P_{evap}</math> - Refrigerant pressure in evaporator (<math>kP_a</math>)</li> <li>○ <math>(m_{evap,ref})_{in}</math> - Refrigerant mass flow rate at evaporator inlet (<math>kg/s</math>)</li> <li>○ <math>(m_{evap,ref})_{out}</math> - Refrigerant mass flow rate at evaporator outlet (<math>kg/s</math>)</li> <li>○ <math>h_j</math> - Refrigerant enthalpy in <math>j^{th}</math>-control volume (<math>kJ/kg</math>)</li> <li>○ <math>\rho_j</math> - Refrigerant density in <math>j^{th}</math>-control volume (<math>kg/m^3</math>)</li> </ul>
Heat absorbed	$Q_{ref,j} = -\alpha_j \frac{A_j}{N_{cells}} (T_j - T_{wall,j})$	<ul style="list-style-type: none"> <li>○ <math>Q_{ref,j}</math> - Heat absorbed by refrigerant in evaporator (<math>kw</math>)</li> <li>○ <math>\alpha_j</math> - Heat transfer coefficient in <math>j^{th}</math>-control volume (<math>kw/m^2\text{°C}</math>)</li> <li>○ <math>A_j</math> - Internal surface of <math>j^{th}</math>-control volume (<math>m^2</math>)</li> </ul>
Wall temperature	$\frac{(MC)_{evap}}{N_{cells}} \frac{dT_{wall,j}}{dt} = -(Q_{ref,j} - Q_{water,j})$	<ul style="list-style-type: none"> <li>○ <math>T_{wall,j}</math> - wall temperature in <math>j^{th}</math>-control volume (<math>\text{°C}</math>)</li> <li>○ <math>(MC)_{evap}</math> - Thermal mass of evaporator wall (<math>kJ/\text{°C}</math>)</li> </ul>
Heat added	$Q_{water,j} = -U_{evap,water} \frac{A_{evap,eff}}{N_{cells}} \left[ T_{wall,j} - (T_{water,in})_{evap} \right]$ $A_{evap,eff} = A_{evap,tube} + \eta_{evap,fin} A_{evap,fin}$	<ul style="list-style-type: none"> <li>○ <math>Q_{water,j}</math> - Heat added by water (<math>kwh</math>)</li> <li>○ <math>A_{evap,eff}</math> - Effective outer surface of evaporator (<math>m^2</math>)</li> <li>○ <math>A_{evap,tube}</math> - Outer surface of evaporator tubes (<math>m^2</math>)</li> <li>○ <math>A_{evap,fin}</math> - Surface of evaporator fins (<math>m^2</math>)</li> </ul>

### 3.5. EXPERIMENTAL INVESTIGATION OF A VC SYSTEM

The four main parts of a typical VC system, along with refrigerant piping and measurement equipment, make up the experimental setup. The compressor is an electrically powered, three-phase inverter motor-driven reciprocating piston in a cylinder that can operate at various speeds.

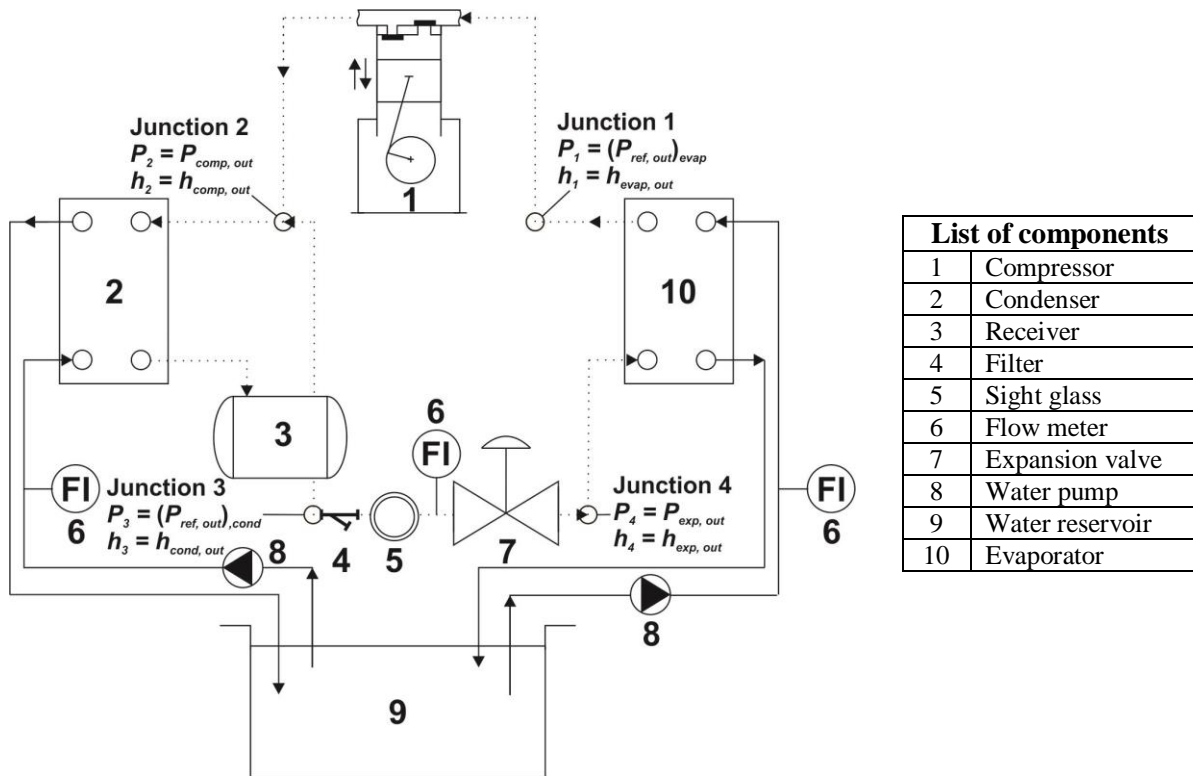


Figure 3.4 Experimental setup

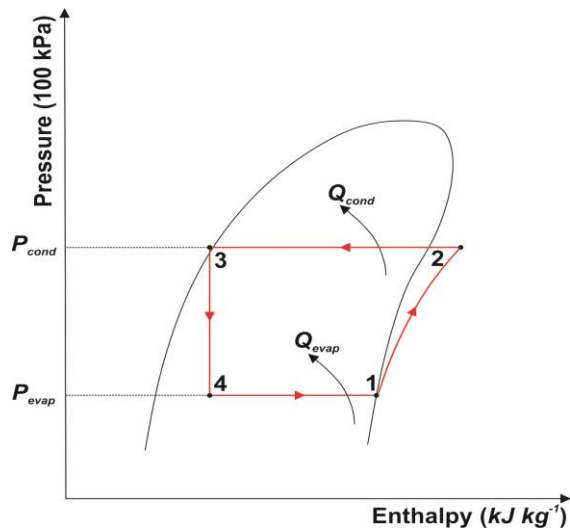


Figure 3.5  $p$ - $h$  diagram of the VC cycle



Recirculated room-temperature water was used as the secondary fluid in plate heat exchangers that made up the condenser and evaporator units. For water storage, a water reservoir was used to maintain constant pressure, temperature and flow rate required for stable operation. A TXV made up the expansion device.

A thermocouple expansion valve and a temperature sensing bulb were used to measure the refrigerant temperature at the TXV and evaporator coil outlets, respectively. At the compressor's inlet and outlet, two electronic pressure transducers were installed to measure the refrigerant pressure on the low- and high-pressure sides.

A receiver is installed on the liquid line of the experimental setup after the condenser in order to collect exceeding refrigerant liquid exiting the condenser. A filter-dryer is installed before the thermostatic expansion valve in order to prevent the passage of any debris by means of a strainer and this contributes in protecting the expansion valve and compressor from failure. The filter-dryer also enables to remove moisture with a desiccant to ensure satisfactory heat transfer between the circulating refrigerant and water. A sight glass is installed on the experimental setup just before the expansion valve so that the operator can check whether bubbles are present in the refrigerant, which indicates the presence of gas downstream of the condenser and therefore requiring an eventual system check or maintenance.

Data acquisition consists in gathering the analog signal transmitted by the thermo-physical transformation undergone by the refrigerant and water during the process of the VC system. The measurement devices installed at various location of the experimental setup such as thermocouples, water flow meters and pressure transducers convert the signal emitted into voltage

signal measurable by the data acquisition equipment. The voltage signal is converted into digit format by the data acquisition equipment so that the computer can depict this signal. A Windows computer running the RA1 software [205] and data logger was the data acquisition system. With a mimic diagram shown on the personal computer (PC) screen, the software enabled real-time control and monitoring of all the measurement device outputs. The inverter motor driving the compressor is equipped with a torque vector control allowing measurement as well as control of the motor torque and the compressor speed with RA1 software [205].

With its temperature rising above saturation (superheating), the refrigerant vapor R134a entered the compressor through junction 1 in Fig. 3.4 and exited through junction 2. High temperature refrigerant entered the condenser through junction 2 to be cooled for superheat removal to allow latent heat removal to occur at constant temperature and pressure whilst causing the phase change from vapor to liquid. The heat removed was carried by the surrounding water stream in the condenser as the refrigerant liquid exited the condenser through junction 3.

The refrigerant liquid stream enters the expansion valve through junction 3 and expands with a sudden drop in pressure before leaving through junction 4 in a low-pressure, liquid-vapor mixture. Through junction 4, a low-temperature refrigerant mixture enters the evaporator where it is heated by the water stream to undergo a phase change to vapor before returning to the compressor through junction 1 to begin a new cycle. Fig. 3.5 shows the refrigerant's thermodynamic cycle in a VC system.

After running for about 10 minutes with the water flow rate set at 50% of its full range through the condenser and at 70% of its full range through the evaporator, the experimental setup attained steady state operating conditions. The speed of the compressor was varied with 5% step increment.

The data were recorded every minute and over 30 minutes for each range of compressor speed setting for steady state investigation. For transient state investigation, data were recorded every second during 10 min before the setup reached steady state. Plots of each data range's average value against the corresponding setting of the compressor speed were made. With minor changes in compressor speed setting, the collected data remained largely unchanged. However, as the compressor speed setting was increased significantly, an important variation of the recorded data was observed.

### 3.6. RESULTS AND DISCUSSION

#### 3.6.1. Steady state modelling

The parameters used for steady state modelling are listed in Table 3.6 as follows:

**Table 3.6** *Steady state parameters [145]*

Parameters	
$V_{ref} = 0.05 \text{ m s}^{-1}$	$\eta_{isen} = 0.65$
$f_{cond} = 1$	$h_{isen,out} = 258.36 \text{ kJ kg}^{-1}$
$f_{evap} = 1$	$D_v = 92.5 \cdot 10^{-6} \text{ m}^3 \text{ s}^{-1}$
$l_{cond} = 0.5 \text{ m}$	$RPM_{comp} = 1000$
$l_{evap} = 0.5 \text{ m}$	$\rho_{txv,in} = 1183.5 \text{ kg m}^{-3}$
$d_{cond} = 0.012 \text{ m}$	$C_{txv} = 10^{-6}$
$d_{evap} = 0.012 \text{ m}$	$T_{Sh,operating} = 4 \text{ }^\circ\text{C}$
$\eta_{vol} = 4.6$	$T_{Sh,static} = 3.5 \text{ }^\circ\text{C}$

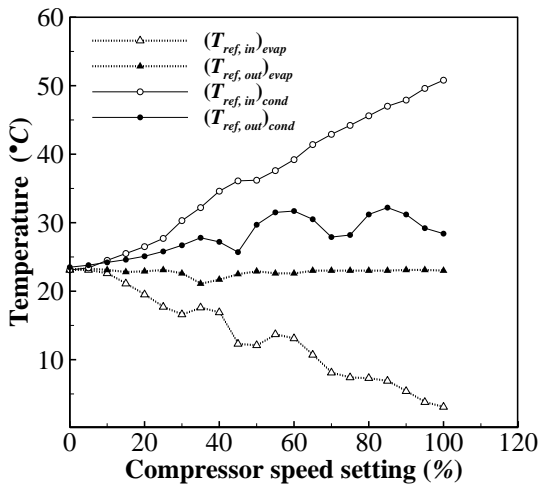


Figure 3.6 Temperature curves of the refrigerant

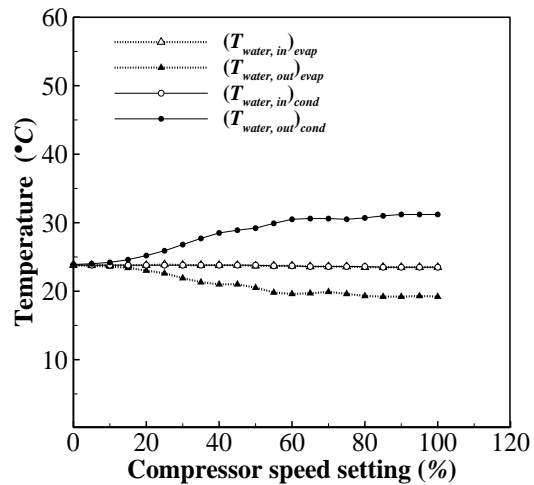
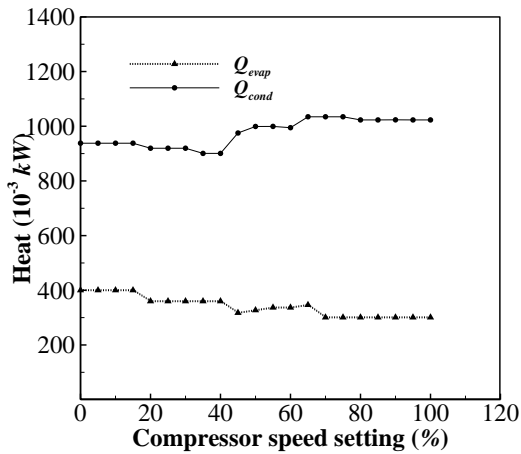
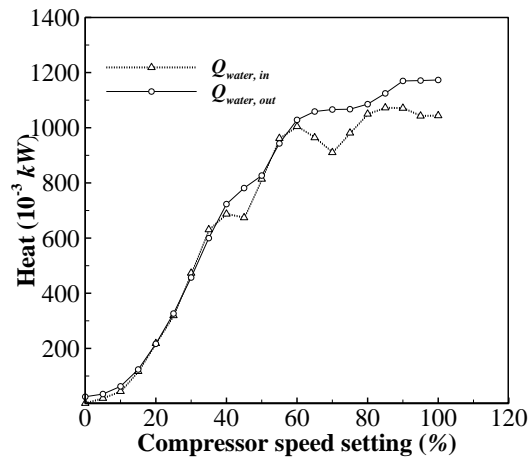


Figure 3.7 Temperature curves of water

Figs. 3.6 and 3.7 show how the refrigerant temperature changes in the VC system as a function of the compressor speed setting and the distribution of the water streams around the condenser and evaporator, respectively. The offsets observed with the curve of the refrigerant temperature at the condenser outlet ( $(T_{ref,out})_{cond}$ ) were due to issues related to the experimental setup however, this was adjusted with a correction factor during the simulation. The heat transfer distribution to and from the refrigerant is presented in Fig. 3.8 whilst its counterpart for the water streams is presented in Fig. 3.9. Fig. 3.10 illustrates the model's experimental data validation for prediction of the pressure through the condenser and evaporator. The model validation with experiments to predict the junction enthalpies is presented in Fig. 3.11. On the other hand, the predicted junction pressures and enthalpies were found from (3.12).



**Figure 3.8** Heat curves of the refrigerant



**Figure 3.9** Heat curves of water

Re-circulated water entered the evaporator and condenser at an average room temperature of 23°C. The refrigerant temperature at the evaporator outlet decreased with increasing compressor speed and stabilized at about 60% compressor speed setting (Fig. 3.4). On the other hand, the refrigerant temperature through the condenser outlet increased as the speed of the compressor was raised and oscillated within 28°C to 32°C at 60% compressor speed setting (Fig. 3.4). As the compressor speed increased so did the refrigerant temperature through the condenser inlet (Fig. 3.4). Similarly, the inlet refrigerant pressure through the condenser also increased with increasing compressor speed (Fig. 3.10). The refrigerant enthalpy through the condenser inlet remained high (Fig. 3.11) because at this point the gas stream at high pressure and temperature carried an important amount of heat. Increasing compressor speed led the refrigerant temperature through the evaporator inlet to decrease.

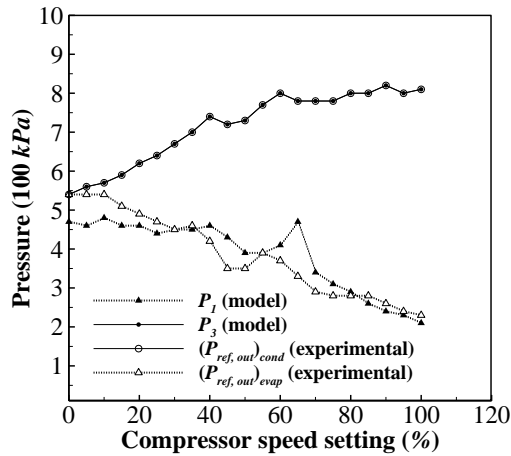


Figure 3.10 Pressure curves of the refrigerant

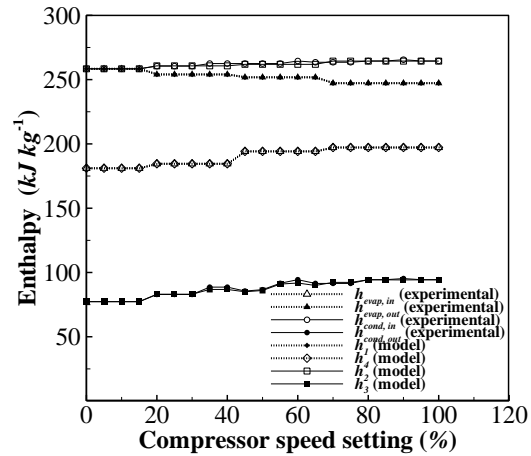


Figure 3.11 Enthalpy curves of the refrigerant

The refrigerant pressure at the evaporator inlet also decreased with increasing compressor speed (Fig. 3.10). The refrigerant mixture carried less heat at low pressure and temperature through the evaporator inlet consequently its enthalpy remained low at this point (Fig. 3.11). At steady state operating conditions of the experimental setup, the heat rejected by the refrigerant through the condenser remained higher than the heat absorbed by the refrigerant through the evaporator (Fig. 3.8). At high compressor speed (roughly 65% compressor speed setting), the heat added to the evaporator and removed from the condenser by the secondary water stream had the same magnitude (Fig. 3.9). The condenser and evaporator curve trends of the refrigerant conditions confirmed the validity of the experimental data.

Some parameter values for steady state modelling (Table 3.6) were used to determine the output parameters of the components of the VC system. For the system of conservation equations at each junction in (3.12), the refrigerant pressure at the compressor outlet and its enthalpy through the expansion valve outlet were inputs so that the modeling outputs could be easily determined using

the Gaussian elimination method. The prediction of the model outputs at each junction was performed by coding the steady state modelling matrix in Matlab using the steady state parameter conditions in Table 3.6 and by solving for the model outputs in (3.9) with a Gaussian elimination method. The results obtained from the Matlab code were plotted against the experimental data for model validation.

The predicted evaporating or low refrigerant pressure was in agreement with the experimental data (Fig. 3.10). However, the evaporating refrigerant pressure was determined by reversing the modelling outputs for each compressor speed setting in order to describe the expansion process occurring in the expansion device otherwise, the distribution of the predicted evaporating pressure would grow linearly with the predicted condensing pressure in a purely analytical point of view. The lowest refrigerant pressure in the system was located at the junctions between the expansion device and evaporator and the compressor. These junctions could be referred to as the VC system's low-pressure side (Fig. 3.1). The condensing pressure, on the other hand, was the same at the junctions between the compressor and condenser and the expansion device. These junctions could be thought of as the VC system's high-pressure side (Fig. 3.1).

With an average value of  $252 \text{ kJ kg}^{-1}$ , the junction enthalpy of the refrigerant at the evaporator outlet was consistent with the experiments (Fig. 3.11) and slightly lower than the refrigerant enthalpy of  $262 \text{ kJ kg}^{-1}$  at the condenser inlet. It was confirmed that downstream of the condenser, heat is removed from the refrigerant by the circulating water stream to produce condensing effects because the predicted outlet refrigerant enthalpy through the condenser was in agreement with experiments at an average of  $87 \text{ kJ kg}^{-1}$ .

The average refrigerant enthalpy through the evaporator inlet was  $190 \text{ kJ kg}^{-1}$ , and it was consistent with experimental data. However, since the inlet and outlet refrigerant enthalpies through the expansion valve are different, the assumption of isenthalpic process along the expansion device, which is frequently adopted in the literature, could not be confirmed. For steady state modelling, the heat removed through the condenser and absorbed through the evaporator was assumed to be constant.

### 3.6.2. Transient state modelling

Relevant parameters used for transient state modelling are listed in Table 3.7 as follows:

**Table 3.7** Transient state parameters [145]

Parameters	
Condenser	Evaporator
$V_{i-1} = V_i = V_{i+1} = 0.008 \text{ m}^3$	$V_{j-1} = V_j = V_{j+1} = 0.008 \text{ m}^3$
$A_{i-1} = A_i = A_{i+1} = 0.02 \text{ m}^2$	$A_{j-1} = A_j = A_{j+1} = 0.02 \text{ m}^2$
$P_{cond}^0 = 540 \text{ kPa}$	$P_{evap}^0 = 540 \text{ kPa}$
$h_{i-1}^0 = h_{cond,in} = 258.4 \text{ kJ kg}^{-1}$	$h_{j-1}^0 = h_{evap,in} = 181.1 \text{ kJ kg}^{-1}$
$h_i^0 = 167.8 \text{ kJ kg}^{-1}$	$h_j^0 = 219.7 \text{ kJ kg}^{-1}$
$h_{i+1}^0 = h_{cond,out} = 77.3 \text{ kJ kg}^{-1}$	$h_{j+1}^0 = h_{evap,out} = 258.4 \text{ kJ kg}^{-1}$
$(m_{cond,ref})_{in} = (m_{cond,ref})_{out} = 0.01 \text{ kg s}^{-1}$	$(m_{evap,ref})_{in} = (m_{evap,ref})_{out} = 0.01 \text{ kg s}^{-1}$



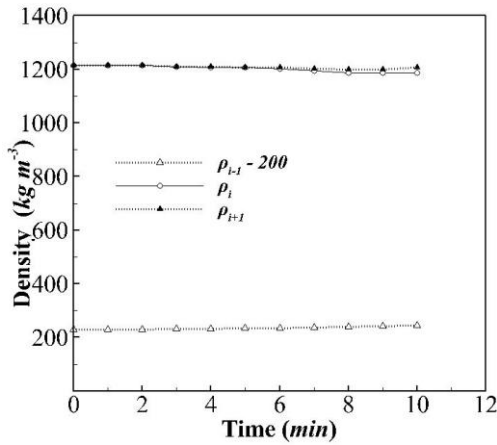


Figure 3.12 Refrigerant density in condenser

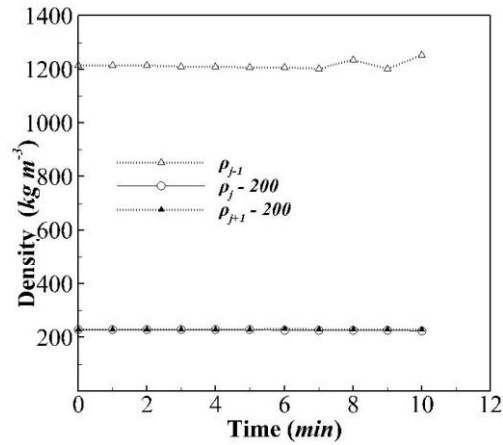


Figure 3.13 Refrigerant density in evaporator

Fig. 3.12 depicts the refrigerant density variation over time in the condenser, whilst Fig. 3.13 shows the same variation over time in the evaporator. Fig. 3.14 shows the temperature change over time in the condenser, whilst Fig. 3.15 shows for the evaporator, the equivalent distribution.

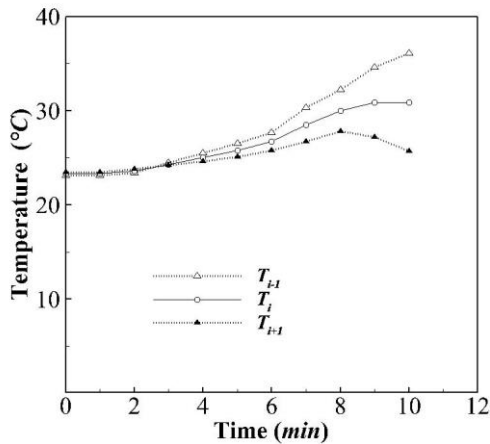


Figure 3.14 Refrigerant temperature in condenser

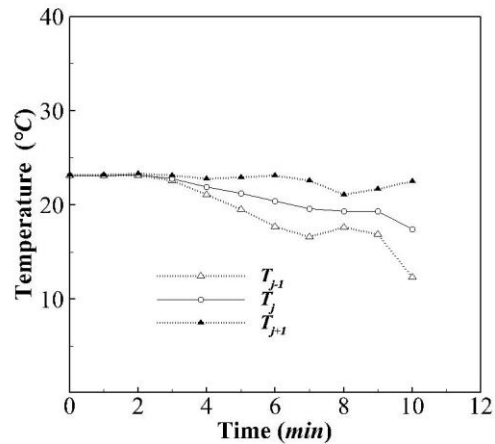


Figure 3.15 Refrigerant temperature in evaporator

Predicted refrigerant enthalpies through the condenser and evaporator are represented along with experimental validation in Fig. 3.16 and Fig. 3.17 respectively. The evaporator modelling was

performed similar to the condenser. Predicted refrigerant pressures through the condenser and evaporator are represented in Fig. 3.18 along with experimental validation.

For the compressor and expansion valve models, a quasi-static formulation was used. The predicted conditions from the evaporator and condenser were used as modelling inputs. The outlet enthalpy, the mass flow rate through the compressor, and the mass flow rate through the expansion valve were each calculated using (3.1), (3.2), and (3.6), respectively. Longitudinal flow through the condenser and evaporator as well as negligible axial conduction were assumed. The condenser and evaporator tubes were circular, thin, uniform, long enough and oriented horizontally.

Assuming that there were minimal variations in the refrigerant conditions between two consecutive time steps, the enthalpy and pressure computed for the previous time step were used as initial conditions for the subsequent time step. Isobaric conditions within the evaporator and condenser were assumed to be sufficient to cancel out pressure drop [166].

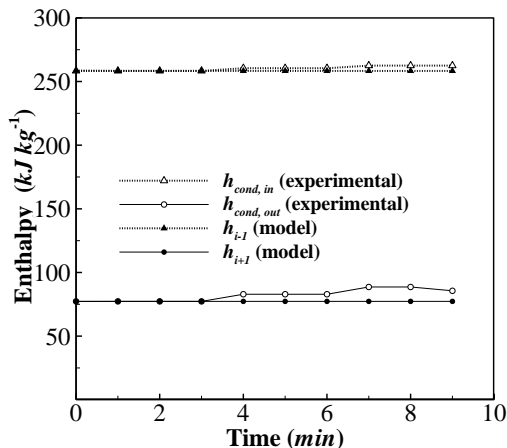


Figure 3.16 Refrigerant enthalpy in condenser

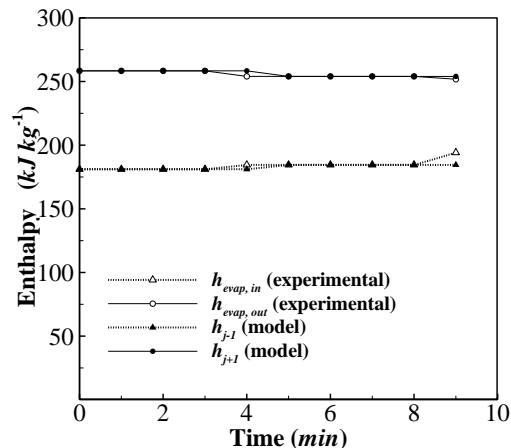


Figure 3.17 Refrigerant enthalpy in evaporator

For every time step, data were logged every second. The values of the predicted conditions were averaged and plotted as they varied with time. The densities within the condenser (Fig. 3.12) and evaporator (Fig. 3.13) did not vary considerably with time as the data were recorded with a narrow delay. As more energy could be stored by gas, the outlet enthalpy of the refrigerant within the condenser was less important than its inlet counterpart. Similarly, within the evaporator, the outlet enthalpy of the refrigerant was more important due to gas storage compared to the inlet enthalpy where energy is stored by a liquid.

Through the condenser, the outlet and inlet refrigerant temperatures were the same for approximately 5 min (Fig. 3.14) then, due to heat absorption by water, significant outlet temperature drop was observed whilst with high pressure gas at the compressor outlet, significant temperature increase was observed. Similar trends were observed on the evaporator side (Fig. 3.15). The experimental results were satisfactory for model validation based on the observation made on the trend of the refrigerant conditions within the evaporator and condenser.

Matlab was used to code (3.31) and adopt the Gaussian elimination method for prediction within the condenser with the solutions being recorded every 60 seconds. Table 3.7 provided the specifications for the pressures and enthalpies' initial conditions. The modelling results obtained with Matlab were validated with experimental data. The condenser model had to be split up into several control volumes for finite volume formulation. The heat transfer coefficient (HTC) was evaluated within each phase of the refrigerant namely, superheat, two-phase and subcooling. The property tables of the R-134a refrigerant were used for evaluation of the specific heat capacities. The correlation of [206], was adopted for HTC evaluation within the superheat and subcool zones

whilst the correlation of [207], was adopted for HTC evaluation within the two-phase zone. The Colburn J-factor was adopted for water's HTC evaluation.

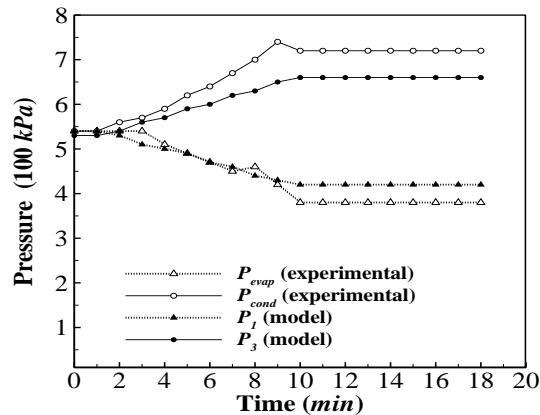


Figure 3.18 Refrigerant pressure in condenser and evaporator

Numerical issues created using the property tables and correlations with discontinuities required a particular attention. An example of occurring numerical issues is the HTC computation for each control volume with varying refrigerant conditions at each time step such as the flow rate, pressure and enthalpy. Numerical issues resulted in slowing the model simulation however, to overcome these issues, integrated smooth function were adopted. Parameters such as the Intermediate enthalpies and flow rates cancelled out with algebraic manipulation. Eq. (3.31) was used to evaluate the lumped enthalpy, mass flow rate and pressure. Lumped enthalpy at the central node was calculated from interpolation of the lumped enthalpies of surrounding nodes under the assumption that the enthalpy distribution was linear.

The experimental results were in agreement with the predicted outlet enthalpy of the refrigerant at the evaporator with an average of  $256 \text{ kJ kg}^{-1}$  (Fig. 3.17) and through the condenser, the average inlet refrigerant enthalpy was  $258 \text{ kJ kg}^{-1}$  (Fig. 3.16). The experiments were in agreement with

the predicted outlet enthalpy of the refrigerant at the condenser with an average of  $77 \text{ kJ kg}^{-1}$  (Fig. 3.16) which confirmed heat removal from the refrigerant by the water downstream the condenser. Predicted and experimental results of the inlet refrigerant enthalpy through the evaporator were in agreement with an average value of  $190 \text{ kJ kg}^{-1}$  (Fig. 3.17).

The experimental data and predicted evaporating pressure were in agreement (Fig. 3.18) however;  $15 \text{ Kpa}$  was subtracted at every time step to obtain a satisfactory evaporating pressure curve. The junctions between the expansion valve and evaporator and the compressor, indicated the low-pressure side of the system (Fig. 3.1). For the condenser model,  $15 \text{ Kpa}$  was incremented at every time step to obtain a satisfactory condensing pressure curve. The experimental data and predicted condensing pressure were in agreement (Fig. 3.18). The junctions between the compressor and condenser and the expansion valve, indicated the high-pressure side of the system (Fig. 3.1).

### **3.7. CONCLUSION**

Using existing component equations, a steady state modelling scheme of VC system was suggested. A steady state modelling matrix was derived to determine the modelling outputs. The steady state matrix used a communication framework to exchange information with the VC system so that the only required parameters for modelling would be the junction pressure and enthalpy. The system of equations for steady state modelling was based on the conservation law at each junction. It was necessary to set up some input parameters in order to solve the system of equations.

There were experiments run, and the recorded data were checked and found to be appropriate for model validation. The predicted evaporating pressure results from steady state modelling agreed with the results of the experiments. The predicted junction enthalpies and the experimental results were both convergent.

It was also found that the condensing pressure increased with increasing compressor speed setting. The evaporating pressure was inversely proportional to the condensing pressure as the flow was expanded through the expansion valve. The results also showed that at steady state conditions with constant water and refrigerant flow rates, more heat was removed from the refrigerant in the condenser than it was added to the evaporator. The results of the steady state modeling could be used to identify the optimum VC system parameters needed to implement an optimum control scheme to increase the effectiveness of the system.

The steady state modelling technique could also be adopted for different type of component modelling equations and its results supported with experimental results. The results obtained could be useful for improving the design of innovative control methods of VC systems. Although not attempted in this work, the developed steady state modelling method could be extended for modelling of complex configuration of VC systems such as systems with single condensing unit combined with multiple evaporating units and expansion valves.

Using existing modelling equations, a transient state modelling scheme of VC system was also suggested. For the finite volume discretization of the PDE's, small control volumes were chosen for the condenser and evaporator modelling. The initial and final values were used to approximate the time derivatives. The adoption of the finite volume scheme was supported by its flexibility in evaluating the dynamics of systems with different configuration with a simple discretization method.

The algebraic equations used for solution tracking were obtained from the discretization of governing equations around the central node of each control volume. The initial values were required and set to initiate the solution tracking at each time step.

The relevance of the experiments was assessed for validation of the predictive model. The predictions of the condensing and evaporating pressures as well as the junction enthalpies were in agreement with experiments. The pressure curves of the condenser and evaporator respectively rose and dropped with time significantly before stabilizing when steady state was reached. No significant variation with time of the enthalpy and density was depicted.

The implementation of optimal controllers using the results of the transient state predictive modelling could be improved to control the refrigerant dynamics in VC systems. Instead of using a quasi-static approach, time varying mass flow rate through the compressor and expansion valve during startup operation should be investigated to improve the predictive transient state model.

The refrigerant phase changes should also be taken into account to accurately assess HTC's through the condenser and evaporator. The pressure drop through the condenser and evaporator models might also require special attention to strengthen the suggested transient state model.

# CHAPTER 4 CONTROL-ORIENTED MODELLING OF THE REFRIGERANT DYNAMICS

## 4.1. INTRODUCTION

The mathematical models developed in the previous chapter enabled to determine the refrigerant conditions such as pressure, temperature and enthalpy during steady and transient operating conditions. These parameters govern the characteristics of the refrigerant dynamics controllable with actuators such as the expansion valve and compressor. The predictive models could track the refrigerant conditions and integrate them into multivariable controllers that could control simultaneously superheat and capacity regulation.

The models in the previous chapter enables to track the refrigerant conditions in steady and transient operating conditions. The steady state model validated with experiments enables the selection of a steady operating point for linearization of nonlinear systems. The transient state model enables optimal design of VC systems for efficient energy usage during startup. Despite the aforementioned, these models require improvements firstly to capture the refrigerant phase changes in the evaporator and condenser and secondly to develop control-oriented models required for implementation of multivariable controllers.

Designing a robust and performant multivariable controller of VC systems requires developing a nonlinear control-oriented model that could be linearized around a steady operating point. Additionally, MPC implementation on multivariable indoor air quality control has consistently



## ***CHAPTER 4 CONTROL-ORIENTED MODELLING OF THE REFRIGERANT DYNAMICS***

---

delivered good results with regards to disturbance rejection and reference tracking. Therefore, it may be worthwhile to investigate MPC implementation for multivariable control of the refrigerant dynamics in VC systems using control-oriented modelling as this system could offer excellent performance with regards to disturbance rejection and reference tracking for superheat and capacity regulation.

The objective of this chapter is first, to develop a nonlinear control-oriented model of the refrigerant dynamics in VC systems integrating the refrigerant phase changes in the heat exchangers based on Navier-Stokes equations adopted in the previous chapter but with additional parameters enabling the model simulation under wide operating conditions. Secondly, the linearization of the nonlinear control-oriented model around a steady operating point. Thirdly, MPC implementation on the linear model for simultaneous superheat and capacity regulation with consideration of the coupling effects between the two variables.

This work contributes in designing a multivariable controller of the refrigerant dynamics in VC systems to control simultaneously the superheat and capacity regulation whilst considering their coupling effects using MPC loop on a nonlinear control-oriented model duly linearized around a steady operating point carefully selected using the steady state model developed and validated with experiments in the previous chapter.

The subsequent sections of this chapter are listed as follows. In section 4.2., the literature study on control-oriented modelling of the refrigerant dynamics is presented. Control-oriented models of the heat exchangers are developed in section 4.3. The state space formulation and the MPC

## ***CHAPTER 4 CONTROL-ORIENTED MODELLING OF THE REFRIGERANT DYNAMICS***

---

implementation on the VC system are discussed respectively in section 4.4. and section 4.5. The results and discussion are presented in section 4.6 and the conclusion in section 4.7.

### **4.2. LITERATURE REVIEW**

Dynamic control of VC systems requires developing simple but accurate control-oriented dynamic models capturing the complex physical transformation of the circulating fluid. Advanced dynamic control schemes contribute to improve the performance and efficiency of VC systems operating across wide range. Dynamic control of VC systems consists in controlling the expansion valve for superheat regulation and the compressor for capacity regulation [208].

Superheat regulation was reported by [209-215]. Capacity regulation on the other hand was reported by [216-224]. SISO controllers, which have inherent restrictions on gain tuning and the coupling between superheat and capacity control, are frequently used to independently control superheat and capacity regulation [225]. Limitations of SISO schemes are addressable by adopting MIMO controllers more robust and performant across wide operating range.

Thermal control of enclosed spaces using VC systems with MIMO MPC has been reported [226-230]. Similar MPC strategies could be implemented for dynamic control of VC systems despite its fundamental difference with thermal control of enclosed spaces. The latter consisting in controlling simultaneously indoor conditions such as temperature, humidity and CO<sub>2</sub> level with the compressor and evaporator fan speeds [228]. The former on the other hand, performs a simultaneous superheat and capacity regulation [225], by actuating the expansion valve and compressor.

## ***CHAPTER 4 CONTROL-ORIENTED MODELLING OF THE REFRIGERANT DYNAMICS***

---

[225], proposed a moving-boundary scheme for a control-oriented model with lumped parameters to represent the refrigerant's physical transformation inside the evaporator and condenser. [231], adopted this model for MIMO control of the refrigerant dynamics in VC systems using combined LQG and gain scheduling schemes. [232, 233], adopted similar control-oriented model for MIMO control of food process and vehicle AC respectively.

[234], presented recent work on dynamic modelling of VC systems for prediction of the refrigerant conditions during start-up and shutdown. This work also reviewed recent works on dynamic modelling of VC systems such as [145, 148, 164, 167, 172]. However, these works were based on long transient modelling more effective for prediction during start-up and shutdown rather than for model-based controller design, which requires short transient for linearization of the model around a steady operating point [225]. Insightful literatures on control-oriented modelling of VC systems have been reported in [235-241] along with MPC implementation on VC systems [242, 243].

[244, 245], adopted PID strategy with auto-tuning for multivariable control of an HVAC system. Decoupling methodology was considered and the auto-tuning demonstrated satisfactory and superior results compared to manual tuning. [246], investigated the effect of PID implementation on a VC system for superheat control using an electronic expansion valve (EEV). The control gains determined with Ziegler-Nichols improved the overall energy consumption of the system. [247], compared ANN, Fuzzy and PID for capacity and superheat control. ANN performed better in terms of energy consumption.

## ***CHAPTER 4 CONTROL-ORIENTED MODELLING OF THE REFRIGERANT DYNAMICS***

---

[248], suggested predictive functional control (PFC) for superheat control with an EEV and the results showed an improved COP of the VC system. [249], adopted MPC for superheat and capacity control on VC systems equipped with multiple evaporators. The controller was tested in a laboratory with an AC system supplying two zones to demonstrate its effectiveness.

[250], implemented MPC on a VC system for superheat and capacity control. The control strategy improved overall COP whilst effectively tracking superheat and capacity. [251], suggested a simulation platform using Simulink for performance evaluation of dynamic HVAC controllers.

[203], suggested a distributed model adopted to control the superheat and capacity of a VC system. The fluid's properties were determined from the equation of [252]. HTC were correlated with [253, 254]. The pressure drop within the evaporator was correlated with [255]. To avoid discontinuities between two-phase and superheat zones within the evaporator, critical quality was determined using the correlation of [256]. Void fraction was correlated with [257]. The compressor was modelled using [258]. The transfer function suggested by [259] was adopted for superheat and capacity control considering [260] to evaluate the control parameters such as heat gain and time constant. The simulation results of the control system were in agreement with performed experiments as superheat remained within set range with minimum error.

### **4.3. CONTROL - ORIENTED MODELLING OF THE HEAT EXCHANGERS**

In this section, one dimensional refrigerant flow through long, thin and horizontal heat exchanger tubes as well as negligible heat conduction axially are the assumptions undertaken for simplicity. We consider cross-flow type of heat exchangers using water as secondary fluid.

**CHAPTER 4 CONTROL-ORIENTED MODELLING OF THE REFRIGERANT DYNAMICS**

The refrigerant flow through the evaporator undergoes phase change due to energy gains, therefore it is split in two areas namely, the liquid-gas mixture area and the superheated gas area. The refrigerant temperature is at saturation and is spatially invariant along the two-phase zone whilst it increases along the single-phase zone through the evaporator outlet. The evaporator model is represented in Fig. 4.1 as follows:

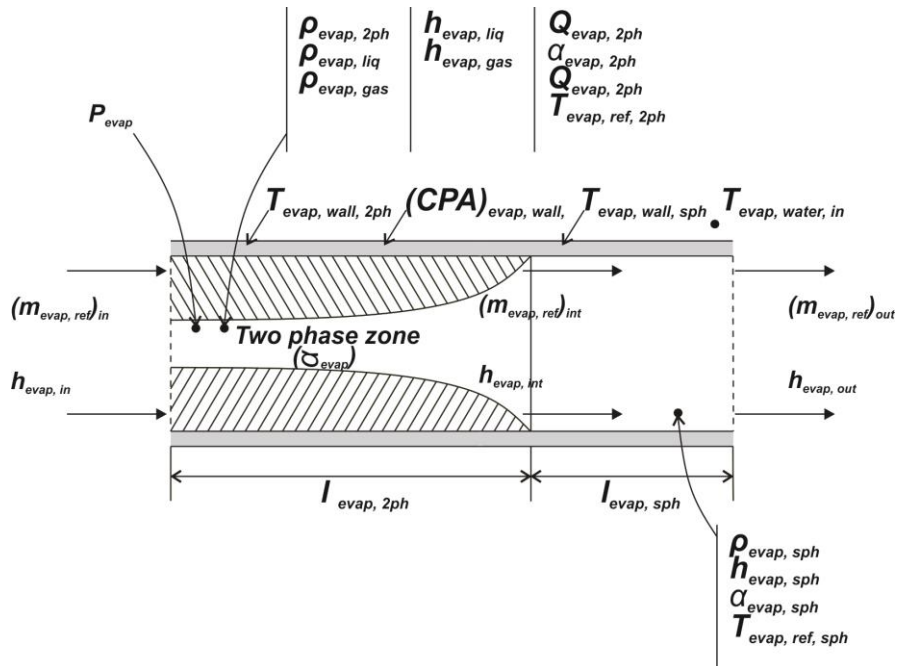


**Figure 4.1** Evaporator model with two-phase and superheat zones

On the other hand, the condenser modelling could be performed similarly to the evaporator but with three area namely, the superheated gas area, the liquid-gas mixture area and the subcool zone.

The condenser model is represented in Fig. 4.2 as follows:

## CHAPTER 4 CONTROL-ORIENTED MODELLING OF THE REFRIGERANT DYNAMICS

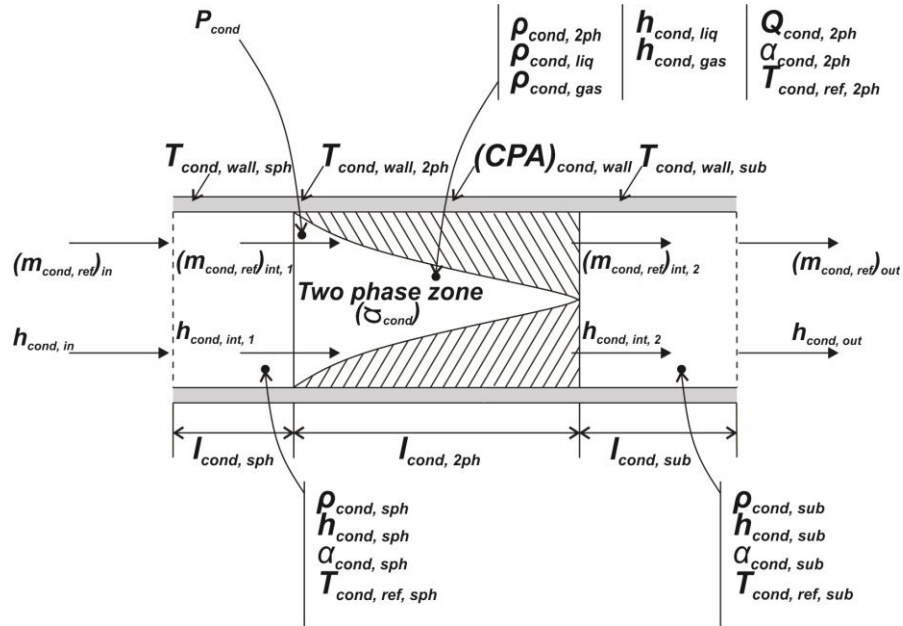


**Figure 4.2** Condenser model with superheat, two-phase and subcool zones

### 4.3.1. Two - phase zone of the evaporator

Using the mean void fraction and the time-invariant principle, the mass conservation along the two-phase area could be written as:

$$\begin{aligned}
 A_{evap} l_{evap,2ph} \frac{d\rho_{evap,2ph}}{dP_{evap}} \frac{dP_{evap}}{dt} + A_{evap} (\rho_{evap,liq} - \rho_{evap,gas}) \frac{dl_{evap,2ph}}{dt} \\
 = (m_{evap,ref})_{in} - (m_{evap,ref})_{int}
 \end{aligned} \tag{4.1}$$

$A_{evap}$	Evaporator surface ( $m^2$ )
$l_{evap,2ph}$	Two-phase length in evaporator ( $m$ )
$\rho_{evap,2ph}$	Density of two-phase refrigerant in evaporator ( $kg\ m^{-3}$ )
$\rho_{evap,liq}$	Density of refrigerant liquid in evaporator ( $kg\ m^{-3}$ )

---

**CHAPTER 4 CONTROL-ORIENTED MODELLING OF THE REFRIGERANT DYNAMICS**


---

$\rho_{evap,gas}$	Density of refrigerant gas in evaporator ( $kg\ m^{-3}$ )
$(m_{evap,ref})_{int}$	Refrigerant mass flow rate at evaporator interface ( $kg\ s^{-1}$ )

where,

$$\rho_{evap,2ph} = \rho_{evap,liq}(1 - \bar{\gamma}_{evap}) + \rho_{evap,gas}\bar{\gamma}_{evap}$$

The energy conservation along the two-phase zone could be expressed as:

$$\begin{aligned}
 & A_{evap}l_{evap,2ph} \left( \frac{d(\rho_{evap,liq}h_{evap,liq})}{dt} (1 - \bar{\gamma}_{evap}) \right. \\
 & \left. + \frac{d(\rho_{evap,gas}h_{evap,gas})}{dt} \bar{\gamma}_{evap} - \frac{dP_{evap}}{dt} \right) \\
 & + A_{evap}(1 - \bar{\gamma}_{evap})(\rho_{evap,liq}h_{evap,liq} \\
 & - \rho_{evap,gas}h_{evap,gas}) \frac{dl_{evap,2ph}}{dt} \\
 & = (m_{evap,ref})_{in} h_{evap,in} - (m_{evap,ref})_{int} h_{evap,int} \\
 & + Q_{evap,2ph}
 \end{aligned} \tag{4.2}$$

$h_{evap,liq}$	Enthalpy of liquid refrigerant in evaporator ( $kJ\ kg^{-1}$ )
$\bar{\gamma}_{evap}$	Evaporator void fraction
$h_{evap,gas}$	Enthalpy of refrigerant gas in evaporator ( $kJ\ kg^{-1}$ )
$h_{evap,in}$	Refrigerant enthalpy at evaporator inlet ( $kJ\ kg^{-1}$ )
$h_{evap,int}$	Refrigerant enthalpy at evaporator interface ( $kJ\ kg^{-1}$ )
$Q_{evap,2ph}$	Heat absorption in evaporator two-phase zone ( $kw$ )

## ***CHAPTER 4 CONTROL-ORIENTED MODELLING OF THE REFRIGERANT DYNAMICS***

where,

$$Q_{evap,2ph} = \alpha_{evap,2ph} \pi d_{evap,in} l_{evap,2ph} (T_{evap,wall,2ph} - T_{evap,ref,2ph})$$

$\alpha_{evap,2ph}$  Heat transfer coefficient in evaporator two-phase zone ( $kw m^{-2} \text{ } ^\circ C^{-1}$ )

$d_{evap,in}$  Evaporator inner diameter ( $m$ )

$T_{evap,wall,2ph}$  Wall temperature in evaporator two-phase zone ( $^\circ C$ )

$T_{evap,water,in}$  Refrigerant temperature in evaporator two-phase zone ( $^\circ C$ )

The wall equation within the two-phase zone could be given as:

$$\begin{aligned} (C\rho A)_{evap,wall} \frac{dT_{evap,wall,2ph}}{dt} \\ = \alpha_{evap,2ph} \pi d_{evap,in} (T_{evap,ref,2ph} - T_{evap,wall,2ph}) \\ + \alpha_{evap,out} \pi d_{evap,out} (T_{evap,water,in} - T_{evap,wall,2ph}) \end{aligned} \quad (4.3)$$

$(C\rho A)_{evap,wall}$  Thermal capacitance at evaporator wall ( $kJ \text{ } ^\circ C^{-1} m^{-1} kg$ )

$\alpha_{evap,out}$  Heat transfer coefficient at evaporator outer surface ( $kw m^{-2} \text{ } ^\circ C^{-1}$ )

$d_{evap,out}$  Evaporator outer diameter ( $m$ )

$T_{evap,water,in}$  Water temperature at evaporator inlet ( $^\circ C$ )

### **4.3.2. Superheat zone of the evaporator**

The mass conservation along the superheat zone could be expressed as:



## **CHAPTER 4 CONTROL-ORIENTED MODELLING OF THE REFRIGERANT DYNAMICS**

$$\begin{aligned}
 A_{evap} l_{evap,sph} \frac{d\rho_{evap,sph}}{dP_{evap}} \frac{dP_{evap}}{dt} + A_{evap} (\rho_{evap,gas} - \rho_{evap,sph}) \frac{dl_{evap,2ph}}{dt} \\
 = (m_{evap,ref})_{int} - (m_{evap,ref})_{out}
 \end{aligned} \tag{4.4}$$

$l_{evap,sph}$  Superheat length in evaporator ( $m$ )

$\rho_{evap,sph}$  Density of superheated refrigerant in evaporator ( $kg\ m^{-3}$ )

The energy conservation along the superheat zone could be expressed as:

$$\begin{aligned}
 A_{evap} l_{evap,sph} \left( \rho_{evap,sph} \frac{dh_{evap,sph}}{dt} - \frac{dP_{evap}}{dt} \right) \\
 = - \left( (m_{evap,ref})_{int} \right. \\
 \left. - \rho_{evap,gas} A_{evap} \frac{dl_{evap,2ph}}{dt} \right) \frac{h_{evap,out} - h_{evap,int}}{2} \\
 - (m_{evap,ref})_{out} \frac{h_{evap,out} - h_{evap,int}}{2} + Q_{evap,sph}
 \end{aligned} \tag{4.5}$$

$h_{evap,sph}$  Enthalpy of superheated refrigerant in evaporator ( $kJ\ kg^{-1}$ )

$h_{evap,out}$  Refrigerant enthalpy at evaporator outlet ( $kJ\ kg^{-1}$ )

$Q_{evap,sph}$  Heat absorption in evaporator superheat zone ( $kw$ )

where,

$$Q_{evap,sph} = \alpha_{evap,sph} \pi d_{evap,in} l_{evap,sph} (T_{evap,wall,sph} - T_{evap,ref,sph})$$

$\alpha_{evap,sph}$  Heat transfer coefficient in evaporator superheat zone ( $kw\ m^{-2} \text{ } ^\circ\text{C}^{-1}$ )

$T_{evap,wall,sph}$  Wall temperature in evaporator superheat zone ( $^\circ\text{C}$ )

## **CHAPTER 4 CONTROL-ORIENTED MODELLING OF THE REFRIGERANT DYNAMICS**

---

$T_{evap,ref,sph}$  Refrigerant temperature in evaporator superheat zone ( $^{\circ}\text{C}$ )

The wall equation within the superheat zone could be expressed as:

$$\begin{aligned}
 (C\rho A)_{evap,wall} & \left( \frac{dT_{evap,wall,sph}}{dt} + \frac{T_{evap,wall,2ph} - T_{evap,wall,sph}}{l_{evap,sph}} \frac{dl_{evap,2ph}}{dt} \right) \\
 & = \alpha_{evap,sph} \pi d_{evap,in} (T_{evap,ref,sph} - T_{evap,wall,sph}) \\
 & + \alpha_{evap,out} \pi d_{evap,out} (T_{evap,water,in} - T_{evap,wall,sph})
 \end{aligned} \tag{4.6}$$

### **4.3.3. Superheat zone of the condenser**

The mass conservation along the superheat zone could be expressed as:

$$\begin{aligned}
 A_{cond} l_{cond,sph} \frac{d\rho_{cond,sph}}{dP_{cond}} \frac{dP_{cond}}{dt} + A_{cond} (\rho_{cond,gas} - \rho_{cond,sph}) \frac{dl_{cond,2ph}}{dt} \\
 = (m_{cond,ref})_{in} - (m_{cond,ref})_{int,1}
 \end{aligned} \tag{4.7}$$

$A_{cond}$  Condenser surface ( $m^2$ )

$l_{cond,sph}$  Superheat length in condenser ( $m$ )

$\rho_{cond,sph}$  Density of superheated refrigerant in condenser ( $kg\ m^{-3}$ )

$(m_{cond,ref})_{int,1}$  Mass flow rate at condenser interface 1 ( $kg\ s^{-1}$ )

The energy conservation along the superheat zone could be expressed as:

## **CHAPTER 4 CONTROL-ORIENTED MODELLING OF THE REFRIGERANT DYNAMICS**

$$\begin{aligned}
 & A_{cond} l_{cond,sph} \left( \rho_{cond,sph} \frac{dh_{cond,sph}}{dt} - \frac{dP_{cond}}{dt} \right) \\
 & = - \left( (m_{cond,ref})_{in} \right. \\
 & \quad \left. - \rho_{cond,gas} A_{cond} \frac{dl_{cond,2ph}}{dt} \right) \frac{h_{cond,int,1} - h_{cond,in}}{2} \\
 & \quad - (m_{cond,ref})_{int,1} \frac{h_{cond,int,1} - h_{cond,in}}{2} + Q_{cond,sph}
 \end{aligned} \tag{4.8}$$

$h_{cond,sph}$  Enthalpy of superheated refrigerant in condenser ( $kJ\ kg^{-1}$ )

$l_{cond,2ph}$  Two-phase length in condenser ( $m$ )

$h_{cond,int,1}$  Refrigerant enthalpy at condenser interface 1 ( $kJ\ kg^{-1}$ )

$Q_{cond,sph}$  Heat absorption in condenser superheat zone ( $kw$ )

where,

$$Q_{cond,sph} = \alpha_{cond,sph} \pi d_{cond,in} l_{cond,sph} (T_{cond,wall,sph} - T_{cond,ref,sph})$$

$\alpha_{cond,sph}$  Heat transfer coefficient in condenser superheat zone ( $kw\ m^{-2}\ ^\circ C^{-1}$ )

$d_{cond,in}$  Condenser inner diameter ( $m$ )

$T_{cond,wall,sph}$  Wall temperature in condenser superheat zone ( $^\circ C$ )

$T_{cond,ref,sph}$  Refrigerant temperature in condenser superheat zone ( $^\circ C$ )

The wall equation within the superheat zone could be expressed as:

## **CHAPTER 4 CONTROL-ORIENTED MODELLING OF THE REFRIGERANT DYNAMICS**

$$\begin{aligned}
 (C\rho A)_{cond,wall} & \left( \frac{dT_{cond,wall,sph}}{dt} + \frac{T_{cond,wall,2ph} - T_{cond,wall,sph}}{l_{cond,sph}} \frac{dl_{cond,2ph}}{dt} \right) \\
 & = \alpha_{cond,sph} \pi d_{cond,in} (T_{cond,ref,sph} - T_{cond,wall,sph}) \\
 & + \alpha_{cond,out} \pi d_{cond,out} (T_{cond,water,in} - T_{cond,wall,sph})
 \end{aligned} \tag{4.9}$$

$(C\rho A)_{cond,wall}$	Thermal capacitance at condenser wall ( $kJ\ ^\circ C^{-1}\ m^{-1}\ kg$ )
$\alpha_{cond,out}$	Heat transfer coefficient at condenser outer surface ( $kw\ m^{-2}\ ^\circ C^{-1}$ )
$d_{cond,out}$	Condenser outer diameter ( $m$ )
$T_{cond,water,in}$	Water temperature at condenser inlet ( $^\circ C$ )

### **4.3.4. Two - phase zone of the condenser**

Applying the mean void fraction and the time-invariant principle, the mass conservation along the two-phase area could be written as follows:

$$\begin{aligned}
 A_{cond} l_{cond,2ph} \frac{d\rho_{cond,2ph}}{dP_{cond}} \frac{dP_{cond}}{dt} + A_{cond} (\rho_{cond,liq} - \rho_{cond,gas}) \frac{dl_{cond,2ph}}{dt} \\
 = (m_{cond,ref})_{int,1} - (m_{cond,ref})_{int,2}
 \end{aligned} \tag{4.10}$$

$\rho_{cond,2ph}$	Density of two-phase refrigerant in condenser ( $kg\ m^{-3}$ )
$\rho_{cond,liq}$	Density of refrigerant liquid in condenser ( $kg\ m^{-3}$ )
$(m_{cond,ref})_{int,2}$	Refrigerant mass flow rate at condenser interface 2 ( $kg\ s^{-1}$ )

where,

$$\rho_{cond,2ph} = \rho_{cond,liq} (1 - \bar{V}_{cond}) + \rho_{cond,gas} \bar{V}_{cond}$$

## **CHAPTER 4 CONTROL-ORIENTED MODELLING OF THE REFRIGERANT DYNAMICS**

$\bar{v}_{cond}$  Condenser void fraction

The energy conservation along the two-phase zone could be expressed as:

$$\begin{aligned}
 & A_{cond} l_{cond,2ph} \left( \frac{d(\rho_{cond,liq} h_{cond,liq})}{dt} (1 - \bar{v}_{cond}) \right. \\
 & \quad \left. + \frac{d(\rho_{cond,gas} h_{cond,gas})}{dt} \bar{v}_{cond} - \frac{dP_{cond}}{dt} \right) \\
 & \quad + A_{cond} (1 - \bar{v}_{cond}) (\rho_{cond,liq} h_{cond,liq} \\
 & \quad - \rho_{cond,gas} h_{cond,gas}) \frac{dl_{cond,2ph}}{dt} \\
 & = (m_{cond,ref})_{int,1} h_{cond,int,1} - (m_{cond,ref})_{int,2} h_{cond,int,2} \\
 & \quad + Q_{cond,2ph}
 \end{aligned} \tag{4.11}$$

$h_{cond,liq}$  Enthalpy of liquid refrigerant in condenser ( $kJ\ kg^{-1}$ )

$h_{cond,gas}$  Enthalpy of refrigerant gas in condenser ( $kJ\ kg^{-1}$ )

$h_{cond,int,2}$  Refrigerant enthalpy at condenser interface 2 ( $kJ\ kg^{-1}$ )

$Q_{cond,2ph}$  Heat absorption in condenser two-phase zone ( $kw$ )

where,

$$Q_{cond,2ph} = \alpha_{cond,2ph} \pi d_{cond,in} l_{cond,2ph} (T_{cond,wall,2ph} - T_{cond,ref,2ph})$$

$\alpha_{cond,2ph}$  Heat transfer coefficient in condenser two-phase zone ( $kw\ m^{-2}\ ^\circ C^{-1}$ )

$T_{cond,wall,2ph}$  Wall temperature in condenser two-phase zone ( $^\circ C$ )

$T_{cond,ref,2ph}$  Refrigerant temperature in condenser two-phase zone ( $^\circ C$ )

## **CHAPTER 4 CONTROL-ORIENTED MODELLING OF THE REFRIGERANT DYNAMICS**

The wall equation within the two-phase zone could be given as:

$$\begin{aligned}
 (C\rho A)_{cond,wall} \frac{dT_{cond,wall,2ph}}{dt} &= \alpha_{cond,2ph} \pi d_{cond,in} (T_{cond,ref,2ph} - T_{cond,wall,2ph}) \\
 &+ \alpha_{cond,out} \pi d_{cond,out} (T_{cond,water,in} - T_{cond,wall,2ph})
 \end{aligned} \tag{4.12}$$

### **4.3.5. Subcool zone of the condenser**

The mass conservation within the subcool zone could be expressed as:

$$\begin{aligned}
 A_{cond} l_{cond,sub} \frac{d\rho_{cond,sub}}{dP_{cond}} \frac{dP_{cond}}{dt} + A_{cond} (\rho_{cond,sub} - \rho_{cond,liq}) \frac{dl_{cond,2ph}}{dt} &= (m_{cond,ref})_{int,2} - (m_{cond,ref})_{out}
 \end{aligned} \tag{4.13}$$

$l_{cond,sub}$  Subcool length in condenser ( $m$ )

$\rho_{cond,sub}$  Density of subcooled refrigerant in condenser ( $kg\ m^{-3}$ )

The energy conservation along the subcool zone could be expressed as:

$$\begin{aligned}
 A_{cond} l_{cond,sub} \left( \rho_{cond,sub} \frac{dh_{cond,sub}}{dt} - \frac{dP_{cond}}{dt} \right) &= - \left( (m_{cond,ref})_{int,2} \right. \\
 &- \rho_{cond,liq} A_{cond} \frac{dl_{cond,sub}}{dt} \left. \right) \frac{h_{cond,out} - h_{cond,int,2}}{2} \\
 &- (m_{cond,ref})_{int,2} \frac{h_{cond,out} - h_{cond,int,2}}{2} + Q_{cond,sub}
 \end{aligned} \tag{4.14}$$

## **CHAPTER 4 CONTROL-ORIENTED MODELLING OF THE REFRIGERANT DYNAMICS**

---

$h_{cond,sub}$             Enthalpy of subcooled refrigerant in condenser ( $kJ\ kg^{-1}$ )

$Q_{cond,sub}$             Heat absorption in condenser subcool zone ( $kw$ )

where,

$$Q_{cond,sub} = \alpha_{cond,sub} \pi d_{cond,in} l_{cond,sub} (T_{cond,wall,sub} - T_{cond,ref,sub})$$

$\alpha_{cond,sub}$             Heat transfer coefficient in condenser subcooled zone ( $kw\ m^{-2} \circ C^{-1}$ )

$T_{cond,wall,sub}$         Wall temperature in condenser subcooled zone ( $\circ C$ )

$T_{cond,ref,sub}$         Refrigerant temperature in condenser subcooled zone ( $\circ C$ )

The wall equation within the subcool zone could be expressed as:

$$\begin{aligned} (C\rho A)_{cond,wall} & \left( \frac{dT_{cond,wall,sub}}{dt} + \frac{T_{cond,wall,2ph} - T_{cond,wall,sub}}{l_{cond,sph}} \frac{dl_{cond,2ph}}{dt} \right) \\ & = \alpha_{cond,sub} \pi d_{cond,in} (T_{cond,ref,sub} - T_{cond,wall,sub}) \\ & + \alpha_{cond,out} \pi d_{cond,out} (T_{cond,water,in} - T_{cond,wall,sub}) \end{aligned} \quad (4.15)$$

### **4.4. STATE SPACE FORMULATION ON THE VC SYSTEM**

The state space formulation could be expressed as:

$$(D\dot{X})_1 = (F(X, U))_1 + (G(Z))_1 \quad (4.16)$$

The decoupling matrix  $(D)_1$  could be defined as:

## CHAPTER 4 CONTROL-ORIENTED MODELLING OF THE REFRIGERANT DYNAMICS

$$(D)_1 = \begin{bmatrix} D_{11} & D_{12} & 0 & 0 & 0 & 0 & 0 & 0 & 0 & 0 & 0 & 0 \\ 0 & 0 & D_{23} & 0 & 0 & 0 & 0 & 0 & 0 & 0 & 0 & 0 \\ D_{31} & D_{32} & 0 & D_{34} & 0 & 0 & 0 & 0 & 0 & 0 & 0 & 0 \\ 0 & D_{42} & 0 & 0 & D_{45} & 0 & 0 & 0 & 0 & 0 & 0 & 0 \\ D_{51} & D_{52} & 0 & 0 & 0 & 0 & 0 & 0 & 0 & 0 & 0 & 0 \\ 0 & 0 & 0 & 0 & 0 & D_{66} & D_{67} & D_{68} & 0 & 0 & 0 & 0 \\ 0 & 0 & 0 & 0 & 0 & 0 & D_{77} & 0 & D_{79} & 0 & 0 & 0 \\ 0 & 0 & 0 & 0 & 0 & D_{86} & D_{87} & 0 & 0 & 0 & 0 & 0 \\ 0 & 0 & 0 & 0 & 0 & 0 & 0 & 0 & 0 & D_{910} & 0 & 0 \\ 0 & 0 & 0 & 0 & 0 & D_{106} & D_{107} & 0 & 0 & 0 & D_{1011} & 0 \\ 0 & 0 & 0 & 0 & 0 & 0 & D_{117} & 0 & 0 & 0 & 0 & D_{1112} \\ 0 & 0 & 0 & 0 & 0 & D_{126} & D_{126} & 0 & 0 & 0 & 0 & 0 \end{bmatrix} \quad (4.17)$$

The components of  $(D)_1$  are given in Table 4.1 as follows:

**Table 4.1** Components of the  $(D)_1$  Matrix

$D_{11} = A_{evap} l_{evap,2ph} \left( \frac{d(\rho_{evap,liq} h_{evap,liq})}{dP_{evap}} (1 - \bar{\gamma}_{evap}) + \frac{d(\rho_{evap,gas} h_{evap,gas})}{dP_{evap}} \bar{\gamma}_{evap} - 1 \right)$
$D_{12} = A_{evap} (1 - \bar{\gamma}_{evap}) (\rho_{evap,liq} h_{evap,liq} - \rho_{evap,gas} h_{evap,gas})$
$D_{23} = (C\rho A)_{evap,wall}$
$D_{31} = -A_{evap} l_{evap,sph}$
$D_{32} = -\rho_{evap,gas} A_{evap} \frac{h_{evap,out} - h_{evap,int}}{2}$
$D_{34} = A_{evap} l_{evap,sph} \rho_{evap,sph}$
$D_{42} = (C\rho A)_{evap,wall} \frac{T_{evap,wall,2ph} - T_{evap,wall,sph}}{l_{evap,sph}}$
$D_{45} = (C\rho A)_{evap,wall}$
$D_{51} = A_{evap} l_{evap,2ph} \left( \frac{d\rho_{evap,2ph}}{dP_{evap}} + \frac{d\rho_{evap,sph}}{dP_{evap}} \right)$
$D_{52} = A_{evap} (\rho_{evap,liq} - \rho_{evap,sph})$
$D_{66} = -A_{cond} l_{cond,sph}$
$D_{67} = -\rho_{cond,gas} A_{cond} \frac{h_{cond,int,1} - h_{cond,in}}{2}$
$D_{68} = A_{cond} l_{cond,sph} \rho_{cond,sph}$
$D_{77} = (C\rho A)_{cond,wall} \frac{T_{cond,wall,2ph} - T_{cond,wall,sph}}{l_{cond,sph}}$
$D_{79} = (C\rho A)_{cond,wall}$



## CHAPTER 4 CONTROL-ORIENTED MODELLING OF THE REFRIGERANT DYNAMICS

$D_{86} = A_{cond} l_{cond,2ph} \left( \frac{d(\rho_{cond,liq} h_{cond,liq})}{dP_{cond}} (1 - \bar{\gamma}_{cond}) + \frac{d(\rho_{cond,gas} h_{cond,gas})}{dP_{cond}} \bar{\gamma}_{cond} - 1 \right)$
$D_{87} = A_{cond} (1 - \bar{\gamma}_{cond}) (\rho_{cond,liq} h_{cond,liq} - \rho_{cond,gas} h_{cond,gas})$
$D_{910} = (C\rho A)_{cond,wall}$
$D_{106} = -A_{cond} l_{cond,sub}$
$D_{107} = -\rho_{cond,liq} A_{cond} \frac{h_{cond,out} - h_{cond,int,2}}{2}$
$D_{1011} = A_{cond} l_{cond,sub} \rho_{cond,sub}$
$D_{117} = (C\rho A)_{cond,wall} \frac{T_{cond,wall,2ph} - T_{cond,wall,sub}}{l_{cond,sph}}$
$D_{1112} = (C\rho A)_{cond,wall}$
$D_{126} = A_{cond} l_{cond,sph} \left( \frac{d\rho_{cond,sph}}{dP_{cond}} + \frac{d\rho_{cond,2ph}}{dP_{cond}} + \frac{d\rho_{cond,sub}}{dP_{cond}} \right)$
$D_{127} = A_{cond} (\rho_{cond,sub} - \rho_{cond,sph})$

The function  $(F)_1$  could be defined as:

$$(F)_1 = [F_1 \ F_2 \ F_3 \ F_4 \ F_5 \ F_6 \ F_7 \ F_8 \ F_9 \ F_{10} \ F_{11} \ F_{12}]^T \quad (4.18)$$

The components of  $(F)_1$  are given in Table 4.2 as:

**Table 4.2** Components of the  $(F)_1$  matrix

$F_1 = (m_{evap,ref})_{in} h_{evap,in} - (m_{evap,ref})_{int} h_{evap,int}$
$F_2 = \alpha_{evap,2ph} \pi d_{evap,in} (T_{evap,ref,2ph} - T_{evap,wall,2ph}) + \alpha_{evap,out} \pi d_{evap,out} (T_{water,in} - T_{evap,wall,2ph})$
$F_3 = - \left( (m_{evap,ref})_{int} + (m_{evap,ref})_{out} \right) \frac{h_{evap,out} - h_{evap,int}}{2}$
$F_4 = \alpha_{evap,sph} \pi d_{evap,in} (T_{evap,ref,sph} - T_{evap,wall,sph}) + \alpha_{evap,out} \pi d_{evap,out} (T_{water,in} - T_{evap,wall,sph})$
$F_5 = (m_{evap,ref})_{in} - (m_{evap,ref})_{out}$
$F_6 = - \left( (m_{cond,ref})_{in} + (m_{cond,ref})_{int,1} \right) \frac{h_{cond,int,1} - h_{cond,in}}{2}$
$F_7 = \alpha_{cond,sph} \pi d_{cond,in} (T_{cond,ref,sph} - T_{cond,wall,sph}) + \alpha_{cond,out} \pi d_{cond,out} (T_{water,in} - T_{cond,wall,sph})$
$F_8 = (m_{cond,ref})_{int,1} h_{cond,int,1} - (m_{cond,ref})_{int,2} h_{cond,int,2}$
$F_9 = \alpha_{cond,2ph} \pi d_{cond,in} (T_{cond,ref,2ph} - T_{cond,wall,2ph}) + \alpha_{cond,out} \pi d_{cond,out} (T_{water,in} - T_{cond,wall,2ph})$

## **CHAPTER 4 CONTROL-ORIENTED MODELLING OF THE REFRIGERANT DYNAMICS**

$F_{10} = - \left( (m_{cond,ref})_{int,2} + (m_{cond,ref})_{int,2} \right) \frac{h_{cond,out} - h_{cond,int,2}}{2}$
$F_{11} = \alpha_{cond,sph} \pi d_{cond,in} (T_{cond,ref,sub} - T_{cond,wall,sub}) + \alpha_{cond,out} \pi d_{cond,out} (T_{water,in} - T_{cond,wall,sub})$
$F_{12} = (m_{cond,ref})_{in} - (m_{cond,ref})_{out}$

The definition of the state variable  $(X)_1$  is as follows:

$$(X)_1 = \begin{bmatrix} P_{evap} \\ l_{evap,2ph} \\ T_{evap,wall,2ph} \\ h_{evap,sph} \\ T_{evap,wall,sph} \\ P_{cond} \\ l_{cond,2ph} \\ h_{cond,sph} \\ T_{cond,wall,sph} \\ T_{cond,wall,2ph} \\ h_{cond,sub} \\ T_{cond,wall,sub} \end{bmatrix} \quad (4.19)$$

The input  $(U)_1$  could be defined as:

$$(U)_1 = \begin{bmatrix} C_{txv} \\ RPM_{comp} \end{bmatrix} \quad (4.20)$$

The function  $(G)_1$  could be defined as:

---

**CHAPTER 4 CONTROL-ORIENTED MODELLING OF THE REFRIGERANT DYNAMICS**


---

$$(G)_1 = \begin{bmatrix} Q_{evap,2ph} \\ 0 \\ Q_{evap,sph} \\ 0 \\ 0 \\ Q_{cond,sph} \\ 0 \\ Q_{cond,2ph} \\ 0 \\ Q_{cond,sub} \\ 0 \\ 0 \end{bmatrix} \quad (4.21)$$

The disturbance  $(Z)_1$  could be defined as:

$$(Z)_1 = [\alpha_{evap,2ph} \quad \alpha_{evap,sph} \quad \alpha_{cond,sph} \quad \alpha_{cond,2ph} \quad \alpha_{cond,sub}]^T \quad (4.22)$$

#### 4.5. MPC IMPLEMENTATION ON THE VC SYSTEM

The nonlinear system could be linearized around a steady operating point  $(X_0, U_0)$  using Taylor first order approximation whilst a close loop MPC could be adopted to reduce the deviations.

$$\begin{cases} (X(k+1))_1 = (AX(k))_1 + (B\Delta U(k))_1 \\ (Y(k))_1 = (CX(k))_1 \end{cases} \quad (4.23)$$

where,

$$(A)_1 = \begin{bmatrix} A_d & 0_9^T \\ CA_d & I_{3 \times 3} \end{bmatrix} \text{ is the state matrix}$$

$$(B)_1 = \begin{bmatrix} B_d \\ CB_d \end{bmatrix} \text{ is the input matrix}$$

## CHAPTER 4 CONTROL-ORIENTED MODELLING OF THE REFRIGERANT DYNAMICS

$$(C)_1 = \begin{bmatrix} 1 & 0 & 0 & 0 & 0 & 0 & 0 & 0 & 0 & 0 & 0 & 0 \\ 0 & 0 & 0 & 1 & 0 & 0 & 0 & 0 & 0 & 0 & 0 & 0 \\ 0 & 0 & 0 & 0 & 0 & 1 & 0 & 0 & 0 & 0 & 0 & 0 \end{bmatrix} \text{ is the output matrix}$$

With,

$$A_d = \left. \frac{\partial F}{\partial X} \right|_{X=X_0, U=U_0} \quad \text{and} \quad B_d = \left. \frac{\partial F}{\partial U} \right|_{X=X_0, U=U_0}$$

The following compact form of the predicted output vector could be written:

$$(Y(k_i))_1 = (FX(k_i))_1 + (\Phi \Delta U(k_i))_1 \quad (4.24)$$

where,

$$(F)_1 = [CA \quad CA^2 \quad CA^3 \quad \dots \quad CA^{N_p}]^T \quad (4.25)$$

And,

$$(\Phi)_1 = \begin{bmatrix} CB & 0 & 0 & \dots & 0 \\ CAB & CB & 0 & \dots & 0 \\ CA^2B & CAB & CB & \dots & 0 \\ \vdots & \vdots & \vdots & \vdots & \vdots \\ CA^{N_p-1}B & CA^{N_p-2}B & CA^{N_p-2}B & \dots & CA^{N_p-N_c}B \end{bmatrix} \quad (4.26)$$

Using the control horizon  $N_c = 2$  and the prediction horizon  $N_p = 24$ , the set point information could be expressed in the data vector as:

$$(R_s)_1 = [1 \quad 1 \quad 1]^T (r(k_i))_1 \quad (4.27)$$

with,

$\bar{R}_s = [1 \quad 1 \quad 1]^T$  and  $r(k_i)$  as the step value of the outputs.

## ***CHAPTER 4 CONTROL-ORIENTED MODELLING OF THE REFRIGERANT DYNAMICS***

The objective with MPC is to reduce errors between the reference values and output feedbacks.

This is expressed as a cost function to find out the optimum inputs, which could be defined as:

$$\begin{aligned}
 (J)_1 = \sum_{i=1}^{12} & \left[ ((R_s)_1 - (Y(k_i))_1)^T ((R_s)_1 - (Y(k_i))_1) \right. \\
 & \left. + (\Delta U(k_i))_1^T \bar{R} (\Delta U(k_i))_1 \right]
 \end{aligned} \tag{4.28}$$

Whilst the second term takes into consideration control action weighting for large or small error, the first term is used for minimizing error.

Eq. (4.24) inserted into (4.28) gives:

$$\begin{aligned}
 (J)_1 = \sum_{i=1}^{12} & \left[ (R_s - FX(k_i) - \Phi \Delta U(k_i))_1^T (R_s - FX(k_i) - \Phi \Delta U(k_i))_1 \right. \\
 & \left. + (\Delta U(k_i))_1^T \bar{R} (\Delta U(k_i))_1 \right]
 \end{aligned} \tag{4.29}$$

The cost function's first derivative could be written as:

$$\left( \frac{\partial J}{\partial \Delta U(k_i)} \right)_1 = \sum_{i=1}^{12} \left[ (R_s - FX(k_i) - \Phi \Delta U(k_i))_1^T (-\Phi) + (\Delta U(k_i))_1^T \bar{R} \right] \tag{4.30}$$

When the derivative is set to zero, the following results:

$$(\Phi^T \Phi + \bar{R}) \sum_{i=1}^{12} (\Delta U(k_i))_1^T = \Phi \sum_{i=1}^{12} (R_s - FX(k_i))_1^T \tag{4.31}$$

Therefore,

**CHAPTER 4 CONTROL-ORIENTED MODELLING OF THE REFRIGERANT DYNAMICS**

$$\sum_{i=1}^{12} (\Delta U(k_i))_1 = ((\Phi^T \Phi + \bar{R})^{-1} \Phi^T)_1 \sum_{i=1}^{12} (\bar{R}_s r(k_i) - FX(k_i))_1 \quad (4.32)$$

**4.6. RESULTS AND DISCUSSION**

Simulink was used to test the MPC using the MPC toolbox. A Simulink control design framework was created by first linearizing the control-oriented model around a steady operating point in Matlab. The MPC toolbox and the linear model were used to evaluate performance. The computed variables in Simulink are presented in Fig. 4.3 as follows:

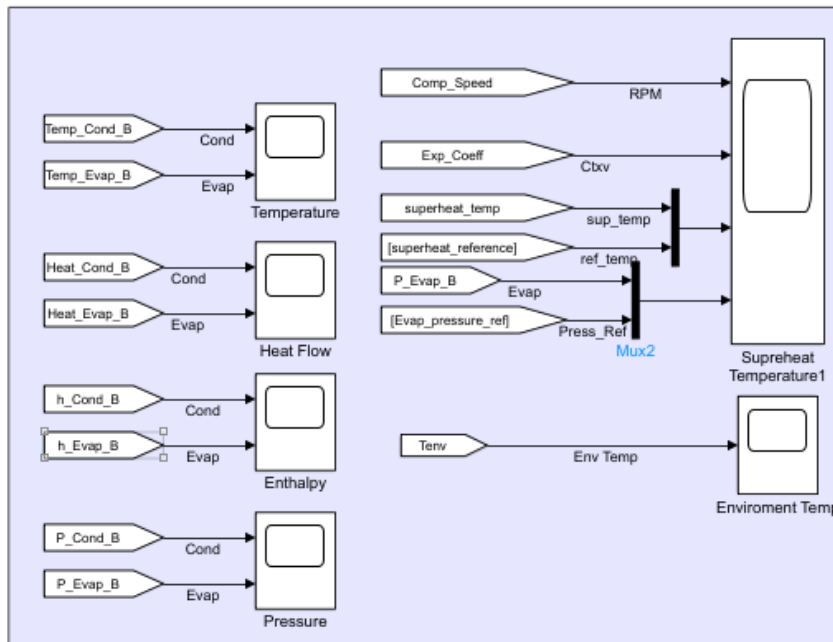


**Figure 4.3** *Computed variables on Simulink*

Two inputs were adopted namely, the compressor speed and the expansion valve opening to control two outputs simultaneously namely the superheat and evaporator pressure (capacity control). Fig. 4.4 describes the MPC adopted to compute the optimal inputs with measured output feedbacks.

**CHAPTER 4 CONTROL-ORIENTED MODELLING OF THE REFRIGERANT DYNAMICS**

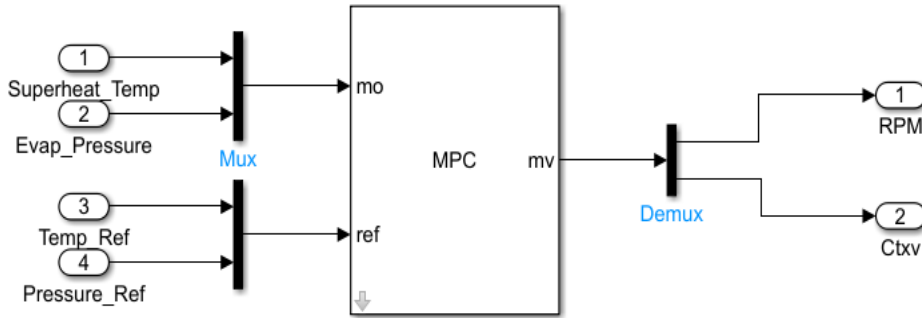


**Figure 4.4** MPC model

The time step was 30 s with the entire simulation lasting 3000 s. Fig. 4.5 summarized the Simulink models adopted for the expansion valve (Fig. 4.5(a)), compressor (Fig. 4.5(b)), evaporator (Fig. 4.5(c)), and condenser (Fig. 4.5(d)).

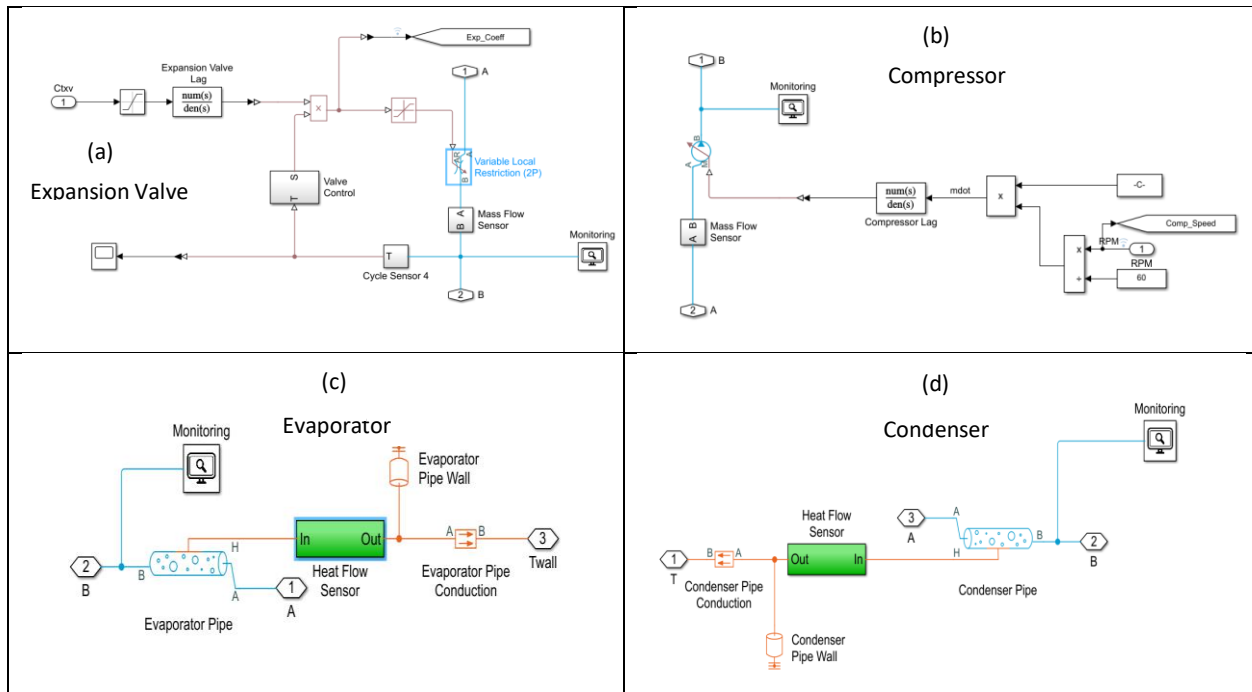


**Figure 4.5** Simulink models of the VC components

(a) Expansion valve. (b) Compressor. (c) Evaporator. (d) Condenser.

## ***CHAPTER 4 CONTROL-ORIENTED MODELLING OF THE REFRIGERANT DYNAMICS***

The expansion valve coefficient and the mass flow rate across the expansion valve were carefully monitored (Fig. 4.5(a)) and so were the compressor speed and the mass flow rate across the compressor (Fig. 4.5(b)). The refrigerant conditions, the wall temperature and the heat flux were also monitored through the evaporator model (Fig. 4.5(c)) and the condenser model (Fig. 4.5(d)). The disturbances affecting the evaporator's outputs namely the variation of the environment temperature (Fig. 4.6(a)) and the absorbed heat (Fig. 4.6(b)) are measured then plotted in Fig. 4.6 along with the mass flow rate responses across the expansion valve (Fig. 4.6(c)) and compressor (Fig. 4.6(d)).

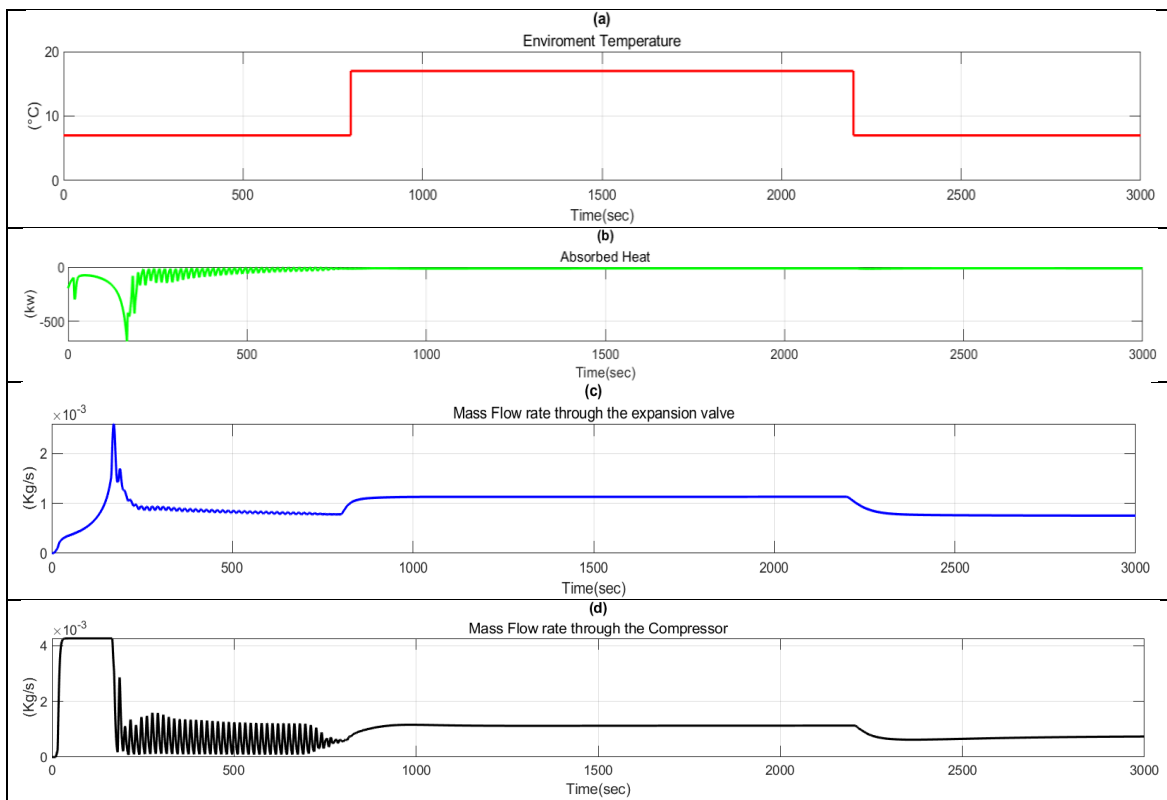


**Figure 4.6** *System responses to disturbances*

*(a) Environment temperature. (b) Absorbed heat. (c) Mass flow rate through the expansion valve.*

*(d) Mass flow rate through the compressor.*



## ***CHAPTER 4 CONTROL-ORIENTED MODELLING OF THE REFRIGERANT DYNAMICS***

Temperature, heat, enthalpy and pressure across the evaporator were measured during the entire simulation. The initial condition for the environment temperature was at 8°C with and the simulation was initiated when the system was turned on. The performance of the MPC controllers was tested using more than 40 parameters. Some parameters such as the geometrical parameters (Table 4.3) were identical to the experiment of [234]. The physical properties of the refrigerant were estimated around a steady operating point using empirical equations and thermodynamic tables. The steady operating point adopted for linearization was found from the experiment of [234] where for cooling operation, superheat is 4°C and evaporator pressure is 3.35 bar.

The key parameters adopted for performance evaluation of the control system are listed in Table 4.3 as follows:

**Table 4.3** *Integrated parameters*

Natural convection	$20 \text{ kw m}^{-2}\text{°C}^{-1}$	Evaporator length	$3 \text{ m}$
Initial pressure	$3.0 \text{ bar}$	Fin convection	$150 \text{ kw m}^{-2}\text{°C}^{-1}$
Initial quality	5%	Pipe diameter	$0.01 \text{ m}$
Time constant	20	Pipe thickness	$0.0005 \text{ m}$
Displacement volume	0.004	Internal surface area	$4.5 \text{ m}^2$
Volumetric efficiency	0.8	External area	$6 \text{ m}^2$
Min throat area	$0.1 \text{ mm}^2$	Foam thickness	$0.03 \text{ m}$
Max throat area	$1.5 \text{ mm}^2$	Copper density	$8940 \text{ kg m}^{-3}$
Min throat temperature	$-23.5\text{°C}$	Copper specific heat	$390 \text{ kJ kg}^{-1}\text{°C}^{-1}$
Max throat temperature	$6.5\text{°C}$	Copper conductivity	$400 \text{ kw m}^{-1}\text{°C}^{-1}$
Condenser length	$3 \text{ m}$	Foam conductivity	$0.03 \text{ kw m}^{-1}\text{°C}^{-1}$

The MPC performance was evaluated following the disturbance rejection criterion (Fig. 4.6) with the refrigerant flow rates through the expansion valve and compressor adjusting to the disturbances and the set point tracking criterion (Fig. 4.7) with MPC tracking the reference points of the superheat and evaporator pressure.

## ***CHAPTER 4 CONTROL-ORIENTED MODELLING OF THE REFRIGERANT DYNAMICS***

---

As the temperature of the environment rose and more heat was absorbed, the refrigerant flow rate into the expansion valve and the compressor increased.

As the environment temperature, varied from 8°C to 18°C from  $t=750$  s to  $t=2250$  s (Fig. 4.6(a)) one could observe the mass flow rates through the expansion valve (Fig. 4.6(c)) and the compressor (Fig. 4.6(d)) varied simultaneously from  $0.008 \text{ kg s}^{-1}$  to  $0.011 \text{ kg s}^{-1}$ .

Similarly, as heat is absorbed through the evaporator (Fig. 4.6(b)) one could observe a simultaneous variation of the mass flow rates through the expansion valve (Fig. 4.6(c)) to a peak of  $0.025 \text{ kg s}^{-1}$  and the compressor to a value of  $0.041 \text{ kg s}^{-1}$  (Fig. 4.6(d)). Mass flow rates through the expansion valve and the compressor adjust simultaneously to overcome sudden disturbances namely environment temperature (Fig. 4.6(a)) and absorbed heat through the evaporator (Fig. 4.6(b)).

**CHAPTER 4 CONTROL-ORIENTED MODELLING OF THE REFRIGERANT DYNAMICS**

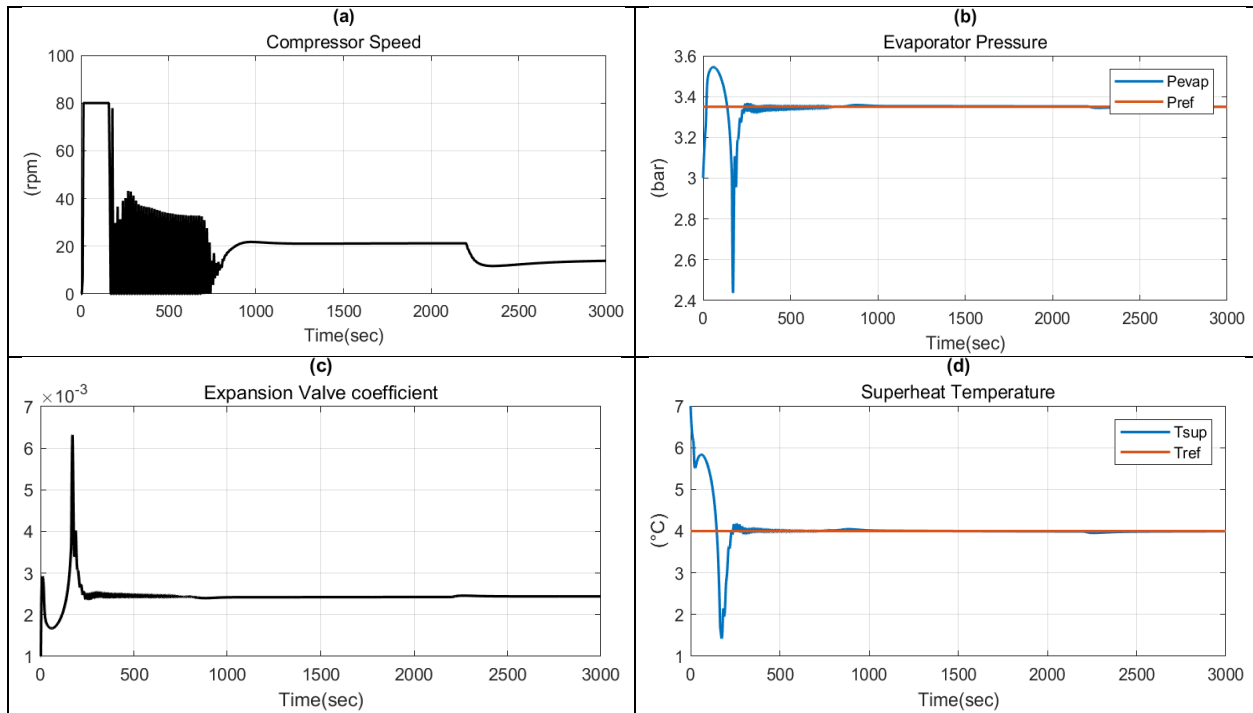


**Figure 4.7** Coupled reference tracking

*(a) Compressor speed. (b) Evaporator pressure. (c) Expansion valve coefficient.*

*(d) Superheat temperature.*

Mass flow rate variations through the expansion valve (Fig. 4.6(c)) and compressor (Fig. 4.6(d)) due to sudden environment temperature (Fig. 4.6(a)) and heat absorbed (Fig. 4.6(b)) changes make the compressor speed (Fig. 4.6(a)) and expansion valve (Fig. 4.6(c)) vary simultaneously to track the reference points of the evaporator pressure (Fig. 4.7(b)) and superheat (Fig. 4.7(d)).

The mass flow rate variations through the expansion valve (Fig. 4.6(c)) and the compressor (Fig. 4.6(d)) due to the variation of the environment temperature (Fig. 4.6(a)) did not have significant effect on the heat absorbed (Fig. 4.6(b)) from 200s onward. This could be explained by the fact that the sudden change in environment temperature of by 10°C (Fig. 4.6(a)) created a slow response

## ***CHAPTER 4 CONTROL-ORIENTED MODELLING OF THE REFRIGERANT DYNAMICS***

---

of the heat absorbed curve (Fig. 4.6(b)). Although not attempted in this work, this numerical issue could be overcome by adopting a ramp rate of temperature instead of a step change in Fig. 4.6(a).

Simultaneous superheat and capacity (or evaporator pressure) control using MPC enhances the system performance as the refrigerant flow rate adjusts continuously to track the reference points through adequate control of the compressor speed and the expansion valve opening. Valve opening and compressor speed rebalance the refrigerant temperature and charge in the system to enhance the VC system's performance.

The control-oriented model was established using component equations similar to [231, 261] however, the refrigerant's dynamics through the heat exchangers were carefully analyzed by considering the two-phase and superheat zones within the evaporator on one hand whilst considering the superheat, two-phase and subcool zone within the condenser on the other hand. The HTC's within the evaporator and condenser were determined with the correlation of [206] within the superheat and subcool zones whilst the correlation of [207] was adopted within the two-phase zones. The water's HTC was determined using Colburn J-factor.

The tables of properties for parameters and correlations created issues encountered while computing HTC's as they varied at each time step with varying enthalpy, pressure and flow rate. The numerical discontinuity was addressed using integrated smooth functions enabling fast output tracking. The refrigerant properties were defined from existing R-134a property tables and integrated to the Matlab code used with the Simulink toolbox which was made of 4 interconnected subsystems namely, the VC system, the MPC system, the reference system, and the environment.

## ***CHAPTER 4 CONTROL-ORIENTED MODELLING OF THE REFRIGERANT DYNAMICS***

---

The control objective was to control simultaneously superheat and evaporator pressure using two manipulated control variables namely compressor speed and expansion valve opening. The control system was therefore defined with two inputs and two outputs. The nonlinear control-oriented model was first linearized around a steady state point carefully selected using experiments. MPC was then adopted to control superheat and evaporator pressure with optimal compressor speed and expansion valve opening. MPC received output feedback values namely superheat and evaporator pressure along with their reference values to calculate optimal compressor speed and expansion valve coefficient.

Environment temperature and absorbed heat were adopted as disturbances to check the controller robustness. Therefore, the effect of varying environment temperature and absorbed heat on superheat and evaporator pressure's feedbacks were tested on the MPC. To determine the optimal expansion valve coefficient and compressor speed using a constraint optimizer with measured superheat and evaporator pressure feedbacks, the formulation of the cost function was adopted. The difference between measured feedbacks and reference values defined the error tracking within the prediction horizon whilst the difference between the current and former control inputs defined the inputs' variation within the control horizon.

Scaling factors with nominal values were adopted to predict superheat and evaporator pressure with consistent scale avoiding therefore scaling related issues. Only the first element of the computed input vectors was adopted for actuation at each time step to avoid instability.

Measured state variables were repeatedly updated within the prediction horizon at each time step to compute the optimal input vectors until reaching the reference values.

## ***CHAPTER 4 CONTROL-ORIENTED MODELLING OF THE REFRIGERANT DYNAMICS***

---

The dynamic formulation of the VC system (4.16) led to 12 state variables but only the feedbacks of the evaporator's pressure and superheat were measured by the MPC. Refrigerant conditions such as temperature, heat, enthalpy and pressure within the evaporator and condenser were also measured in Simulink (Fig. 4.3) and could be adopted for other control purposes such as controlling the condensing pressure and subcooling. In this work, MPC was only adopted to compute optimal compressor speed and expansion valve opening to track superheat and evaporator pressure's reference values considering the coupling effects and the disturbances.

Normalized internal energy from the refrigerant p-h chart was adopted for evaluation of the fluid characteristics during the simulation so that the refrigerant temperature could be determined knowing its pressure and internal energy. The control objective in Fig. 4.7 is to track the reference values of 4°C for superheat (Fig. 4.7(b)) and 3.35 bar for evaporator pressure (Fig. 4.7(d)). Reference tracking is made using optimal compressor speed (Fig. 4.7(a)) and expansion valve coefficient (Fig. 4.7(c)) during the entire simulation started with the initial environment temperature and heat absorbed respectively at 8°C (Fig. 4.6(a)) and 0 kw (Fig. 4.6(b)).

At  $t=200$  s heat is absorbed (Fig. 4.6(b)) and the refrigerant mass flow rate through the expansion valve (Fig. 4.6(c)) and the compressor (Fig. 4.6(d)) automatically increased to allow more refrigerant to circulate through the evaporator tubes so that heat could be absorbed rapidly preventing therefore the output responses from hunting making the MPC robust to sudden disturbances.

With the disturbances, the refrigerant flow rate variation into the expansion valve (Fig. 4.6(c)) and the compressor (Fig. 4.6(d)) are respectively linked to the expansion valve opening (Fig. 4.7(c))

## ***CHAPTER 4 CONTROL-ORIENTED MODELLING OF THE REFRIGERANT DYNAMICS***

---

and the compressor speed (Fig. 4.7(a)) therefore, disturbance rejection could be tested and validated with Figs. 4.6 and 4.7.

Simultaneous control of superheat (Fig. 4.7(d)) and evaporating pressure (Fig. 4.7(b)) could be conflicting due to the coupling effect between the two variables. The MPC could generate dire performance without a careful consideration of the coupling effects between the two outputs as well as between the compressor speed and expansion valve opening. For illustration, at  $t=750s$  to  $t=2250s$  the environment temperature rose by  $10^{\circ}C$  causing automatically the mass flow rate through the expansion valve (Fig. 4.6(c)) and the compressor (Fig. 4.6(d)) to increase. However, only the compressor speed varied (Fig. 4.7(a)) during that period as the expansion valve opening (Fig. 4.7(c)) stabilize rapidly so that superheat target could be maintained without a deviation of the evaporator pressure from its reference value.

### **4.7. CONCLUSION**

A nonlinear control-oriented model of a VC system was formulated with 12 state variables and 2 inputs. The nonlinear model was implemented on Simulink using R-134a tables and physical parameters from experimental work. It was then possible to implement MPC for dynamic multivariable control by linearizing the nonlinear model around a steady state point. The control objective was defined to regulate simultaneously superheat and evaporator pressure. MPC was implemented on Simulink so that the superheat and evaporator pressure's feedbacks could be measured to compute the two optimal inputs namely the expansion valve opening and the compressor speed.

## ***CHAPTER 4 CONTROL-ORIENTED MODELLING OF THE REFRIGERANT DYNAMICS***

---

The controller performances were evaluated in terms of the controller's robustness to withstand disturbances and its ability to track the reference values. In the presence of sudden disturbances such as the environment temperature and the heat absorbed in the evaporator, the controller response was satisfactory since the refrigerant mass flow rates through the expansion valve and the compressor varied accordingly as optimal values of the expansion valve opening and the compressor speed were automatically actuated to keep track of the reference settings.

The coupling effects between superheat and evaporator pressure were also considered by the MPC since the reference values were tracked simultaneously with optimal expansion valve opening and compressor speed whose individual control action did not tradeoff the MPC robustness to disturbance rejection and reference tracking. Although not attempted in this work, experimental validations are required to strengthen this model with the integration of operating constraints due to system dynamics, thermal mass and inertia to evaluate their effects on the modelling outputs.



# CHAPTER 5 CONTROL-ORIENTED MODELLING OF THE INDOOR AIR CONDITIONS

## 5.1. INTRODUCTION

In the previous chapter, a nonlinear control-oriented model was developed then linearized around a steady operating point for MPC implementation to control superheat and capacity simultaneously considering the coupling effects between both variables. MPC was implemented using a methodology similar to the multivariable control of indoor air conditions such as temperature, humidity and CO<sub>2</sub> level.

There is a fundamental difference between superheat and capacity control versus indoor air control as explained in the previous chapter however, both controls are interdependent for air-conditioning using VCAC systems as heat transfer occurs between the refrigerant and indoor air streams through the evaporator coils. Therefore, control of indoor air temperature, humidity and CO<sub>2</sub> level could be linked to superheat and capacity control of the refrigerant to enhance heat transfer between the two streams namely, the refrigerant and indoor air without excluding other factors such as climate conditions, building envelope and orientation required for optimal control of indoor air conditions.

MPC implementation for simultaneous control of indoor air temperature, humidity and CO<sub>2</sub> level has demonstrated satisfactory performance in recent works as presented in the subsequent survey.

The coupling effects between temperature and humidity requires a robust controller

## ***CHAPTER 5 CONTROL-ORIENTED MODELLING OF THE INDOOR AIR CONDITIONS***

---

implementation for satisfactory performance. Limitations of SISO controllers such as the commonly adopted PID loops are obvious when coupling effects between temperature and humidity are considered. Moreover, disturbances require anew tuning.

MPC enables the integration of coupling effects and hold out disturbances. However, effective CO<sub>2</sub> level control is required to ensure indoor comfort. Fresh air temperature is required to regulate the level of indoor CO<sub>2</sub> through natural or mechanical ventilation whilst maintaining the load balance within range. Suggestion to determine an optimal steady state point for linearization of the system prior to implement MPC might seem sufficiently comprehensive. However, consideration of an optimal fresh air volume for CO<sub>2</sub> level control might create issues without a control loop implemented for fresh air temperature.

The aforementioned issues, related to varying fresh air temperature, may eventually make the supply fan and compressor speeds rise, therefore, increasing the energy demand to prevent from the load imbalance which could alter the performance of the controller to track the set reference point with limited delays. The simplest solution to prevent from load imbalance associated to fresh air supply could be, a PID loop implementation for control of the fresh air temperature. A combined PID-MPC could provide satisfactory performance for VCAC control like Chiller-FCU systems and is worth a detailed investigation.

The objective of the chapter is to apply a sub layer PID and an upper layer MPC on a Chiller-FCU to control indoor air temperature, humidity and CO<sub>2</sub> level simultaneously without load imbalance associated to fresh air supply. The PID-MPC implemented in the subsequent sections and the VC controller from the previous chapter could be integrated as a multilayer control loop of integrated

## ***CHAPTER 5 CONTROL-ORIENTED MODELLING OF THE INDOOR AIR CONDITIONS***

---

VCAC systems to control simultaneously the refrigerant dynamics and the indoor air conditions. The multilayer control loop could be segmented in upstream controller, which is the multivariable controller of the refrigerant dynamics and downstream controller, which is the PID-MPC controller of indoor air temperature, humidity and CO<sub>2</sub> level.

This work makes two contributions. In order to prevent imbalanced loads and level-out the room temperature and outdoor air, a fresh air processing system with a sub layer PID loop is first implemented on a primary heat exchanger. This will reduce the compressor's speed and enhance energy saving. Secondly, an upper layer MPC loop with optimal control actions is used to simultaneously control the temperature, humidity, and CO<sub>2</sub> level. When PID-MPC loops are combined, it is possible to achieve acceptable performances with an implementation that best reflects practicality.

The subsequent sections of this chapter are listed as follows. In section 5.2., the literature study on control-oriented modelling of the indoor air conditions is presented. The chiller-FCU setup is presented in section 5.3. The implementation of the sub layer PID and the upper layer MPC are presented respectively in section 5.4., and section 5.5. The results and discussion are elaborated in section 5.6., followed by the conclusion in section 5.7.

### **5.2. LITERATURE REVIEW**

Due to their simplicity, PID controllers are commonly used in HVAC systems. Through gains tuning, they modify the input signal [262], which may change the overshoots, settling time, and disturbance rejection performances. PID performances could be affected by dynamic HVAC processes [263]. But, [264] reported some acceptable

## ***CHAPTER 5 CONTROL-ORIENTED MODELLING OF THE INDOOR AIR CONDITIONS***

---

PID performance for controlling temperature and humidity. With anew tuning, poor PID performance [265-268] can be addressed.

PID is not robust with changing humidity and temperature conditions. The performance is further diminished by the coupling effect between temperature and humidity. An advanced scheme like MPC can address robustness and coupling effect.

Multivariable control is made possible by MPC implementation, which also eventually integrates coupling effect [269]. It outlines the constraints for the optimization of the cost function [270] to find the optimal control input that enables energy savings for HVAC systems bound by disturbances under various operating conditions [271-275]. Predictions with MPC are made within a time setting using previously recorded data.

The computed control input at each time setting could be used to modify output and disturbance rejection. MPC could be implemented from any data-oriented model, including grey and black box models [276-278] that are appropriate for data evaluation. Utilizing weather forecasts, MPC implementation on a solar-powered HVAC system [279] showed satisfactory performance.

An approach to determine an optimal control strategy for chilled water systems was proposed by [280]. They demonstrated that a quadratic cost function could represent the energy consumption of a cooling unit in terms of uncontrolled and controlled variables. A range of conditions of their approach resulted with the determination of near to optimal control set. [281], used the approach of [280] to develop an optimal control for a chilled water unit. The energy consumption of the chilled water unit under the condition of uncontrolled variables could be reduced by selecting optimal setting of chilled water, condenser water and supply air temperature.

## ***CHAPTER 5 CONTROL-ORIENTED MODELLING OF THE INDOOR AIR CONDITIONS***

---

[282], studied the short-time room air conditioner simulation method using response factor with the aim of developing an optimized control algorithm for room air conditioner. Their results showed an acceptable level of their simulation method to evaluate the energy consumption of a room air conditioner. An optimal control strategy was developed by [283] using an input-output linearization controller design and a nonlinear controller design optimized with Matlab-Simulink response optimizer as well as a nonlinear programming scheme. The results displayed a better energy saving in comparison with the conventional controllers. Decoupling matrix approach was adopted by [284], for MIMO HVAC control. The remarkable benefit of this novel approach was its simplicity as it led to stable matrix considering coupling effects among control variables often required for implementation of multivariable controllers.

[285], used feedback linearization and back stepping scheme for nonlinear control of moisture and heat loads of HVAC systems. The results disclosed a system with quick value tracking of the humidity and temperature associated with optimized energy consumption in the presence of transient loads. Other advanced strategies for temperature and humidity control could be found in literatures namely, fuzzy logic controller [286-290] and neural network controller [291-293].

According to [294], MPC implementation on HVAC systems improves set point tracking and disturbance rejection. Without deteriorating indoor comfort, simultaneous temperature and humidity control with MPC achieved satisfactory performance [295]. The energy-saving features of MPC implementation on HVAC systems were reviewed by [296, 297]. When compared to PID controllers alone, PID-MPC controllers for the processing and purification of active pharmaceutical ingredients [298] performed better.

## ***CHAPTER 5 CONTROL-ORIENTED MODELLING OF THE INDOOR AIR CONDITIONS***

---

Given the coupling effect between temperature and humidity [228], MPC implementation on a DX AC was chosen for simultaneous CO<sub>2</sub> level, temperature, and humidity control [229, 230]. Disturbance rejection and set point tracking worked well.

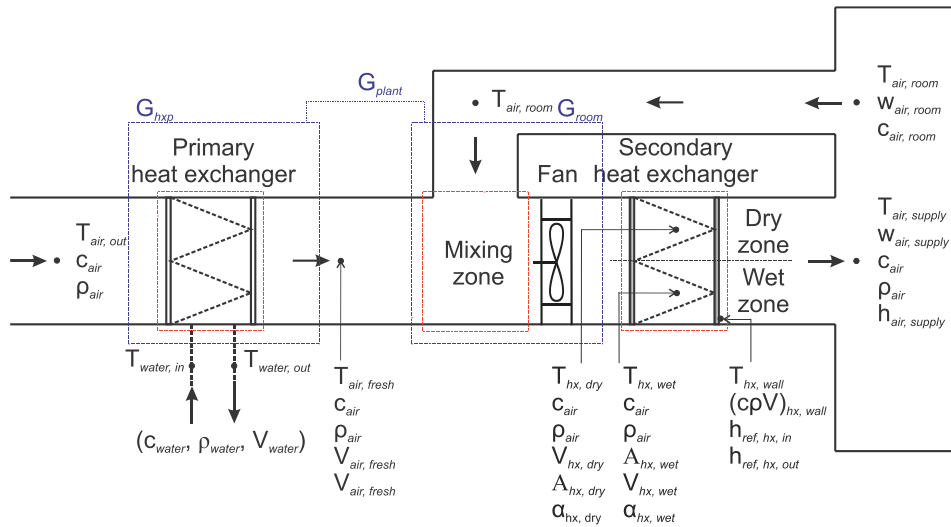
### **5.3. CHILLER – FCU SETUP**

Fig. 5.1 shows the setup of a Chiller-FCU. A chiller with pipes carrying cold water is connected to a primary heat exchanger, through which warm outdoor air is forced. Outside air and cold water can transfer heat, allowing room and fresh air temperatures to be identical in the mixing zone.

To ensure fresh air supply without additional loads and prevent from imbalanced loads that could increase the compressor and supply fan speeds, the primary heat exchanger is used for outdoor air cooling. Further downstream, as mixed air passes through the secondary heat exchanger to reach the room air settings, more heat is removed.

The secondary heat exchanger is used to cool the air while removing moisture therefore, it is divided in wet zone where the refrigerant in two-phase mixture undergoes phase change as a result of heat transfer with mixed room and fresh air. The secondary heat exchanger is also divided in dry zone where refrigerant is superheated as it leaves the heat exchanger.

## CHAPTER 5 CONTROL-ORIENTED MODELLING OF THE INDOOR AIR CONDITIONS



**Figure 5.1** Chiller-FCU Setup

Chiller-FCU are used primarily in large cooling applications, like high-rise office buildings and large theaters, where cooling with dehumidification and fresh air renewal are absolutely necessary. [264, 299, 300], reported equivalent setups for fault detection and dynamic control.

### 5.4. SUB LAYER PID

By adjusting the chiller's control valve, the control objective is to keep the temperature of the fresh air closer to room temperature.

#### 5.4.1. Primary heat exchanger modelling

The primary heat exchanger's dynamic equation could be written as follows:

$$\begin{aligned}
 C_{air}\rho_{air}V_{air,fresh} \frac{dT_{air,fresh}}{dt} &= C_{air}\rho_{air}\dot{V}_{air,fresh}(T_{air,out} - T_{air,fresh}) \\
 &\quad - C_{water}\rho_{water}\dot{V}_{water}(T_{water,in} - T_{water,out})
 \end{aligned} \tag{5.1}$$

## **CHAPTER 5 CONTROL-ORIENTED MODELLING OF THE INDOOR AIR CONDITIONS**

$C_{air}$	Specific heat of air ( $kJ\ kg^{-1}\ ^\circ C^{-1}$ )
$\rho_{air}$	Air density ( $kg\ m^{-3}$ )
$V_{air,fresh}$	Fresh air volume ( $m^3$ )
$T_{air,fresh}$	Fresh air temperature ( $^\circ C$ )
$\dot{V}_{air,fresh}$	Fresh air flow rate ( $m^3\ s^{-1}$ )
$T_{air,out}$	Outdoor air temperature ( $^\circ C$ )
$C_{water}$	Specific heat of water ( $kJ\ kg^{-1}\ ^\circ C^{-1}$ )
$\rho_{water}$	Water density ( $kg\ m^{-3}$ )
$\dot{V}_{water}$	Water flow rate ( $m^3\ s^{-1}$ )
$T_{water,in}$	Inlet water temperature ( $^\circ C$ )
$T_{water,out}$	Outlet water temperature ( $^\circ C$ )

Laplace transformation on (5.1) assuming constant fresh air volume and temperature yields to:

$$\begin{aligned}
 C_{air}\rho_{air}V_{air,fresh}sT(s)_{air,fresh} + C_{air}\rho_{air}\dot{V}_{air,fresh}T(s)_{air,fresh} \\
 = C_{air}\rho_{air}\dot{V}_{air,fresh}T(s)_{air,out} \\
 + C_{water}(T_{water,out} - T_{water,in})\dot{m}(s)_{water}
 \end{aligned} \tag{5.2}$$

The primary heat exchanger model's transfer function between  $\dot{m}(s)_{water}$  and  $T(s)_{air,fresh}$  could be expressed as:

$$G_{hxp}(s) = \frac{C_{water}(T_{water,out} - T_{water,in})}{C_{air}\rho_{air}\dot{V}_{air,fresh} \left( \frac{V_{air,fresh}}{\dot{V}_{air,fresh}} s + 1 \right)} \tag{5.3}$$

Eq. (5.3) could be re-written as:



---

**CHAPTER 5 CONTROL-ORIENTED MODELLING OF THE INDOOR AIR CONDITIONS**


---

$$G_{hxp}(s) = \frac{K_1}{\tau_1 s + 1} \quad (5.4)$$

$$K_1 = \frac{c_{water}(T_{water,out} - T_{water,in})}{c_{air}\rho_{air}\dot{V}_{air,fresh}} \text{ is the gain}$$

$$\tau_1 = \frac{V_{air,fresh}}{\dot{V}_{air,fresh}} \text{ is the thermal time}$$

### 5.4.2. Room modelling

The energy conservation in the thermal room could be stated as:

$$\begin{aligned} c_{air}\rho_{air}V_{air,supply} \frac{dT_{air,supply}}{dt} \\ = c_{air}\rho_{air}\dot{V}_{air,supply}(T_{air,fresh} - T_{air,supply}) + Q_{air,fresh} \end{aligned} \quad (5.5)$$

$V_{air,supply}$	Supply air volume ( $m^3$ )
$\dot{V}_{air,supply}$	Flow rate of supply air ( $m^3 s^{-1}$ )
$T_{air,supply}$	Supply air temperature ( $^{\circ}C$ )
$Q_{air,fresh}$	Fresh air load ( $kw$ )

Laplace transformation on (5.5) leads to:

$$\begin{aligned} c_{air}\rho_{air}V_{air,supply}sT(s)_{air,supply} + c_{air}\rho_{air}\dot{V}_{air,supply}T(s)_{air,supply} \\ = c_{air}\rho_{air}\dot{V}_{air,supply}T(s)_{air,fresh} + Q_{air,fresh} \end{aligned} \quad (5.6)$$

The transfer function of the room model between  $T(s)_{air,fresh}$  and  $T(s)_{air,supply}$  could be expressed as:

---

**CHAPTER 5 CONTROL-ORIENTED MODELLING OF THE INDOOR AIR CONDITIONS**


---

$$G_{room}(s) = \frac{1}{\frac{V_{air,supply}}{\dot{V}_{air,supply}} s + 1} \quad (5.7)$$

Eq. (5.7) could be re-written as:

$$G_{room}(s) = \frac{K_2}{\tau_2 s + 1} \quad (5.8)$$

$K_2 = 1$  is the gain

$\tau_2 = \frac{V_{air,supply}}{\dot{V}_{air,supply}}$  is the thermal time

### 5.4.3. Plant modelling

The plant model's transfer function between  $\dot{m}(s)_{water}$  and  $T(s)_{air,supply}$  could be defined as:

$$G_{plant}(s) = G_{room}(s) \times G_{hxp}(s) = \frac{K_1 K_2}{(\tau_1 s + 1)(\tau_2 s + 1)} \quad (5.9)$$

**Table 5.1** Parameters of the plant model

$C_{air}$	1.005 kJ/kg°C
$\rho_{air}$	1.2 kg/m <sup>3</sup>
$V_{air,supply}$	360 m <sup>3</sup>
$\dot{V}_{air,supply}$	1.1 m <sup>3</sup> /s
$V_{air,fresh}$	84.56 m <sup>3</sup>
$\dot{V}_{air,fresh}$	3.02 m <sup>3</sup> /s
$C_{water}$	4.184 kJ/kg°C
$T_{water,out} - T_{water,in}$	5°C
$T_{air,out}$	28°C

Using the air and water parameters in Table 5.1,  $G_{plant}(s)$  could be expressed as:

**CHAPTER 5 CONTROL-ORIENTED MODELLING OF THE INDOOR AIR CONDITIONS**

$$G_{plant}(s) = 5.74 \frac{1.09 \times 10^{-4}}{s^2 + 0.039s + 1.09 \times 10^{-4}} \quad (5.10)$$

Fig. 5.2 shows the open loop plant model's block diagram as follows:

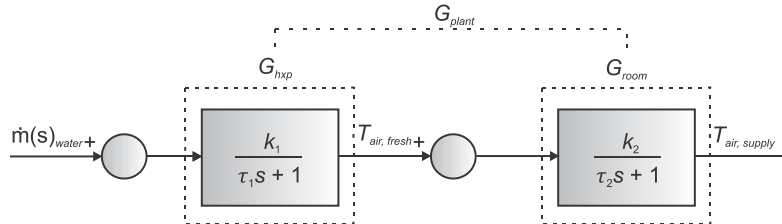


**Figure 5.2** Block diagram of the open loop plant

**5.4.4. PID implementation on the primary heat exchanger**

The transfer function of the PID loop could be stated as follows:

$$G_c(s) = \frac{K_d s^2 + K_p s + K_i}{s} \quad (5.11)$$

$K_d$	Derivative gain
$K_p$	Proportional gain
$K_i$	Integral gain

Due to the close loop's series arrangement of the PID and plant models, the following expression could be used to represent the overall transfer function:

$$G_{overall}(s) = G_c(s) \times G_{plant}(s) \quad (5.12)$$

Fig. 5.3, shows the closed loop sub layer controller's block diagram as follows:

**CHAPTER 5 CONTROL-ORIENTED MODELLING OF THE INDOOR AIR CONDITIONS**

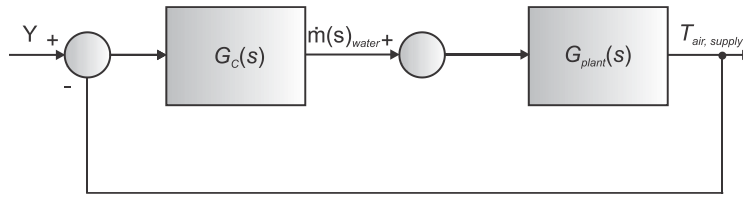


**Figure 5.3** PID block diagram

**5.5. UPPER LAYER MPC**

By adjusting the compressor, supply fan speeds, and fresh air intake, the control goal is to maintain indoor temperature, humidity, and CO2 level simultaneously within settings.

**5.5.1. Dynamic modelling**

Indoor temperature:

$$\begin{aligned}
 C_{air}\rho_{air}V_{air,room} \frac{dT_{air,room}}{dt} & \\
 & = C_{air}\rho_{air}\dot{V}_{air,supply}(T_{air,supply} - T_{air,room}) + Q_{air,room}
 \end{aligned}
 \tag{5.13}$$

$V_{air,room}$  Room air volume ( $m^3$ )

$T_{air,room}$  Room air temperature ( $^{\circ}C$ )

$Q_{air,room}$  Room air load ( $kw$ )

Air temperature in dry cooling zone:

$$\begin{aligned}
 C_{air}\rho_{air}V_{hx,dry} \frac{dT_{hx,dry}}{dt} & \\
 & = C_{air}\rho_{air}\dot{V}_{air,supply}(T_{air,room} - T_{hx,dry}) \\
 & + \alpha_{hx,dry}A_{hx,dry} \left( T_{hx,wall} - \frac{T_{hx,dry} + T_{air,room}}{2} \right)
 \end{aligned}
 \tag{5.14}$$

---

**CHAPTER 5 CONTROL-ORIENTED MODELLING OF THE INDOOR AIR CONDITIONS**


---

$V_{hx,dry}$	Air volume at heat exchanger's dry zone ( $m^3$ )
$T_{hx,dry}$	Air temperature at heat exchanger's dry zone ( $^{\circ}C$ )
$\alpha_{hx,dry}$	Heat transfer coefficient at heat exchanger's wet zone ( $kw m^{-2}^{\circ}C^{-1}$ )
$T_{hx,wall}$	Wall temperature at heat exchanger ( $^{\circ}C$ )

Supply air temperature and humidity:

$$\begin{aligned}
 C_{air}\rho_{air}V_{hx,wet} \frac{dT_{air,supply}}{dt} + \rho_{air}V_{hx,wet}h_{latent,vap} \frac{dW_{air,supply}}{dt} \\
 = C_{air}\rho_{air}\dot{V}_{air,supply}(T_{hx,dry} - T_{air,supply}) \\
 + \rho_{air}\dot{V}_{air,supply}h_{latent,vap}(W_{air,room} - W_{air,supply}) \\
 + \alpha_{hx,wet}A_{hx,wet} \left( T_{hx,wall} - \frac{T_{hx,dry} + T_{air,supply}}{2} \right)
 \end{aligned} \tag{5.15}$$

$V_{hx,wet}$	Air volume at heat exchanger's wet zone ( $m^3$ )
$h_{latent,vap}$	Water's latent heat of vaporization ( $kJ kg^{-1}$ )
$W_{air,supply}$	Supply air's moisture content ( $kg kg^{-1} dry air$ )
$W_{air,room}$	Room air's moisture content ( $kg kg^{-1} dry air$ )
$\alpha_{hx,wet}$	Heat transfer coefficient at heat exchanger's wet zone ( $kw m^{-2}^{\circ}C^{-1}$ )
$A_{hx,wet}$	Heat transfer area at heat exchanger's wet zone ( $m^2$ )

Wall temperature:

---

**CHAPTER 5 CONTROL-ORIENTED MODELLING OF THE INDOOR AIR CONDITIONS**


---

$$\begin{aligned}
 (C\rho V)_{hx,wall} \frac{dT_{hx,wall}}{dt} &= \alpha_{hx,dry} A_{hx,dry} \left( \frac{T_{hx,dry} + T_{air,room}}{2} - T_{hx,wall} \right) \\
 &+ \alpha_{hx,wet} A_{hx,wet} \left( \frac{T_{hx,dry} + T_{air,supply}}{2} - T_{hx,wall} \right) \\
 &+ \dot{m}_{ref} (h_{ref,hx,out} - h_{ref,hx,in})
 \end{aligned} \tag{5.16}$$

$(C\rho V)_{hx,wall}$  Thermal capacitance at heat exchanger wall ( $kJ\ ^\circ C^{-1}\ m^{-2}kg$ )

$\dot{m}_{ref}$  Refrigerant mass flow rate ( $kg\ s^{-1}$ )

$h_{ref,hx,out}$  Refrigerant enthalpy at heat exchanger's outlet ( $kJ\ kg^{-1}$ )

$h_{ref,hx,in}$  Refrigerant enthalpy at heat exchanger's inlet ( $kJ\ kg^{-1}$ )

Indoor humidity:

$$\begin{aligned}
 \rho_{air} V_{air,room} h_{latent,vap} \frac{dW_{air,room}}{dt} &= \rho_{air} \dot{V}_{air,supply} h_{latent,vap} (W_{air,supply} - W_{air,room})
 \end{aligned} \tag{5.17}$$

The relationship between supply air temperature and moisture [27, 226] could be expressed as:

$$\frac{dW_{air,supply}}{dt} = 3.96 \times 10^{-5} \frac{dT_{air,supply}}{dt} + 8.5 \times 10^{-5} \tag{5.18}$$

Indoor CO<sub>2</sub> level:

$$V_{air,room} \frac{dC_{air,room}}{dt} = \dot{V}_{air,supply} (C_{air,supply} - C_{air,room}) \tag{5.19}$$

---

**CHAPTER 5 CONTROL-ORIENTED MODELLING OF THE INDOOR AIR CONDITIONS**


---

$C_{air,room}$  Room air CO<sub>2</sub> level (*ppm*)

$C_{air,supply}$  Supply air CO<sub>2</sub> level (*ppm*)

### 5.5.2. State space formulation on the VCAC system

The formulation for the state space could be as follows:

$$(D\dot{X})_2 = (F(X, U))_2 + (G(Z))_3 \quad (5.20)$$

The decoupling matrix  $(D)_2$  could be defined as:

$$(D)_2 = \begin{bmatrix} D_{11} & 0 & 0 & 0 & 0 & 0 & 0 \\ 0 & D_{22} & 0 & 0 & 0 & 0 & 0 \\ 0 & 0 & D_{33} & 0 & 0 & D_{36} & 0 \\ 0 & 0 & 0 & D_{44} & 0 & 0 & 0 \\ 0 & 0 & 0 & 0 & D_{55} & 0 & 0 \\ 0 & 0 & D_{63} & 0 & 0 & D_{66} & 0 \\ 0 & 0 & 0 & 0 & 0 & 0 & D_{77} \end{bmatrix} \quad (5.21)$$

The components of  $(D)_2$  are given in Table 5.2 as follows:

**Table 5.2** Components of the  $(D)_2$  Matrix

$D_{11} = C_{air}\rho_{air}V_{air,room}$
$D_{22} = C_{air}\rho_{air}V_{hx,dry}$
$D_{33} = C_{air}\rho_{air}V_{hx,wet}$
$D_{44} = (C\rho V)_{hx,wall}$
$D_{55} = \rho_{air}V_{air,room}h_{latent,vap}$
$D_{36} = \rho_{air}V_{hx,wet}h_{latent,vap}$
$D_{63} = 3.96 \times 10^{-5}$
$D_{66} = 1$
$D_{77} = V_{air,room}$

The function  $(F)_2$  could be defined as:

---

**CHAPTER 5 CONTROL-ORIENTED MODELLING OF THE INDOOR AIR CONDITIONS**


---

$$(F)_2 = [F_1 \ F_2 \ F_3 \ F_4 \ F_5 \ F_6 \ F_7]^T \quad (5.22)$$

The components of  $(F)_2$  are given in Table 5.3 as:

**Table 5.3** Components of the  $(F)_2$  matrix

$F_1 = C_{air}\rho_{air}\dot{V}_{air,supply}(T_{air,supply} - T_{air,room})$
$F_2 = C_{air}\rho_{air}\dot{V}_{air,supply}(T_{air,room} - T_{hx,dry})$ $+ \alpha_{hx,dry}A_{hx,dry}\left(T_{hx,wall} - \frac{T_{hx,dry} + T_{air,room}}{2}\right)$
$F_3 = C_{air}\rho_{air}\dot{V}_{air,supply}(T_{hx,dry} - T_{air,supply})$ $+ \rho_{air}\dot{V}_{air,supply}h_{latent,vap}(W_{air,room} - W_{air,supply})$ $+ \alpha_{hx,wet}A_{hx,wet}\left(T_{hx,wall} - \frac{T_{hx,dry} + T_{air,supply}}{2}\right)$
$F_4 = \alpha_{hx,dry}A_{hx,dry}\left(\frac{T_{hx,dry} + T_{air,room}}{2} - T_{hx,wall}\right)$ $+ \alpha_{hx,wet}A_{hx,wet}\left(\frac{T_{hx,dry} + T_{air,supply}}{2} - T_{hx,wall}\right)$ $+ \dot{m}_{ref}(h_{ref,hx,out} - h_{ref,hx,in})$
$F_5 = \rho_{air}\dot{V}_{air,supply}h_{latent,vap}(W_{air,supply} - W_{air,room})$
$F_6 = 8.5 \times 10^{-5}$
$F_7 = \dot{V}_{air,supply}(C_{air,supply} - C_{air,room})$

The state variable  $(X)_2$  could be defined as:

$$(X)_2 = \begin{bmatrix} T_{air,room} \\ T_{hx,dry} \\ T_{air,supply} \\ T_{hx,wall} \\ W_{air,room} \\ W_{air,supply} \\ C_{air,room} \end{bmatrix} \quad (5.23)$$

The input  $(U)_2$  could be defined as:



---

**CHAPTER 5 CONTROL-ORIENTED MODELLING OF THE INDOOR AIR CONDITIONS**


---

$$(U)_2 = \begin{bmatrix} \dot{V}_{air,room} \\ \dot{m}_{ref} \\ \dot{V}_{air,supply} \end{bmatrix} \quad (5.24)$$

The function  $(G)_2$  could be defined as:

$$(G)_2 = [Q_{air,room} \quad 0 \quad 0 \quad 0 \quad 0 \quad 0 \quad 0]^T \quad (5.25)$$

where the disturbance  $(Z)_2 = Q_{air,room}$

### 5.5.3. MPC implementation on the VCAC system

Similar to Section 4.5 and considering the three outputs namely, the room temperature, humidity and CO<sub>2</sub> level the nonlinear system could be linearized around a steady operating point  $(X_0, U_0)$  as follows:

$$\begin{cases} (X(k+1))_2 = (AX(k))_2 + (B\Delta U(k))_2 \\ (Y(k))_2 = (CX(k))_2 \end{cases} \quad (5.26)$$

where,

$$(A)_2 = \begin{bmatrix} A_d & 0_3^T \\ CA_d & I_{3 \times 3} \end{bmatrix} \text{ is the state matrix}$$

$$(B)_2 = \begin{bmatrix} B_d \\ CB_d \end{bmatrix} \text{ is the input matrix}$$

$$(C)_2 = \begin{bmatrix} 1 & 0 & 0 & 0 & 0 & 0 & 0 \\ 0 & 0 & 0 & 0 & 1 & 0 & 0 \\ 0 & 0 & 0 & 0 & 0 & 0 & 1 \end{bmatrix} \text{ is the output matrix}$$

The compact form of the predicted output vector could be stated as follows:

---

**CHAPTER 5 CONTROL-ORIENTED MODELLING OF THE INDOOR AIR CONDITIONS**


---

$$(Y(k_i))_2 = (FX(k_i))_2 + (\Phi\Delta U(k_i))_2 \quad (5.27)$$

where,

$$(F)_1 = [CA \quad CA^2 \quad CA^3 \quad \dots \quad CA^{N_p}]^T \quad (5.28)$$

and,

$$(\Phi)_2 = \begin{bmatrix} CB & 0 & 0 & \dots & 0 \\ CAB & CB & 0 & \dots & 0 \\ CA^2B & CAB & CB & \dots & 0 \\ \vdots & \vdots & \vdots & \vdots & \vdots \\ CA^{N_p-1}B & CA^{N_p-2}B & CA^{N_p-2}B & \dots & CA^{N_p-N_c}B \end{bmatrix} \quad (5.29)$$

$N_p = 24$  for the prediction horizon, and  $N_c = 3$  for the control horizon. The set point information could be represented by the following data vector:

$$(R_s)_2 = [1 \quad 1 \quad 1]^T (r(k_i))_2 \quad (5.30)$$

with,

$\bar{R}_s = [1 \quad 1 \quad 1]^T$  and  $r(k_i)$  as the step value of the outputs.

The set point is chosen to be between 24°C - 26°C, with 50%-60% relative humidity and an adequate fresh air volume, in accordance with the ASHRAE comfort zone. Minimizing deviations between the set point and predicted output is the objective of the MPC loop. To find the best course of control action, the aforementioned objective is turned into a cost function expressed as follows:

$$(J)_2 = \sum_{i=1}^7 \left[ ((R_s)_2 - (Y(k_i))_2)^T ((R_s)_2 - (Y(k_i))_2) + (\Delta U(k_i))_2^T \bar{R} (\Delta U(k_i))_2 \right] \quad (5.31)$$

## **CHAPTER 5 CONTROL-ORIENTED MODELLING OF THE INDOOR AIR CONDITIONS**

---

Whilst the second term takes into account control action weighting for large or small deviations, the first term carries the objective of minimizing the deviations.

Eq. (5.27) inserted into (5.31) results in:

$$(J)_2 = \sum_{i=1}^7 \left[ (R_s - FX(k_i) - \Phi \Delta U(k_i))_2^T (R_s - FX(k_i) - \Phi \Delta U(k_i))_2 + (\Delta U(k_i))_2^T \bar{R} (\Delta U(k_i))_2 \right] \quad (5.32)$$

The cost function's first derivative could be written as:

$$\left( \frac{\partial J}{\partial \Delta U(k_i)} \right)_2 = \sum_{i=1}^7 \left[ (R_s - FX(k_i) - \Phi \Delta U(k_i))_2^T (-\Phi) + (\Delta U(k_i))_2^T \bar{R} \right] \quad (5.33)$$

The following equation results from setting the derivative to zero:

$$(\Phi^T \Phi + \bar{R}) \sum_{i=1}^7 (\Delta U(k_i))_2^T = \Phi \sum_{i=1}^7 (R_s - FX(k_i))_2^T \quad (5.34)$$

therefore,

$$\sum_{i=1}^7 (\Delta U(k_i))_2 = ((\Phi^T \Phi + \bar{R})^{-1} \Phi^T)_2 \sum_{i=1}^7 (\bar{R}_s r(k_i) - FX(k_i))_2 \quad (5.35)$$

## **5.6. RESULTS AND DISCUSSION**

### **5.6.1. Sub layer PID**

The sub layer controller was used to pre-cool the outdoor air. As the roots of its characteristic equation were both negative, the plant model was stable. A sufficient amount of PID tuning could

**CHAPTER 5 CONTROL-ORIENTED MODELLING OF THE INDOOR AIR CONDITIONS**

result in satisfactory performance, as evidenced by the uncontrolled plant's transient response (Fig. 5.4), which had a small steady state error of -4.74 and a settling time of 21 min. The convolution theorem [301] is used in Matlab to determine the transient response of the close loop (Fig. 5.5) to a step input.

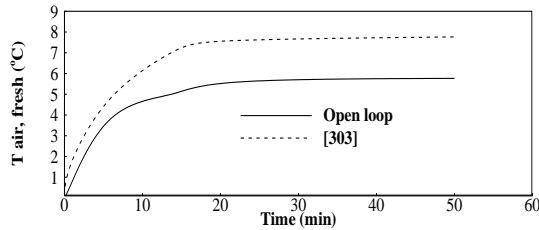


**Figure 5.4** Open loop's response

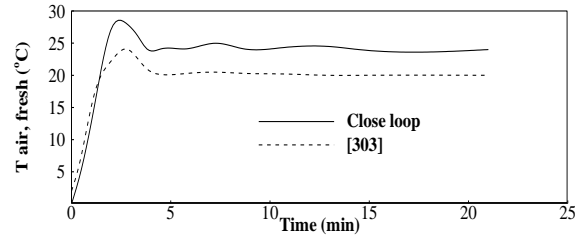


**Figure 5.5** Close loop's response

The PID gains calculated with the Ziegler-Nichols table [302, 303] using the parameters L, T, and R [304] are shown in Table 5.4:

**Table 5.4** Ziegler-Nichols parameters and gains

Parameters	L	0.5 min	Gains	K <sub>p</sub>	9.3
	T	22.8 min		K <sub>i</sub>	0.02
	R	0.004		K <sub>d</sub>	0.06

In Figs. 5.4 and 5.5, the transient responses of the open and close loops are depicted and verified using the work of [303]. In Figs. 5.4 and 5.5, the sampling period is 1 min. By measuring the plant steady state error following a step input, the plant rising time for its response to move from 10% to 90% of its final value and the plant settling time to stabilize within a range of  $\delta = \pm 2\%$  of its steady state, the plant characteristics are evaluated using a method similar to [303].

The performance indicators are presented in Table 5.5 as follows:

---

**CHAPTER 5 CONTROL-ORIENTED MODELLING OF THE INDOOR AIR CONDITIONS**


---

**Table 5.5 Plant performance indicators**

Plant	Open loop	Close loop
Steady state error	-4.74	0.04
Maximum overshoot		16.9%
Settling time	21 min	2.8 min
Rising time	12.2 min	1.7 min

The sub layer controller was tested with step inputs of the water mass flow rates for the open and close loop. PID tuning is necessary to ascertain  $K_d = 0.06$  to reduce the settling time and decrease the overshoot then  $K_p = 9.3$  to reduce the rise time and  $K_i = 0.02$  to cancel out the steady state error. The primary heat exchanger (Fig. 5.1) was used to process 28°C outdoor air for fresh air intake, which released energy to chilled water to balance the room air temperature, set initially at 24°C.

Removal of moisture and pollutants that are harmful to occupants through fresh air temperature control improved IAQ. As the fresh air is pre-cooled to room temperature, the compressor and supply fan speeds can be lowered, increasing comfort without increasing energy demand. PID implementation for fresh air control was in accordance with ASHRAE recommendations because the steady state error was close to zero and the maximum overshoot and settling time of the fresh air temperature (Fig. 5.5) were less than the recommended values of 30% and 3 min, respectively (Table 5.5). The rising time was reduced by the PID loop from 12.2 min (Fig. 5.4) when the plant was uncontrolled to 1.7 min (Fig. 5.5).

### 5.6.2. Upper layer MPC

## ***CHAPTER 5 CONTROL-ORIENTED MODELLING OF THE INDOOR AIR CONDITIONS***

To maintain adequate indoor air quality whilst allowing fresh air intake if the CO<sub>2</sub> level rose above preset levels, the compressor and supply fan speeds were regulated by the upper layer MPC. 03 inputs and 03 outputs, along with 07 state variables, represented the dynamic system.

To predict future system behavior, the state space formulation was used. The output reached the set point quickly without a smooth transition when the control action was not given any weight. Smoother responses required more time to reach a steady state where they gradually decreased as the energy required for set point tracking was dispersed over a longer period of time after adopting the weighting factor.

The dynamics of the FCU required specific MPC testing. Set point tracking and disturbance rejection are used to carry out MPC assessment. Table 5.6, contains a list of the testing parameters [230] as follows:

**Table 5.6** *MPC parameters*

Compressor speed setting	50%
Supply fan speed setting	50%
Moisture content	0.011 $kgkg^{-1}$ dry air
Refrigerant flow rate	3.100 $m^3s^{-1}$
Outdoor air temperature	28°C

Fig. 5.6 describes the block diagram of the adopted close loop MPC.

## CHAPTER 5 CONTROL-ORIENTED MODELLING OF THE INDOOR AIR CONDITIONS

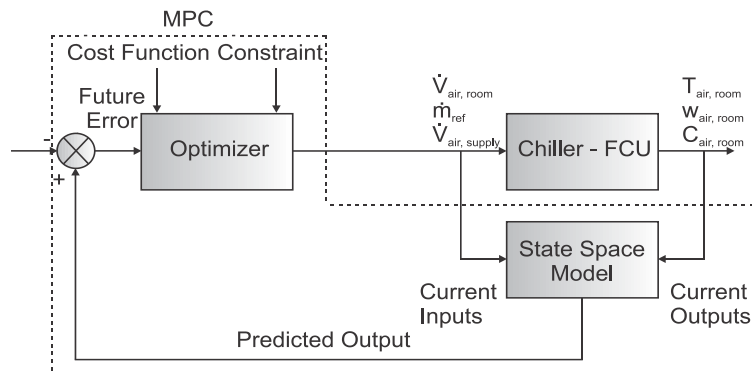


**Figure 5.6** MPC block diagram

Using the MPC toolbox, MPC was tested on Simulink. The upper layer controller's mathematical model was implemented in Simulink, and a framework for Simulink control design was developed by linearizing the model around a steady state point. The performance of the linearized model was assessed with an MPC toolbox.

The number of inputs was set to 3, which included the fresh air intake, supply and compressor fan speeds. The reference points for temperature, relative humidity, and CO2 level were set at 23.5°C, 50%, and 780.1 ppm, respectively. The prediction and control horizons were set at 24 and 3, respectively. The simulation was run for 60 minutes with a sampling interval of 0.5 minutes.

The cost function was used to monitor the deviation of the inputs and the outputs. A cost function optimizer with constraints was adopted to evaluate the inputs' variation. A difference bounded by the set point and predicted output served to define the error tracking within a finite prediction horizon. A difference bounded by the past and present control actions served as the definition to track the input variation within a finite control horizon. To resolve the scaling issue and enable scale-consistent output prediction, scaling factors were used for both the input variation and error

## ***CHAPTER 5 CONTROL-ORIENTED MODELLING OF THE INDOOR AIR CONDITIONS***

---

tracking. The scaling factors were set by nominal values determined with the modelling input and output.

Instability outside the receding horizon framework resulted from the cost function's formulation over a finite future time to identify an ideal input vector. As a result, for a given time setting, only the first element of the input vector was used for output control. The state variables were updated once the future time setting was attained to compute the new input vector, and only its first element was used for the most recent regulation. Up until the set point was reached, this operation was carried out repeatedly over the prediction horizon.

### **5.6.2.1. Set point tracking assessment**

Tracking indoor settings requires control actions that adapt to shifting circumstances. In Figs. 5.7 and 5.8, the sampling period is 0.5 minutes. In Fig. 5.7, fresh air was admitted to maintain indoor environment within settings whilst the compressor and supply fan speeds varied as the set temperature changed. For approximately 5 minutes, the compressor's speed increased from 2000 to 3500 rpm (Fig. 5.7(a)), stabilized for another 5 minutes then, gradually decreased to settle at 2250 rpm as the temperature decreased from 24°C to 23.5°C (Fig. 5.7(b)).



## CHAPTER 5 CONTROL-ORIENTED MODELLING OF THE INDOOR AIR CONDITIONS

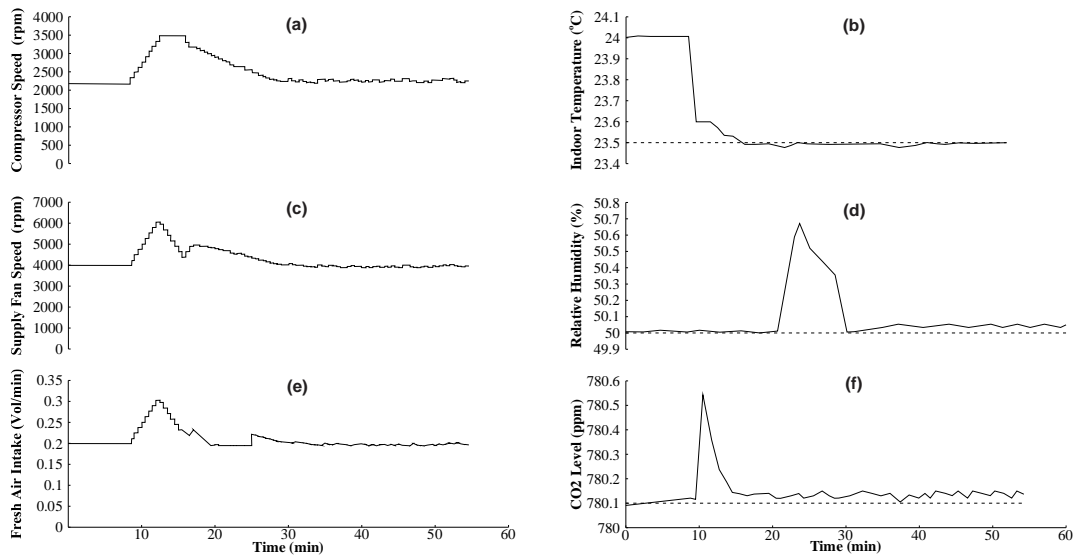


**Figure 5.7** Temperature set point tracking

(a) Compressor speed. (b) Indoor Temperature. (c) Supply fan speed. (d) Relative humidity.  
 (e) Fresh air intake. (f) CO<sub>2</sub> level.

The supply fan speed increased from 4000 rpm to 6000 rpm (Fig. 5.7(c)) for about 5 min then it dropped gradually to 4200 rpm for 5 min. The supply fan speed then briefly increased to 5000 rpm for a swift period of time before declining once more and eventually settling at 4100 rpm. Except for the time period of 22–28 min, when humidity increased to 50.7% in response to the temperature being set from 24°C to 23.5°C, 10 min earlier (Fig. 5.7(b)), humidity did not change significantly (Fig. 5.7(d)), it varied below 50.5%.

The admitted fresh air volume (given in vol/min with 1 vol=1 m<sup>3</sup>) did not significantly change, it did rise gradually from 0.2 vol/min to 0.3 vol/min before falling back to 0.2 vol/min (Fig. 5.7(e)). Except for the period of 10-15 minutes when the CO<sub>2</sub> level was 780.6 ppm, the CO<sub>2</sub> level remained unchanged (Fig. 5.7(f)).

## ***CHAPTER 5 CONTROL-ORIENTED MODELLING OF THE INDOOR AIR CONDITIONS***

---

The speeds of the compressor and supply fan increased simultaneously (Figs. 5.7(a) and 5.7(c)) as the set temperature varied from 24°C to 23.5°C (Fig. 5.7(b)), allowing them to maintain the indoor settings. As a result of the continuous cooling, the fan speed decreased more quickly than the compressor speed, preventing excessive dehumidification. This proved that the coupling effect between temperature and humidity could be reduced by adjusting the compressor and supply fan speeds simultaneously. With fresh air intake (Fig. 5.7(e)) carefully pre-cooled at 24°C (Fig. 5.5) and mixed with the room air upstream the secondary heat exchanger (Fig. 5.1), CO<sub>2</sub> level (Fig. 5.7(f)) was controlled with the PID controller to avoid imbalanced loads that might require compressor and supply fan speed increases.

### **5.6.2.2. Disturbance rejection assessment**

In Figs. 5.8(c) and 5.8(f), as sensible (loads to be removed indoor for cooling) and latent (loads to be removed for dehumidification) loads increased, temperature (5.8(b)) and humidity (5.8(e)) increased with a time delay of approximately 10 min likely due to the slow variation of the air pressure and density. The magnitude and pattern of the sensible and latent loads were identified following [27]. As temperature and humidity should be maintained within settings regardless of sudden load changes, the compressor and supply fan speeds varied to uphold indoor settings as sensible and latent loads increased.

## CHAPTER 5 CONTROL-ORIENTED MODELLING OF THE INDOOR AIR CONDITIONS

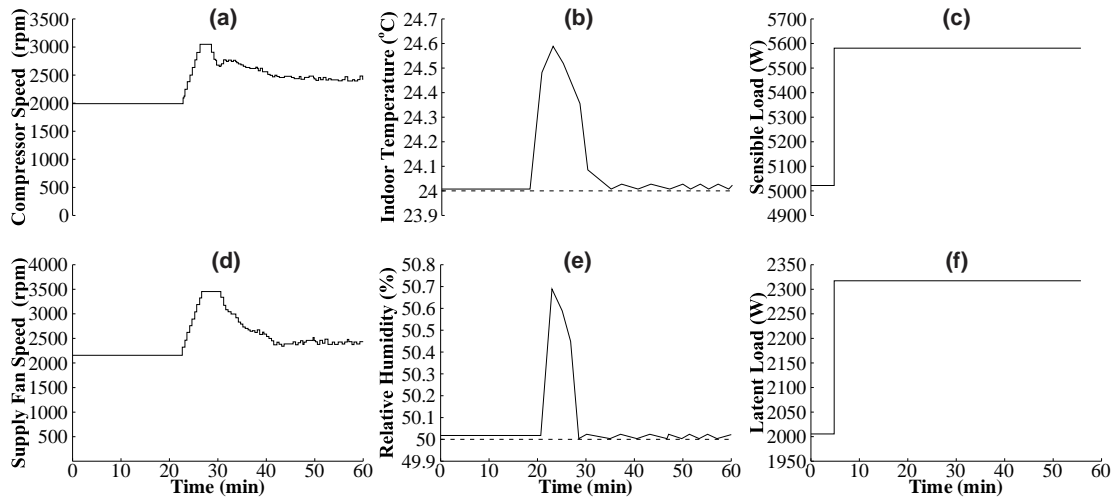


**Figure 5.8** System responses to load variation

(a) Compressor speed. (b) Indoor temperature. (c) Sensible load. (d) Supply fan speed.

(a) Relative humidity. (b) Latent load.

When the sensible load increased (Fig. 5.8(c)) over the course of 22–26 minutes, the compressor's speed was increased (Fig. 5.8(a)) to remove the load as quickly as possible and prevent a temperature offset (Fig. 5.8(b)) above 24.5°C. To prevent humidity offset (Fig. 5.8(e)) above 50.5% within the time range of 20–28 minutes with increasing latent load (Fig. 5.8(f)), the supply fan speed increased (Fig. 5.8(d)). To better remove moisture from the return air, the supply fan speed decreased more rapidly (Fig. 5.8(d)) than the compressor speed (Fig. 5.8(a)) once the predetermined target was reached.

As the compressor and supply fan speeds increased simultaneously (Figs. 5.8(a) and 5.8(d)) to withstand load variation and maintain the indoor settings within range, sensible and latent loads variation (Figs. 5.8(c) and 5.8(f)) impacted the temperature and humidity variation (Figs. 5.8(b) and 5.8(e)) to an extent where the deviations from the set points were respectively 0.5°C and 0.5%. The ability of the MPC to withstand disturbances was demonstrated by the simultaneous

## ***CHAPTER 5 CONTROL-ORIENTED MODELLING OF THE INDOOR AIR CONDITIONS***

---

variation of compressor and supply fan speed with varying load conditions to maintain the indoor settings within range.

Without taking into account the coupling effects that frequently result in poor controller performance, conflicting compressor and supply fan speed control could be misleading. Despite the high dehumidification risk, the compressor speed increased to improve cooling and keep the temperature within the desired range (Fig. 5.8(a)). By quickly reducing the supply fan speed (Fig. 5.8(d)) in comparison to the compressor speed (Fig. 5.8(a)), the humidity level was kept within acceptable limits without compromising the temperature setting.

### **5.7. CONCLUSION**

With a sublayer PID for processing outdoor air and an upper layer MPC for simultaneous temperature, humidity, and CO<sub>2</sub> level regulation, two controllers were put into place. Regarding stability, steady state error, settling time, rise time, and maximum overshoot, the PID performance was satisfactory. The receding horizon framework was used to establish a cost function to determine an optimal control action for MPC implementation. With regards to set point tracking and disturbance rejection, MPC performance was adequate.

Fresh air pre-cooling improved CO<sub>2</sub> level control without imbalanced loads because the temperatures of the fresh air and room air were leveled out, necessitating less cooling with the critical load removal upstream the mixing zone. The MPC took into account the coupling effect between temperature and humidity to improve performances. Conflicting compressor and supply fan speeds were resolved without compromising the indoor settings as the compressor speed

## ***CHAPTER 5 CONTROL-ORIENTED MODELLING OF THE INDOOR AIR CONDITIONS***

---

occasionally increased whilst the supply fan speed decreased. Under changing loads, MPC maintained its robustness.

By combining PID and MPC, this work showed that indoor air quality (IAQ) could be improved whilst maintaining acceptable control performance. To control a single parameter whose setting has no impact on other parameters, PID is more suitable. PID was used to control the outdoor air temperature so that fresh air intake could occur without causing load imbalance. MPC is appropriate for controlling several parameters at once whose settings might be closely connected. MPC was chosen to control simultaneously the indoor temperature, humidity and CO<sub>2</sub> level whilst considering the coupling effect between temperature and humidity.

Since using a PID loop for temperature control to prevent imbalanced loads caused by fresh air intake enables satisfactory set point tracking performance without having to increase the compressor and supply fan speeds to correct the imbalance, the value of this work is demonstrated. This research might be expanded to assess how much energy a Chiller-FCU uses overall in comparison to a system without a PID loop.

## CHAPTER 6 CONCLUSION AND FUTURE WORK

### 6.1. INTRODUCTION

This chapter summarizes and discuss the key findings detailed throughout this work. In section 6.2., the overall conclusion of this work is introduced whilst the suggestions for future work are presented in section 6.3.

### 6.2. CONCLUSION

Modelling and control of VC systems integrated to AC systems to capture the refrigerant dynamics and the variation of indoor air conditions were discussed throughout this work. From the literatures, most of the dynamic models adopted for VC systems are developed from the conservation equations of mass, momentum and energy. This is to capture the dynamic behavior of the fluid circulating through the VC cycle but also to evaluate with more accuracy the variation of the indoor air conditions with varying loads.

Typical VC systems are designed to self-adjust to load variations with varying compressor speed. However, to deepen our understanding of the fluid's dynamic behavior and the variations of the indoor air conditions, comprehensive mathematical models are required for prediction and control purposes. At first a steady and transient state models were developed followed by a control-oriented model to control the refrigerant dynamics in VC systems and finally a control-oriented model to control the indoor air conditions.

Due to a lack of detailed methodology and the abundance of analytical or computational schemes that cannot be objectively evaluated, the steady and transient state modeling techniques of VC systems suggested in many research works are typically difficult to replicate. To address this problem, this work first presented the development of a steady state modeling approach based on the first principles and flexible enough to be applied to various prediction problems.

The results of the experiments used to validate the steady state model were satisfactory. The model's outputs, including the enthalpy at each junction and the refrigerant evaporating pressure, agreed with the available experimental data. The suggested steady state modeling approach could be used in conjunction with other existing mathematical models of the VC system's components. The steady state modeling approach could be used to find a VC system's ideal parameters so that the system's efficiency can be increased by designing and testing low-cost, effective control strategies. The modeling of VC systems with complex configurations, such as those with a single condenser and numerous evaporators, could also be done using the suggested steady state modelling technique.

A technique derived from mass and energy conservation equations represented by the Navier-Stokes equations was used for the transient state modelling. The governing equations were discretized for the heat exchanger models using a finite volume scheme. Transient state modelling matrices were established after the condenser and evaporator were divided into 3 and n-control volumes, respectively. The results of the experiments used to validate the transient state model were satisfactory. The results of the model, such as the pressure of the refrigerant across the condenser and evaporator, are consistent with those of the experiments. The suggested transient

state modelling method could be used for prediction of the ideal start-up parameters. The results of the modelling could be applied for the development of enhanced performance's VC systems.

Following the steady and transient state models, a multivariable MPC was developed on a VC system to control simultaneously the superheat and evaporator pressure. A nonlinear control-oriented model was implemented with 12 state variables and 2 inputs using the steady state models for the expansion valve and compressor on one hand and more detailed Navier-Stokes equations for the condenser and evaporator.

The control-oriented model considered phase changes in the condenser and evaporator so that the refrigerant dynamics could be captured with more accuracy. The nonlinear model was linearized around a steady state point determined from the experiments adopted for validation of the steady state model. MPC was implemented on the linearized model to compute optimal expansion valve opening and compressor speed with measured feedbacks of superheat and evaporator pressure.

The control-oriented model and MPC were implemented on Simulink using 4 interconnected subsystems namely, the VC system, the MPC system, the reference system and the environment. The coupling effects between superheat and evaporator pressure was considered. MPC performance was satisfactory in terms of disturbance rejection and reference tracking considering the coupling effects.

Finally, to improve the performance of a Chiller-FCU in terms of controlling simultaneously the indoor temperature, humidity, and CO<sub>2</sub> level, a hybrid PID-MPC controller was implemented. The sublayer PID was used to process the outdoor air and level-out the room and fresh air temperatures.



Pre-cooled outdoor air kept the compressor and supply fan speeds from increasing and prevented from delaying set point tracking due to imbalanced loads caused by fresh air intake.

For simultaneous control of indoor temperature, humidity, and CO<sub>2</sub> level, the upper layer MPC was implemented. An optimal input was determined using a cost function whilst taking into account the coupling effect between temperature and humidity. MPC was used to withstand disturbances as well. In terms of stability, settling time, and maximum overshoot, PID performance was reliable. In terms of set point tracking and disturbance rejection, MPC performance was adequate.

### **6.3. FUTURE WORK**

The operating trend of VC systems is usually nonlinear and transient. VC systems are designed to run within a wide range of operating conditions. The nonlinear operating trend contribute in energy saving in a sense that the system could self-regulate to run faster or slower depending on the cooling or heating requirement at a particular time. The transient trend enables the system to adjust in time its set value in order to maintain thermal comfort. The wide range of operating conditions allows the system to run efficiently under various weather conditions spanning from low to high temperatures. Therefore, nonlinear controllers are designed to regulate the nonlinearity, time-varying of VC systems under any acceptable operating condition.

In line with above statement, one could suggest to develop and implement a nonlinear controller with multilayers to control simultaneously the refrigerant dynamics and the indoor air conditions. The nonlinear multilayer controller could be made of a sub layer MPC loop to control simultaneously superheat and capacity regulation and an upper layer MPC loop for simultaneous control of indoor air temperature, humidity and CO<sub>2</sub> level.

The integrated nonlinear multilayer controller could be built upon the models proposed in this work for control of the refrigerant dynamics and indoor air conditions. The Simulink model adopted in this work and presented in the Appendix section could be adopted for implementation of the nonlinear multilayer controller.

Upon successful implementation of the nonlinear multilayer controller, one could extend the work to develop an accurate fault detection model of VC system integrated in AC units to obtain a unique model enabling simultaneous control of the refrigerant dynamics and indoor air conditions along with fault detection.

## REFERENCES

- [1] K. Fu, and Z. Deng, “Current situation of energy consumption in Guangzhou railway station and analysis on the potential of energy conservation,” *Journal of Sustainable Development*, vol. 2, pp. 117 - 120, 2009.
- [2] C. Sanama, “Mathematical modelling of flow downstream of an orifice under flow-accelerated corrosion,” Pretoria, 2017, *Masters Dissertation, University of Pretoria*.
- [3] C. Sanama, M. Sharifpur, J. P. Meyer, "Mathematical modeling of orifice downstream flow under flow-accelerated corrosion," *Nuclear Engineering and Design*, vol. 326, pp. 285-289, 2018.
- [4] P. Novak, N. Mendez, G. Oliveira, “Simulation and analysis of a secondary HVAC system using Matlab/Simulink platform,” *ASME International Mechanical Engineering Congress and Exposition*, Anaheim, USA, 13 - 19 November, 2004.
- [5] J. V. Candy, “Model-based signal processing,” *John Wiley & Sons*, New York, 2006.
- [6] P. S. Agachy, Z. K. Nagy, M. V. Cristea, A. I. Lucaci, “Model based control,” *John Wiley & Sons*, New York, 2006.
- [7] J. Ma, D. Kim, J. E. Braun, “A trajectory piecewise-linear approach to model order reduction of vapor compression cycles,” *18<sup>th</sup> International Refrigeration and Air Conditioning Conference*, Purdue, USA, 24 - 28 May, 2021.

## **REFERENCES**

---

- [8] J. Ma, D. Kim, J. E. Braun, “A nonlinear model order reduction framework for dynamic vapor compression cycles via proper orthogonal decomposition,” *18<sup>th</sup> International Refrigeration and Air Conditioning Conference*, Purdue, 24 - 28 May, 2021.
- [9] J. Ma, D. Kim, J. E. Braun, “Development of a fast method for retrieving thermodynamic properties to accelerate transient vapor compression cycle simulation,” *17<sup>th</sup> International Refrigeration and Air Conditioning Conference*, Purdue, 09 - 12 July, 2018.
- [10] J. Ma, “Reduced order modelling for vapor compression systems via proper orthogonal decomposition,” *Masters Dissertation, Purdue University*, Purdue, 2019.
- [11] J. Ma, D. Kim, J. E. Braun, “Proper orthogonal decomposition for reduced order dynamic modeling of vapor compression systems,” *International Journal of Refrigeration*, vol. 132, pp. 145-155, 2021.
- [12] V. Zucatti, H. F. S. Lui, D. B. Pitz, W. R. Wolf, “Assesment of reduced-order modeling strategies for convective heat transfer,” *Numerical Heat Transfer, Part A: Applications*, vol. 77, pp. 702-729, 2020.
- [13] B. Xu, A. Yebi, M. Hoffman, S. Onori, “A rigorous model order reduction framework for waste heat recovery systems based on proper orthogonal decomposition and Garlekin projection,” *IEEE Transactions on Control Systems Technology*, vol. 2, pp. 635 - 643, 2018.
- [14] E. Rodriguez, B.P. Rasmussen, “A nonlinear reduced-order modeling method for dynamic two-phase flow heat exchanger simulations,” *Science and Technology for the Built Environment*, vol. 22, pp. 164-177, 2016.

## ***REFERENCES***

---

- [15] D. Kim, J. Ma, J. E. Braun, E. A. Groll, “Fuzzy modeling approach for transient vapor compression and expansion cycle simulation,” *International Journal of Refrigeration*, vol. 121, pp. 114-125, 2020.
- [16] J. K. White, “A trajectory piecewise-linear approach to model order reduction of nonlinear dynamical systems,” *PhD Thesis, MIT*, Boston, 2003.
- [17] K. Kunisch, S. Volkwein, “Control of the Burges equation by a reduced-order approach using proper orthogonal decomposition,” *Journal of Optimization Theory and Applications*, vol. 102, pp. 345-371, 1999.
- [18] B. B. King, E. W. Sachs, “Semidefinite programming techniques for reduced-order systems with guaranteed stability margins,” *Computational Optimization and Applications*, vol. 17, pp. 37-59, 2000.
- [19] S. Prajma, “POD model reduction with stability guarantee,” *Transactions of the 42<sup>nd</sup> IEEE International Conference on Decision and Control*, vol. 5, pp. 5254-5258, 2003.
- [20] G. Kerschen, J. C. Golinval, A. F. Vakakis, L. A. Bergman, “The method of proper orthogonal decomposition for dynamical characterization and order reduction of mechanical systems: an overview,” *Nonlinear Dynamics*, vol. 41, pp. 147-169, 2005.
- [21] Y. Yao, W. Wang, M. Huang, “A state-space dynamic model for vapor compression refrigeration system based on moving-boundary formulation,” *International Journal of Refrigeration*, vol. 60, pp. 174-189, 2015.

## ***REFERENCES***

---

- [22] L. C. Schurt, C. J. L. Hermes, A. T. Neto, “Assessment of the controlling envelope of a model-based multivariable controller for vapor compression refrigeration systems,” *Applied Thermal Engineering*, vol. 30, pp. 1598-1546, 2010.
- [23] P. Sivak, D. Hroncova, “State-space model of a mechanical system in Matlab/Simulink,” *Procedia Engineering*, vol. 48, pp. 629-635, 2012.
- [24] Y. Yao, M. Huang, J. Chen, “State-space model for dynamic behavior of vapor compression liquid chiller,” *International Journal of Refrigeration*, vol. 36, pp. 2128-2147, 2013.
- [25] L. Zhao, M. Zaheeruddin, “Dynamic simulation and analysis of a water chiller refrigeration system,” *Applied Thermal Engineering*, vol. 25, pp. 2258-2271, 2005.
- [26] Y. Yao, Z. Lian, Z. Hou, X. Zhou, “Optimal operation of a large cooling system based on an empirical model,” *Applied Thermal Engineering*, vol. 24, pp. 2303-2321, 2004.
- [27] Q. Qi, S. Deng, “Multivariable control of air temperature and humidity in a direct expansion (DX) air conditioning (A/C) system,” *Building & Environment*, vol. 44, pp. 1659-1667, 2009.
- [28] Q. Qi, S. Deng, X. Xu, M. Y. Chan, “Improving degree of superheat control in a direct expansion (DX) air conditioning (A/C) system,” *International Journal of Refrigeration*, vol. 33, pp. 125-134, 2010.
- [29] T. Tigrek, “Nonlinear adaptive optimal control of HVAC systems,” *Masters Dissertation*, Graduate College of the University of Iowa, Iowa City, 2001.

## ***REFERENCES***

---

- [30] C. G. Nesler, “Adaptive control of thermal processes in buildings,” *IEEE Control Systems Magazine*, vol. 6, pp. 9-13, 1986.
- [31] L. Hongli, D. Peiyong, Y. Qingmei, L. Hui, Y. Xiuwen, “A novel adaptive energy-efficient controller for the HVAC systems,” *24<sup>th</sup> Chinese Control and Decision Conference (CCDC)*, pp. 1402-1406, Taiyuan, China, 23 - 25 May, 2012.
- [32] L. D. Landau, R. Lozano, M. M’Saad, A. Karimi, “Adaptive control (Algorithms, Analysis and Applications),” *Communication and Control Engineering, Springer*, Ed. 2, London, 2011.
- [33] D. W. U. Perera, C. F. Pfeiffer, N. O. Skeie, “Control of temperature and energy consumption in buildings – A review,” *Energy & Environment*, vol. 5, pp. 471-484, 2014.
- [34] Y. Yan, J. Zhou, Y. Lin, W. Yang, P. Wang, G. Zhang, “Adaptive optimal control model for building cooling and heating sources,” *Energy and Buildings*, vol. 40, pp. 1394-1401, 2008.
- [35] H. Moradi, M. Saffar-Avval, F. Bakhtiari-Nejad, “Nonlinear multivariable control and performance of an air-handling unit,” *Energy and Buildings*, vol. 43, pp. 805-813, 2011.
- [36] S. Yang, M. P. Wan, B. Feng Ng, S. Dubey, G. P. Henze, W. Chen, K. Baskaran, “Experimental study of model predictive control for an air-conditioning system with dedicated outdoor air system,” *Applied Energy*, vol. 257, Paper ID 113920, 2020.

## ***REFERENCES***

---

- [37] M. Fiorentini, J. Wall, Z. Ma, J. H. Braslavsky, P. Cooper, “Hybrid model predictive control of a residential HVAC system with on-site thermal energy generation and storage,” *Applied Energy*, vol. 187, pp. 465-479, 2017.
- [38] T. Zhang, M. P. Wan, B. Feng Ng, S. Yang, “Model predictive control for building energy reduction and temperature regulation,” *2018 IEEE Green Technologies Conference (GreenTech)*, pp. 100-106, Austin, USA, 04 - 06 April, 2018.
- [39] Y. Ma, F. Borelli, B. Hancey, B. Coffey, S. Bengea, P. Haves, “Model predictive control for the operation of building cooling systems,” *IEEE Transactions on Control System Technologies*, vol. 20, pp. 796-803, 2012.
- [40] I. Hazyuk, C. Ghiaus, D. Penhouet, “Optimal temperature control of intermittently heated buildings using model predictive control: Part I-Building modeling,” *Building and Environment*, vol. 51, pp. 379-387, 2012.
- [41] X. Chen, Q. Wang, J. Srebic, “Occupant feedback based model predictive control for thermal comfort and energy optimization: A chamber experimental evaluation,” *Applied Energy*, vol. 164, pp. 341-351, 2016.
- [42] S. Yang, W. M. Pun, C. Wanyu, B. Feng Ng, Z. Deqing, “An adaptive robust model predictive control for indoor climate optimization and uncertainties handling in buildings,” *Building and Environment*, vol. 163, Paper ID 106326, 2019.
- [43] S. Yang, M. P. Wan, B. Feng Ng, S. Dubey, G. P. Henze, S. K. Rai, “Experimental study of a model predictive control system for active chilled beam (ACB) air-conditioning system,” *Energy and Buildings*, Paper ID 109451, 2019.



## ***REFERENCES***

---

- [44] D. Lee, R. Ooka, S. Ikeda, W. Choi, Y. Kwak, “Model predictive control of building energy systems with thermal energy storage in response to occupancy variations and time-variant electricity prices,” *Energy and Buildings*, Paper ID 110291, 2020.
- [45] M. Aftab, C. Chen, C. K. Chau, T. Rahwan, “Automatic HVAC control with real-time occupancy recognition and simulation-guided model predictive control in low-cost embedded system,” *Energy and Buildings*, vol. 154, pp. 141-156, 2017.
- [46] Q. Yang, J. Zhu, X. Xu, J. Lu, “Simultaneous control of indoor air temperature and humidity for a chilled water based airconditioning system using neural networks,” *Energy and Buildings*, vol. 110, pp.159-169, 2016.
- [47] S. Yang, M. P. Wan, B. Feng Ng, T. Zhang, S. Babu, Z. Zhang, W. Chen, S. Dubey, “State-space thermal model incorporating humidity and thermal comfort for model predictive control in buildings,” *Energy and Buildings*, vol. 170, pp. 25-39, 2018.
- [48] M. Castilla, J. D. Alvarez, J. E. Normey-Rico, F. Rodriguez, “Thermal comfort control using a non-linear MPC strategy: A real case of study in a bioclimatic building,” *Journal of Process Control*, vol. 24, pp. 703-713, 2014.
- [49] C. B. Chiou, C. H. Chiou, C. M. Chu, S. L. Lin, “The study of energy-saving strategy for direct expansion air conditioning system,” *Energy and Buildings*, vol. 40, pp. 1660-1665, 2008.
- [50] S. Hashimoto, T. Matsuda, H. Shinbayashi, H. Yoshida, F. Wang, K. Shiota, “An energy-saving method for air-conditioning system by using weather forecast,” *Air Conditioning and the Low Carbon Cooling Challenge*, London, UK, 27 - 29 July, 2008.

## ***REFERENCES***

---

- [51] F. Wang, H. Yoshida, B. Li, N. Umemiya, S. Hashimoto, T. Matsuda, H. Shinbayashi, "Evaluation and optimization of air-conditioner energy saving control considering indoor thermal comfort," *Building Simulation*, Glasgow, Scotland, 27 - 30 July, 2009.
- [52] Z. Ma, S. Wang, "Energy efficient control of variable speed pumps in complex building central air-conditioning systems," *Energy and Buildings*, vol. 41, pp. 197-205, 2009.
- [53] K. Zhao, X. Liu, T. Zhang, Y. Jiang, "Performance of temperature and humidity independent control air-conditioning system in an office building," *Energy and Buildings*, vol. 43, pp. 1895-1903, 2011.
- [54] N. Ghaddar, M. Mossolly, K. Ghali, "Optimal control strategy for a multi-zone air conditioning system using a genetic algorithm," *Energy*, vol. 34, pp. 58-66, 2009.
- [55] N. Wang, J. Zhang, X. Xia, "Energy consumption of air conditioners at different temperature set points," *Energy and Buildings*, vol. 65, pp. 412-418, 2013.
- [56] L. Zadeh, "Fuzzy sets," *Information and Control*, vol. 8, pp. 338-353, 1965.
- [57] E. Mamdani, "Applications of fuzzy algorithms for control of a simple dynamic plant," *IEEE Proceedings*, vol. 121, pp. 1585-1588, 1964.
- [58] T. Tagaki, M. Sugeno, "Fuzzy identification of systems and its applications to modeling and control," *IEEE Transactions on systems, Man and Cybernetics*, pp. 116-132, Tokyo, 1985.
- [59] H. Zhang, D. Liu, "Fuzzy Modeling and Fuzzy Control," *Birkhauser*, Boston, 2006.

## ***REFERENCES***

---

- [60] R. Alcalá, J. Alcalá-Fdez, M. J. Gacto, “Improving fuzzy logic controllers obtained by experts: A case study in HVAC systems,” *Applied Intelligence*, vol. 31, pp. 15-30, 2009.
- [61] D. Kolokotsa, D. Tsiavos, G. S. Stavrakakis, K. Kalaitzakis, E. Antonidakis, “Advanced fuzzy logic controllers design and evaluation for buildings' occupants thermal-visual comfort and indoor air quality satisfaction,” *Energy and Buildings*, vol. 33, pp. 531-543, 2001.
- [62] W. Huang, H. N. Lam, “Using generic algorithms to optimize controller parameters for HVAC systems,” *Energy and Buildings*, vol. 26, pp. 277-282, 1997.
- [63] R. Alcalá, J. M. Benitez, J. Casillas, O. Cordon, R. Perez, “Fuzzy control of HVAC systems optimized by genetic algorithms,” *Applied Intelligence*, vol. 18, pp. 155-177, 2003.
- [64] J. H. Holland, “Adaptation in natural and artificial systems,” *The University of Michigan Press*, Michigan, 1975.
- [65] D. E. Goldberg, “Generic algorithms in search, optimization, and machine learning,” *Addison-Wesley*, Reading, 1989.
- [66] W. B. Hudson, “Introduction and overview of artificial neural networks in instrumentation and measurement applications,” *IEEE Instrumentation and Measurement Technology Conference*, Irvine, USA, 18 - 20 May, 1996.
- [67] D. Daponte, D. Grimaldi, “Artificial neural networks in measurements,” *Measurement*, vol. 23, pp. 93-115, 1998.

## ***REFERENCES***

---

- [68] P. K. Simpson, "Foundation of neural network," *Adaptive control systems technology symposium*, Pittsburg, USA, 24 - 25 October, 1994.
- [69] H. N. Wu, H. X. Li, "Garlekin/neural-network-based design of guaranteed cost control for nonlinear distributed parameter systems," *IEEE Transactions on Neural Networks*, vol. 19, pp. 795-807, 2008.
- [70] M., Ghiassi, H. Saidane, "A dynamic architecture for artificial neural networks," *Neurocomputing*, vol. 63, pp. 397-413, 2005.
- [71] C. R. Bradshaw, E. A. Groll, "A comprehensive model of a novel rotating spool compressor," *International Journal of Refrigeration*, vol. 36, pp. 1974-1981, 2013.
- [72] G. Kemp, N. Garrett, E. Groll, "Novel rotary spool compressor design and preliminary prototype performance," *International Compressor Engineering Conference*, Purdue, USA, 14 - 17 July, 2008.
- [73] G. Kemp, I. Elwood, E. Groll, "Evaluation of prototype rotating spool compressor in liquid flooded operation," *International Compressor Engineering Conference*, Purdue, USA, 12 - 15 July, 2010.
- [74] G. Kemp, J. Orosz, C. Bradshaw, E. Groll, "Spool compressor tip seal design considerations and testing," *International Compressor Engineering Conference*, Purdue, USA, 16 - 19 July, 2012.

## ***REFERENCES***

---

- [75] G. Kemp, J. Orosz, C. Bradshaw, E. Groll, “Spool seal design and testing for the spool compressor,” *International Compressor Engineering Conference*, Purdue, USA, 16 - 19 July, 2012.
- [76] C. J. Deschamps, R. T. S. Ferreira, A. T. Prata, “Turbulent flow through valves of reciprocating compressors,” *International Compressor Engineering Conference*, Purdue, USA, 23 - 26 July, 1996.
- [77] C. J. Deschamps, A. T. Prata, R. T. S. Ferreira, “Turbulent flow through reed types valves of reciprocating compressors,” *ASME, Advanced Energy System Division (AES)*, vol. 36, pp. 151-161, 1996.
- [78] T. T. Rodrigues, J. L. Gasche, J. Militzer “Flow simulation through moving hermetic compressor valves using the immersed boundary method,” *International Refrigeration and Air Conditioning Conference*, Purdue, USA, 12 - 15 July, 2010.
- [79] H. Soumerai, “History in the air conditioning and refrigeration industry: Breakthrough of large positive displacement rotary compressors in the second half of the 20<sup>th</sup> century,” *ASHRAE Web Publication, A Look Back at HVAC&R*, 2010.
- [80] K. Ooi, T. Wong, “A computer simulation of a rotary compressor for household refrigerators,” *Applied Thermal Engineering*, vol. 17, pp. 65-78, 1997.
- [81] J. Kim, E. Groll, “Feasibility study of a bowtie compressor with novel capacity-modulation,” *International Journal of Refrigeration*, vol. 30, pp. 1427-1438, 2007.

## ***REFERENCES***

---

- [82] M. Jovane, “Modelling and analysis of a novel rotary compressor,” *PhD Thesis, Purdue University*, West Lafayette, 2007.
- [83] M. Mathison, J. Braun, E. Groll, “Modelling of a two-stage rotary compressor,” *HVAC&R Research*, vol. 14, pp. 719-748, 2008.
- [84] M. Mathison, “Modelling and evaluation of advanced compression techniques for vapor compression equipment,” *PhD Thesis, Purdue University*, West Lafayette, 2011.
- [85] I. Bell, “Theoretical and experimental analysis of liquid flooded compression in scroll compressors,” *PhD Thesis, Purdue University*, West Lafayette, 2011.
- [86] C. Bradshaw, E. Groll, S. Garimella, “A comprehensive model of a miniature-scale linear compressor for electronics cooling,” *International Journal of Refrigeration*, vol. 34, pp. 63-73, 2011.
- [87] X. Zhang, D. Ziviani, J. E. Braun, E. A. Groll, “Modeling the dynamic characteristics and performance of linear compressors,” *International Compressor Engineering Conference*, Purdue, USA, 9 - 12 July, 2018.
- [88] X. Zhang, D. Ziviani, J. E. Braun, E. A. Groll, “Theoretical analysis of dynamic characteristics in linear compressors,” *International Journal of Refrigeration*, vol. 109, pp. 114-127, 2020.
- [89] M. Park, J. Lee, H. Kim, Y. Ahn, “Experimental and numerical study of heat transfer characteristics using the heat balance in linear compressor,” *International Journal of Refrigeration*, vol. 74, pp. 550-559, 2017.

## ***REFERENCES***

---

- [90] H. Kim, C. G. Roh, J. K. Kim, J. M. Shin, J. K. Hwang, “An experimental and numerical study on dynamic characteristic of linear compressor in refrigeration system,” *International Journal of Refrigeration*, vol. 32, pp. 1536-1543, 2009.
- [91] A. Jomde, A. Anderson, V. Bhojwani, S. Kedia, N. Jangale, K. Kolas, P. Khedkar, “Modeling and measurement of a moving coil oil-free linear compressor performance for refrigeration application using R134a,” *International Journal of Refrigeration*, vol. 88, pp. 182-194, 2018.
- [92] W. Wang, X. Tai, “Characteristic of a miniature linear compressor,” *International Compressor Engineering Conference*, Purdue, USA, 12 - 15 July, 2010.
- [93] X. You, L. Qiu, C. Duan, X. Jiang, C. Huang, X. Zhi, “Study on the stroke amplitude of linear compressor,” *Applied Thermal Engineering*, vol. 129, pp. 1488-1495, 2018.
- [94] L. Ding, Y. Wu, “Output characteristics of miniature linear compressor at hundred-hertz with different connecting tubes,” *International Journal of Refrigeration*, vol. 124, pp. 114-121, 2021.
- [95] G. D. Librado, E. E. R. Vasquez, L. A. M. Santiyanes, J. H. P. Vasquez, C. A. N. Martin, “Transient analysis of a single-stage vapor compression refrigeration system using lumped parameter approaches,” *International Journal on Advances in Systems and Measurements*, vol. 11 pp. 352-362, 2018.
- [96] Z. Li, K. Liang, X. Chen, Z. Zhu, Z. Zhu, H. Jiang, “A comprehensive numerical model of a vapour compression refrigeration system equipped with a variable displacement compressor,” *Applied Thermal Engineering*, vol. 204, Paper ID 117967, 2022.

## ***REFERENCES***

---

- [97] K. J. Samuel, R. T. K. Raj, G. Edison, “An overview of parameters influencing the performance of hermetic reciprocating compressor for domestic applications,” *International Journal of Air Conditioning and Refrigeration*, vol. 26, Paper ID 1830003, 2018.
- [98] A. Burgstaller, D. Nagy, R. Almbauer, W. Lang, “Influence of the main parameters of the suction valve on the overall performance of a small hermetic reciprocating compressor,” *International Compressor Engineering Conference*, Purdue, USA, 14 - 17 July, 2008.
- [99] H. P. Bloch, J. J. Hoefner, “Reciprocating compressors: Operation and maintenance,” *Gulf Professional Publishing*, 1996.
- [100] A. Angeletti, M. E. Biancolini, E. Costa, M. Urbinati, “Optimization of reed valves dynamics by means of fluid structure interaction modeling,” *4<sup>th</sup> European Automotive Simulation Conference*, Munich, Germany, 06 - 07 July, 2009.
- [101] F. Barbi, J. L. Gasche, A. D. S. Neto, M. M. Villar, R. S. Lima, “Numerical simulation of the flow through a compressor-valve model using immersed-boundary method,” *Engineering Applications of Computational Fluid Mechanics*, vol. 10, pp. 255 - 271, 2016.
- [102] J. L. Gosche, B. Franco, “Evaluation of an immersed boundary method for solving the fluid structure interaction problem in refrigeration compressor valves,” *11<sup>th</sup> World Congress on Computational Mechanics, 5<sup>th</sup> European Conference on Computational Mechanics, 6<sup>th</sup> European Conference on Computational Fluid Dynamics*, Barcelona, Spain, 20 - 25 July, 2014.



## ***REFERENCES***

---

- [103] F. F. Matos, C. J. Deschamps, A. T. T. Prata, “A two-dimensional simulation model for reciprocating compressors with automatic valves,” *International Compressor Engineering Conference*, Purdue, USA, 17 - 20 July, 2006.
- [104] K. A. James, R. W. James, “Transient analysis of the thermostatic expansion valve for refrigeration system evaporators using mathematical models,” *Transactions of the Institute of Measurement and Control*, vol. 9, pp. 198-205, 1987.
- [105] M. R. Conde, P. Sutura, “A mathematical simulation model for thermostatic expansion valves,” *Heat Recovery System*, Chapter 12, pp. 271-282, 1992.
- [106] P. Mithraratne, N. E. Wijeyesundera, “An experimental and numerical study of hunting in thermostatic-expansion-valve-controlled evaporators,” *International Journal of Refrigeration*, vol. 25, pp. 992-998, 2002.
- [107] C. Aprea, R. Mastrullo, “Experimental evaluation of electronic and thermostatic expansion valves performances using R22 and R407C,” *Applied Thermal Engineering*, vol. 22, pp. 205-218, 2002.
- [108] R. Lazzarin, M. Noro, “Experimental comparison of electronic and thermostatic expansion valves performances in air conditioning plant,” *International Journal of Refrigeration*, vol. 31, pp. 113-118, 2008.
- [109] F. W. Yu, K. T. Chan, H. Y. Chu, “Constraints of using thermostatic expansion valves to operate air-cooled chillers at lower condensing temperatures,” *Applied Thermal Engineering*, vol. 26, pp. 2470-2478, 2006.

## ***REFERENCES***

---

- [110] L. Renato, N. Daniele, N. Marco, “Electronic expansion valves vs. thermal expansion valves,” *ASHRAE Journal*, vol. 51, pp. 34-38, 2009.
- [111] S. Jayaprakash, N. K. Choo, “Performance study of thermostatic and electronic expansion valves of a water-cooled scroll chiller,” *5<sup>th</sup> Asian Conference on Refrigeration and Air Conditioning ACRA 2010 – Green Breeze from Asia: Frontiers of Refrigerants, Heat Transfer and System*, Tokyo, Japan, 07 - 09 June, 2010.
- [112] D. P. Finn, C. J. Doyle, “Control and optimization issues associated with algorithm-controlled refrigerant throttling devices,” *ASHRAE Transactions*, vol. 106, Paper ID DA-00-4-2, 2000.
- [113] H. Wan, “A review of electronic expansion valve correlations for air-conditioning and heat pump system,” *17<sup>th</sup> International Refrigeration and Air Conditioning Conference*, Purdue, 09 - 12 July 2018.
- [114] A. Behfar, D. P. Yuill, Y. Yu, “Supermarket system characteristic and operating faults (RP – 1615),” *Science and Technology for the Built Environment*, vol. 24, pp. 1104 - 1113, 2018.
- [115] *ASHRAE, Refrigeration handbook (SI)*, Chapter 44, 1994.
- [116] D. Ndiaye, “Etude numérique et expérimentale de la performance en régime transitoire de pompes à chaleur eau-air en cyclage,” *PhD Thesis, Université de Montréal, Ecole Polytechnique de Montréal*, Montréal, 2007.

## ***REFERENCES***

---

- [117] D. Ndiaye, M. Bernier, “Modelling the bleed port of a thermostatic expansion valve,” *International Journal of refrigeration*, vol. 32, pp. 826-836, 2009.
- [118] D. Wirz, “Commercial Refrigeration: For Air Conditioning Technicians,” *Cengage Learning*, Clifton Park, NY Delmar, 2009.
- [119] E. J. Dillman, “Thermostatic Expansion Valve,” *Patent US 2539062 A*, 1951.
- [120] I. W. Eames, A. Milazzo, G. G. Maidment, “Modelling thermostatic expansion valve,” *International Journal of Refrigeration*, vol. 38, pp. 189-197, 2014.
- [121] I. W. Eames, T. Brown, G. G. Maidment, J. Missenden, J. A. Evans, M. J. Swain, S. J. James, “An interactive refrigeration system simulator software,” *1<sup>st</sup> IIR International Conference on Sustainability and the Cold Chain*, Cambridge, UK, 29 - 31 March, 2010.
- [122] I. W. Eames, T. Brown, G. G. Maidment, J. A. Evans, “Description and validation of a computer based refrigeration system simulator,” *Computers and Electronics in Agriculture*, vol. 85, pp. 53-63, 2012.
- [123] A. Behfar, D. Yuill, “Evaluation of gray box thermostatic expansion valve mass flow models,” *International Journal of Refrigeration*, vol. 96, pp. 161-168, 2018.
- [124] R. W. Zappe, “Valve Selection Handbook: Engineering Fundamentals for Selecting Manual valves, Check Valves, Pressure relief Valves, and Rupture Discs,” *Gulf Professional Publishing*, 1999.

## ***REFERENCES***

---

- [125] A. Behfar, D. P. Yuill, Y. Yu, “Automated fault detection and diagnosis methods for supermarket equipment,” *Science and Technology for the Built Environment*, vol. 23, pp. 1242-1266, 2017.
- [126] T. M. Harm, “Charge inventory system modeling and validation for unitary air conditioners,” *PhD Thesis, Purdue University*, West Lafayette, 2002.
- [127] V. Payne, D. L. O’Neal, “A mass flow rate correlation for refrigerants and refrigerant mixtures flowing through short tubes,” *HVAC&R Research*, vol. 10, pp. 73-87, 2004.
- [128] V. Mulay, A. Kulkarni, D. Agonafer, ASME Fellow, R. Schmidt, ASME Fellow, “Effect of location and the properties of thermostatic expansion valve sensor bulb on the stability of a refrigeration system,” *Journal of Heat Transfer*, vol. 127, pp. 85-94, 2005.
- [129] Y. Makwana, D. Agonafer, ASME Fellow, D. Manole, “Impact of TXV and compressor in the stability of a high-end computer refrigeration system,” *Journal of Electronic Packaging*, vol. 126, pp. 554-559, 2004.
- [130] N. Hariharan, B. P. Rasmussen, “Parameter estimation for dynamic HVAC models with limited sensor information,” *IEEE American Control Conference*, Baltimore, USA, 30 June - 02 July, 2010.
- [131] H. Cheung, J. E. Braun, “Simulation of fault impacts for vapor compression systems by inverse modeling. Part I: Component modeling and validation,” *HVAC&R Research*, vol. 19, pp. 892-906, 2013.

## ***REFERENCES***

---

- [132] C. C. Hiller, L. R. Glicksman, "Improving heat-pump performance via compressor capacity control analysis and test," *MIT*, Massachusetts, 1976.
- [133] G. L. Davis, T. C. Scott, "Component modelling requirements for refrigeration system simulation," *Proceedings of the International Compressor Engineering Conference*, pp. 401-408, 1976.
- [134] R. D. Ellison, F. A. Creswick, "A computer simulation of steady-state performance of air-to-air heat pumps," *Oak Ridge National Laboratory*, Tennessee, 1978.
- [135] R. D. Ellison, C. K. Rice, "Heat pump model update," *Oak Ridge National Laboratory*, Tennessee, 1979.
- [136] J. E. Flower, "Analytical modelling of heat pump units as a design aid for performance prediction," *Lawrence Livermore Laboratory*, California, 1978.
- [137] F. W. Ahrens, "Heat pump modelling, simulation and design," *Nato, Advanced Study Institute on Heat Pump Fundamentals*, Espinho, 1980.
- [138] W. M. Kays, "Compact heat exchangers," *McGraw-Hill*, New York, 1984.
- [139] A. E. Dabiri, "A steady-state computer simulation model for air-to-air heat pumps," *ASHRAE Transactions*, vol. 88, pp. 973-987, 1982.
- [140] A. E. Dabiri, C. K. Rice, "A compressor simulation model with corrections for the levels of suction gas superheat," *ASHRAE Transactions*, vol. 87, pp. 771-782, 1981.
- [141] M. L. Martins Costa, J. A. R. Parise, "A three-zone simulation model for air-cooled condensers," *Heat Recovery Systems and CHP*, vol. 13, pp. 97-113, 1993.

## ***REFERENCES***

---

- [142] M. J. S. Lemos, E. L. Zapparoli, "Steady-state numerical solution of vapor compression refrigeration units," Proceedings of the *International Refrigeration and Air Conditioning Conference*, pp. 235-240, 1996.
- [143] J. Liu, W. Wei, G. Ding, C. Zhang, M. Fukaya, K. Wang, T. Inagaki, "A general steady state mathematical model for fin-and-tube heat exchanger based on graph theory," *International Journal of Refrigeration*, vol. 27, pp. 965-973, 2004.
- [144] G. L. Ding, "Recent developments in simulation techniques for vapour-compression refrigeration systems," *International Journal of Refrigeration*, vol. 30, pp. 1119-1133, 2007.
- [145] J. M. Winkler, "Development of a component based simulation tool for the steady state and transient analysis of vapour compression systems," *PhD Thesis, Maryland: Faculty of the Graduate School of the University of Maryland, College Park, Maryland*, 2009.
- [146] J. Winkler, V. Aute, R. Radermacher, "Comprehensive investigation of numerical methods in simulating a steady-state vapor compression system," *International Journal of Refrigeration*, vol. 31, pp. 930-942, 2008.
- [147] J. M. Belman, J. Navarro-Esbri, D. Ginestar, V. Millian, "Steady-state model of a variable speed vapor compression system using R134a as working fluid," *International Journal of Energy Research*, vol. 34, pp. 933-945, 2010.
- [148] F. Bagheri, "Development of efficient air conditioning and refrigeration system for service vehicles," *PhD Thesis, School of Mechatronic Systems Engineering, Faculty of Applied Science, Simon Fraser University, Vancouver*, 2016.

## ***REFERENCES***

---

- [149] M. Beshr, V. Aute, R. Radermacher, "Steady state modeling of advanced vapor compression systems with multiple air and refrigerant loops," *12<sup>th</sup> IEA Heat Pump Conference*, Rotterdam, Netherlands, 11 - 14 May, 2010.
- [150] G. Panaras, E. Mathioulakis, V. Belessiotis, "A semi-analytical refrigeration cycle modelling approach for a heat pump hot water heater," *International Journal of Sustainable Energy*, vol. 37, pp. 393-414, 2018.
- [151] J. Woods, E. Bonnema, "Regression-based approach to modeling emerging HVAC technologies in Energy Plus: A case study using a Vuilleumier-Cycle heat pump," *Energy and Buildings*, vol. 186, pp. 195-207, 2019.
- [152] A. A. Bukshaisha, B. M. Fronk, "Simulation of membrane heat pump system performance for space cooling," *International Journal of Refrigeration*, vol. 99, pp. 371-381, 2019.
- [153] S. A. Klein, "Engineering Equation Solver," *F-Chart Software*, Madison, 2017, .
- [154] G. L. Wedekind, B. L. Bhatt, B. I. Beck, "A system mean void fraction model for predicting various transient phenomena associated with two-phase evaporating and condensing flows," *International Journal of Multiphase Flow*, vol. 4, pp. 97 - 114, 1978.
- [155] M. Dhar, W. Soedel, "Transient analysis of vapor compression refrigeration systems," *15<sup>th</sup> International Congress of Refrigeration*, Venice, Italy, 23 - 29 September, 1979.
- [156] J. Chi, D. A. Didion, "A simulation model of the transient performance of a heat pump," *International Journal of Refrigeration*, vol. 5, pp. 176-184, 1982.

## ***REFERENCES***

---

- [157] J. W. MacArthur, "Theoretical analysis of the dynamic interactions of vapor compression heat pumps," *Energy Conservation Management*, vol. 24, pp. 49 – 66, 1984a.
- [158] J. W. MacArthur, "Transient heat pump behavior: A theoretical investigation," *International Journal of Refrigeration*, vol. 7, pp. 123 – 132, 1984b.
- [159] J. W. MacArthur, E. W. Grald, "Prediction of cyclic heat pump performance with a fully distributed model and a comparison with experimental data," *ASHRAE Transactions*, vol. 93, pp. 1159 - 1178, 1987.
- [160] P. Welsby, S. Devotta, P. J. Diggory, "Steady and dynamic state simulations of heat-pumps. Part I: literature review," *Applied Energy*, vol. 31, pp. 189-203, 1988.
- [161] J. Nyers, G. Stoyan, "A dynamical model adequate for controlling the evaporator of a heat pump," *International Journal of Refrigeration*," vol. 17, pp. 101 -108, 1994.
- [162] M. Willatzen, N. B. O. L. Pettit, L. Ploug-Sorensen, "A general dynamic simulation model for evaporators and condensers in refrigeration. Part I: Moving-boundary formulation of two-phase flows with heat exchange," *International Journal of Refrigeration*, vol. 21, pp. 398 – 403, 1998.
- [163] N. B. O. L. Pettit, M. Willatzen, L. Ploug-Sorensen, "A general dynamic simulation model for evaporators and condensers in refrigeration. Part II: Simulation and control of an evaporator," *International Journal of Refrigeration*, vol. 21, pp. 404-414, 1998.



## ***REFERENCES***

---

- [164] T. L. McKinley, A. G. Alleyne, "An advanced nonlinear switched heat exchanger model for vapor compression cycles using the moving - boundary method," *International Journal of Refrigeration*, vol. 31, pp. 1243-1264, 2008.
- [165] B. Li, A. G. Alleyne, "A full dynamic model of a HVAC vapor compression interacting with dynamic environment," *American Control Conference*, St. Louis, USA, 10 - 12 June, 2009.
- [166] W. J. Zhang, C. L. Zhang, G. L. Ding, "On three forms of momentum equation in transient modeling of residential refrigeration systems," *International Journal of Refrigeration*, vol. 32, pp. 938 - 944, 2009.
- [167] R. Link, C. J. Deschamps, "Numerical modeling of startup and shutdown transients in reciprocating compressors," *International Journal of Refrigeration*, vol. 34, pp. 1398 – 1414, 2011.
- [168] B. P. Rasmussen, "Dynamic modeling of vapor compression systems - Part I: Literature review," *HVAC and R Research*, vol. 18, pp. 934 - 955, 2012.
- [169] B. P. Rasmussen, B. Shenoy, "Dynamic modeling for vapor compression systems - Part II: Simulation Tutorial," *HVAC and R Research*, vol. 18, pp. 956-973, 2012.
- [170] H. Satyavada, S. Baldi, "A novel modelling approach for condensing boilers based on hybrid dynamical systems," *Machines*, vol. 4, pp. 1 - 10, 2016.
- [171] H. Pangborn, "Dynamic modeling, validation, and control for vapor compression systems," *Masters Dissertation, University of Illinois at Urbana - Champaign, Illinois*, 2015.

## ***REFERENCES***

---

- [172] H. Pangborn, A. G. Alleyne, N. Wu, "A comparison between finite volume and switched moving boundary approaches for dynamic vapor compression system modeling," *International Journal of Refrigeration*, vol. 53, pp. 101 - 114, 2015.
- [173] M. C. Diniz, C. J. L. Hernez, C. J. Deschamps, "Transient simulation of small capacity reciprocating compressor in on-off controlled refrigerators," *International Journal of Refrigeration*, vol. 102, pp. 12 - 21, 2019.
- [174] M. C. Diniz, C. Melo, C. J. Deschamps, "Experimental performance assessment of a hermetic reciprocating compressor operating in a household refrigerator under on-off cycling conditions," *International Journal of Refrigeration*, vol. 88, pp. 587 - 598, 2018.
- [175] W. E. Murphy, V. W. Goldschmidt, "Cyclic characteristic of a typical residential air conditioner: modeling of start-up transients," *ASHRAE Transactions*, vol. 91 (Part 2), pp. 427-444, 1985.
- [176] M. W. Browne, P. K. Bansal, "Transient simulation of vapour-compression packaged liquid chillers," *International Journal of Refrigeration*, vol. 25, pp. 597-610, 2002.
- [177] C. Melo, R. Ferreira, R. Pereira, C. Negrao, "Dynamic behaviour of a vapor compression refrigerator: a theoretical and experimental analysis," *International Refrigeration and Air Conditioning Conference*, Purdue, 1988.
- [178] J. V. C. Vargas, J. A. R. Parise, "Simulation in transient regime of a heat pump with closed-loop and on-off control," *International Journal of Refrigeration*, vol. 18, pp. 235-243, 1995.

## ***REFERENCES***

---

- [179] R. O. Nunes, L. F. N. Castro, L. Machado, R. N. N. Koury, “Distributed and nonsteady-state model of an air cooler working with R22 and R410A,” *International Journal of Refrigeration*, vol. 24, Paper ID 1650008, 2016.
- [180] W. Li, Y. Chu, P. Xu, Z. Yang, Y. Ji, L. Ni, Y. Bao, K. Wang, “A transient model for the thermal inertia of chilled-water systems during demand response,” *Energy and Buildings*, vol. 150, pp. 383-395, 2017.
- [181] S. M. Sami, T. N. Duong, Y. Mercadier, N. Galanis, “Prediction of transient response of heat pumps,” *ASHRAE Transactions*, vol. 93 (Part 2), pp. 471-490, 1987.
- [182] J. W. MacArthur, E. W. Grald, “Unsteady compressible two-phase flow model for predicting cyclic heat pump performance and a comparison with experimental data,” *International Journal of Refrigeration*, vol. 12, pp. 29-41, 1989.
- [183] Z. J. Chen, W. H. Lin, “Dynamic simulation and optimal matching of a small scale refrigeration system,” *International Journal of Refrigeration*, vol. 14, pp. 329-335, 1991.
- [184] J. Judge, R. Radermacher, “A heat exchanger model for mixtures and pure refrigerant cycle simulations,” *International Journal of Refrigeration*, vol. 20, pp. 244-255, 1997.
- [185] T. Rossi, J. Braun, “A real-time transient model for air conditioners,” *Proceedings of 20th International Congress of Refrigeration*, Sydney, Australia, 19 - 24 September, 1999.
- [186] R. N. N. Koury, L. Machado, K. A. R. Ismail, “Numerical simulation of variable speed refrigeration system,” *International Journal of Refrigeration*, vol. 24, pp. 192-200, 2001.

## ***REFERENCES***

---

- [187] F. Schiavo, F. Casella, “Object-oriented modelling and simulation of heat exchangers with finite element methods,” *Mathematical and Computer Modelling of Dynamical System*, vol. 13, pp. 211-235, 2007.
- [188] C. J. L. Hermes, C. Melo, “Assessment of the energy performance of household refrigerators via dynamic simulation,” *Applied Thermal Engineering*, vol. 29, pp. 1153-1165, 2009.
- [189] R. N. N. Koury, R. N. Faria, R. O. Nunes, K. A. R. Ismail, L. Machado, “Dynamic model and experimental study of an air-water heat pump for residential use,” *International Journal of Refrigeration*, vol. 24, pp. 192-200, 2001.
- [190] E. Berger, S. Posch, M. Heimeil, R. Almbauer, M. Eichinger, A. Stupnik, “Transient 1D heat exchanger model for the simulation of domestic cooling cycles working with R600a,” *Science and Technology for the Built Environment*, vol. 21, pp. 1010-1017, 2015.
- [191] J. Wu, E. Gagnière, F. Couenne, B. Hamroun, T. Latour, C. Jallut, “A hybrid transient model for simulation of air-cooled refrigeration systems: description and experimental validation,” *International Journal of Refrigeration*, vol. 53, pp. 142-154, 2012.
- [192] C. R. Laughman, H. Qiao, V. Aute, R. Radermacher, “A comparison of transient heat pump cycle models using alternative flow description,” *Science and Technology for the Built Environment*, vol. 21, pp. 666-680, 2015.
- [193] M. J. P. Janssen, J. A. de Wit, L. J. M. Kuijpers, “Cycling losses in domestic appliances: an experimental and theoretical analysis,” *International Journal of Refrigeration*, vol. 15, pp. 152-158, 1992.

## ***REFERENCES***

---

- [194] X. D. He, S. Liu, H. H. Asada, “Moving-interface model of two-phase flow heat exchanger dynamics for control of vapor-compression cycle,” *Heat Pump and Refrigeration Systems Design, Analysis and Applications: Proceedings of the International Mechanical Engineering Congress and Exposition (Advanced Energy Systems Series)*, vol. 32, pp. 69-75, 1994.
- [195] W. J. Zhang, C. L. Zhang, “A generalized moving-boundary model for transient simulation of dry-expansion evaporators under larger disturbances,” *International Journal of Refrigeration*, vol. 29, pp. 119-1127, 2006.
- [196] L. C. Schurt, C. J. L. Hermes, A. T. Neto, “A model-driven multivariable controller for vapor compression refrigeration systems,” *International Journal of Refrigeration*, vol. 32, pp. 1672-1682, 2009.
- [197] B. Li, A. G. Alleyne, “A dynamic model of a vapor compression cycle with shut-down and start-up operations,” *International Journal of Refrigeration*, vol. 33, pp. 538-552, 2010.
- [198] J. N. Esbri, V. Millian, A. Mota-Babiloni, F. Moles, G. Verdu, “Effect of mean void fraction correlations on a shell-and-tube evaporator dynamic model performance,” *Science and Technology for the Built Environment*, vol. 21, pp. 1059-1072, 2015.
- [199] S. Yang, J. C. Ordonez, “Integrative thermodynamic optimization of a vapor compression refrigeration system based on dynamic system responses,” *Applied Thermal Engineering*, vol. 135, pp. 493-503, 2018.

## ***REFERENCES***

---

- [200] S. Bendapudi, J. E. Braun, E. A. Groll, “A comparison of moving-boundary and finite-volume formulations for transients in centrifugal chillers,” *International Journal of Refrigeration*, vol. 31, pp. 1437-1452, 2008.
- [201] N. Liang, S. Shao, C. Tian, Y. Yan, “Dynamic simulation of variable capacity refrigeration systems under abnormal conditions,” *Applied Thermal Engineering*, vol. 30, pp. 1205-1214, 2010.
- [202] E. Rodriguez, B. Rasmussen, “A comparison of modeling paradigms for dynamic evaporator simulations with variable fluid phases,” *Applied Thermal Engineering*, Vol. 112, pp. 1326-1342, 2017.
- [203] J. Garcia, T. Ali, W. M. Duarte, A. Khosravi, L. Machado, “Comparison of transient response of an evaporator model for water refrigeration system working with R1234yf as a drop-in replacement for R134a,” *International Journal of Refrigeration*, vol. 91, pp. 211-222, 2018.
- [204] S. A. Bendapudi, J. E. Braun, “A review of literature on dynamic models of vapor compression equipment,” *Herrick Laboratories, Purdue University*, West Lafayette, 2002.
- [205] Armfield Ltd., “Instruction manual: RA1 vapour – compression refrigeration unit,” *Bridge House*, Hampshire, 2009.
- [206] V. Gnielinski, “New equations for heat and mass transfer in the turbulent flow in pipes and channels,” *NASA, Technical Report A*, vol. 752, pp. 22020, 1975.

## ***REFERENCES***

---

- [207] M. Dobson, J. Chato, “Condensation in smooth horizontal tubes,” *Journal of Heat Transfer*, vol. 120, pp. 193, 1998.
- [208] B. P. Rasmussen, A. G. Alleyne, “Dynamic modelling and advanced control of air conditioning and refrigeration systems,” *University of Illinois*, Report, Urbana, 2006.
- [209] W. F. Stoecker, “Stability of an evaporator valve control loop,” *ASHRAE Transactions*, vol. 72, 1966.
- [210] H. Najork, “Investigations on the dynamical behavior of evaporators with thermostatic expansion valve,” *13<sup>th</sup> International Congress of Refrigeration*, pp. 759-769, 1973.
- [211] P. M. T. Broersen, M. F. G. Vand der Jagt, “Hunting of evaporators controlled by a thermostatic expansion valve,” *ASME Journal of Dynamic Systems, Measurement & Control*, vol. 2, pp. 130-135, 1980.
- [212] W. D. Gruhle, R. Isermann, “Modeling and control of a refrigerant evaporator,” *ASME Journal of Dynamic Systems, Measurement & Control*, vol. 9, pp. 235-240, 1985.
- [213] K. A. James, R. W. James, A. Dunn, “A critical survey of dynamic mathematical models of refrigeration systems and heat pumps and their components,” *IoEE Technical Memorandum*, South Bank Polytechnic, Paper ID 97, 1985.
- [214] G. A. Ibrahim, “Effect of sudden changes in evaporator external parameters on a refrigeration system with an evaporator controlled by thermostatic expansion valve,” *International Journal of Refrigeration*, vol. 24, pp. 556-576, 2001.

## ***REFERENCES***

---

- [215] C. Zhijiu, Z. Ruiqi, W. Yezheng, W. Chen, “Experimental investigation of a minimum stable superheat control system of an evaporator,” *International Journal of Refrigeration*, vol. 25, pp. 1137-1142, 2002.
- [216] D. L. Boyd, “Capacity control of reciprocating compressors used in refrigeration systems,” *Purdue e-Pubs*, Purdue, 1972.
- [217] S. A. Tassou, C. J. Marquand, “Comparison of the performance of capacity-controlled and conventional-controlled heat pumps,” *Applied Energy*, vol. 14, pp. 241-256, 1988.
- [218] T. Q. Qureshi, S. A. Tassou, “Variable speed capacity control in refrigeration systems,” *Applied Thermal Engineering*, vol. 16, pp. 103-113, 1996.
- [219] M. Yaqub, S. M. Zubair, “Capacity control for refrigeration and air-conditioning systems: a comparative study,” *Journal of Energy Resources Technology*, vol. 123, pp. 92-99, 2001.
- [220] D. A. Hickman, J. Slupsky, B. M. Chrisman, T. J. Hurley, “Development, field testing and implementation of automated, hydraulically controlled, variable volume loading systems for reciprocating compressors,” *4<sup>th</sup> International Pipeline Conference*, Calgary, Canada, 30 September - 03 October, 2002.
- [221] J. H. Huh, M. J. Brandemuehl, “Optimization of air-conditioning system operating strategies for hot and humid climates,” *Energy and Buildings*, vol. 40, pp. 1202-1213, 2008.



## ***REFERENCES***

---

- [222] D. Li, H. Wu, J. Gao, “Experimental study on stepless capacity regulation for reciprocating compressor based on novel rotary control valve,” *International Journal of Refrigeration*, vol. 36, pp.1701-1713, 2013.
- [223] L. Wang, G. B. Liu, Y. Y. Zhao, L. L. Li, “Performance comparison of capacity control methods for reciprocating compressors,” *9<sup>th</sup> International Conference on Compressors and their Systems*, London, UK, 05 - 09 September, 2015.
- [224] Y. Wang, Z. Jiang, J. Zhang, C. Zhou, W. Liu, “Performance analysis and optimization of reciprocating compressor with stepless capacity control system under variable load conditions,” *International Journal of Refrigeration*, vol. 94, pp. 174-185, 2018.
- [225] X. D. He, S. Liu, H. H. Asada, “Modeling of vapor compression cycles for multivariable feedback control of HVAC systems,” *ASME Journal of Dynamic Systems, Measurement & Control*, vol. 119, pp. 183-191, 1997.
- [226] Q. Qi, S. Deng, “Multivariable control-oriented modelling of a direct expansion (DX) air conditioning (A/C) system,” *International Journal of Refrigeration*, vol. 40, pp. 841-849, 2008.
- [227] L. Jingyun, L. Ping, “Temperature and humidity control with a model predictive control method in the air-conditioning system,” *2017 International Conference on Advanced Mechatronic Systems*, Xiamen, China, 06 - 09 December, 2017.
- [228] J. Mei, B. Zhu, X. Xia, “Model predictive control for optimizing indoor air temperature and humidity in a direct expansion air conditioning system,” *IEEE 27th Chinese Control and Decision Conference (CCDC)*, Qingdao, China, 23 - 25 May, 2015.

## ***REFERENCES***

---

- [229] J. Mei, X. Xia, “Energy-efficient predictive control of indoor thermal comfort and air quality in a direct expansion air conditioning system,” *Applied Energy*, vol. 195, pp. 439-452, 2017.
- [230] J. Mei, “Energy Efficiency Control of Direct Expansion Air Conditioning Systems,” *PhD Thesis, University of Pretoria*, Pretoria, 2018.
- [231] X. D. He, S. Liu, H. H. Asada, H. Itoh, “Multivariable control of vapor compression systems,” *HVAC&R Research*, vol.4, pp. 205-230, 1998.
- [232] D. Leducq, J. Guilpart, G. Trystram, “Low order dynamic model of a vapor compression cycle for process control design,” *Journal of Food Process Engineering*, vol. 6, pp. 67-91, 2003.
- [233] R. Shah, B. P. Rasmussen, A. G. Alleyne, “Application of a multivariable adaptive control strategy to automotive air conditioning systems,” *International Journal of Adaptive Control and Signal Processing*, vol. 18, pp. 199-221, 2004.
- [234] C. Sanama, X. Xia, “Transient state modelling and experimental investigation of the thermal behavior of a vapor compression system,” *Mathematical Problems in Engineering*, vol. 2021, pp. 1 - 14, 2021.
- [235] X. D. He, “Dynamic modeling and multivariable control of vapor compression cycles in air conditioning systems,” *PhD Thesis, MIT*, Boston, 1996.
- [236] B. P. Rasmussen, “Control-oriented modeling of transcritical vapor compression systems,” *Masters Dissertation, University of Illinois at Urbana-Champaign*, Illinois, 2002.

## ***REFERENCES***

---

- [237] R. Shah, A. G. Alleyne, C. W. Bullard, B. P. Rasmussen, P. S. Hrnjak, “Dynamic modeling and control of single and multi-evaporator subcritical vapor compression systems,” *ACRC Technical Report 216, Air Conditioning and Refrigeration Center, University of Illinois at Urbana-Champaign, Illinois, 2003.*
- [238] B. D. Eldredge, A. G. Alleyne, “Improving the accuracy and scope of control-oriented vapor compression cycle system models,” *ACRC Technical Report 246, Air Conditioning and Refrigeration Center, University of Illinois at Urbana-Champaign, Illinois, 2006.*
- [239] B. Li, “Dynamic modeling and control of vapor compression cycle systems with shut-down and start-up operations,” *Masters Dissertation, University of Illinois at Urbana-Champaign, Illinois, 2009.*
- [240] B. Li, N. Jain, B. Mohs, S. Munns, V. Patnaik, J. Berge, A. G. Alleyne, “Dynamic modeling of refrigerated transport systems with cooling-mode/heating-mode switch operations,” *HVAC&R Research*, vol. 18, pp. 974-996, 2012.
- [241] J. M. Fasl, “Modeling and control of hybrid vapor compression cycles,” *Masters Dissertation, University of Illinois at Urbana-Champaign, Illinois, 2013.*
- [242] A. Gustavsson, “Dynamic modeling and model predictive control of a vapor compression system,” *Masters Dissertation, Linkoping University, Linkoping, 2012.*
- [243] Y. Huang, A. Khajepour, F. Bagheri, M. Barhami, “Modelling and optimal energy-saving control of automotive air-conditioning and refrigeration systems,” *Proceedings of the Institution of Mechanical Engineers, Part D: Journal of Automobile Engineering*, vol. 231, pp. 291 - 309, 2017.

## ***REFERENCES***

---

- [244] Q. Q. Wang, C. C. Hang, Y. Zhang, Q. Bi, “Multivariable controller auto-tuning with its application in HVAC systems,” *Proceedings of the American Control Conference*, vol. 6, pp. 4353-4357, 1999.
- [245] Q. Bi, W. J. Cai, Q. G. Wang, C. C. Hang, E. L. Lee, Y. Sun, K. D. Liu, Y. Zhang, B. Zou, “Advanced controller auto-tuning and its application in HVAC systems,” *Control Engineering Practice*, vol. 8, pp. 633-644, 2000.
- [246] S. S. Franco, J. R. Henriquez, A. A. V. Ochoa, J. A. P. Da Costa, K. A. Ferraz, “Thermal analysis and development of PID control for electronic expansion device of vapor compression refrigeration systems,” *Applied Thermal Engineering*, vol. 206, Paper ID 118130, 2022.
- [247] O. Ekren, S. Sahin, Y. Isler, “Comparison of different controllers for variable speed compressor and electronic expansion valve,” *International Journal of Refrigeration*, vol. 33, pp. 1161-1168, 2010.
- [248] H. Fallahsohi, C. Changenet, S. Place, C. Ligeret, X. Lin-Shi, “Predictive functional control of an expansion valve for minimizing the superheat of an evaporator,” *International Journal of Refrigeration*, vol. 33, pp. 409-418, 2010.
- [249] D. J. Burns, S. A. Bortoff, “Exploiting refrigerant distribution for predictive control of multi-evaporator vapor compression systems,” *2017 IEEE conference on Control Technology and Applications (CCTA)*, Kohala Coast, USA, 27 - 30 August, 2017.
- [250] X. Yin, S. Li, “Energy efficient predictive control for vapor compression refrigeration cycle system,” *IEEE/CAA Journal of Automatica Sinica*, vol. 5, pp. 953-960, 2018.

## ***REFERENCES***

---

- [251] Y. Chen, S. Treado, “Development of a simulation platform based on dynamic models for HVAC control analysis,” *Energy and Buildings*, vol. 68, pp. 376-386, 2014.
- [252] A. C. Cleland, “Computer subroutines for rapid evaluation of refrigerant thermodynamic properties,” *International Journal of Refrigeration*, vol. 9, pp. 346-351, 1986.
- [253] O. E. Turgut, M. T. Coban, M. Asker, “Saturated flow boiling heat transfer correlation for small channels based on R134a experimental data,” *Arabian Journal for Science and Engineering*, vol. 41, pp. 1921-1939, 2016.
- [254] F. Dittus, L. Boelter, “Heat Transfer in Automobile Radiators of the Tubular Type,” *International Communications in Heat and Mass Transfer*, vol. 12, pp. 3 – 22, 1985.
- [255] Y. Xu, X. Fang, “A new correlation of two-phase frictional pressure drop for evaporating flow in pipes,” *International Journal of Refrigeration*, vol. 35, pp. 2039-2050, 2012.
- [256] L. Wojtan, T. Ursenbacher, J. R. Thome, “Investigation of flow boiling in horizontal tubes: Part I – A new diabatic two-phase flow pattern map,” *International Journal of Heat and Mass Transfer*, vol. 48, pp. 2955-2969, 2005.
- [257] S. Z. Rouhani, E. Axelsson, “Calculation of void volume fraction in the subcooled and quality boiling regions,” *International Journal of Heat and Mass Transfer*, vol. 13, pp. 383-393, 1970.
- [258] R. G. Kapadia, S. Jain, R. S. Agarwal, “Transient characteristics of split air-conditioning systems using R-22 and R-410A as refrigerants,” *HVAC&R Research*, vol. 15, pp. 617-649, 2009.

## ***REFERENCES***

---

- [259] A. Outtagarts, P. Haberschill, M. Lallemand, “The transient response of an evaporator fed through an electronic expansion valve,” *International Journal of Energy Research*, vol. 21, pp. 793-807, 1997.
- [260] P. Haberschill, L. Gay, P. Aubouin, M. Lallemand, “Dynamic model of a vapor-compression refrigerating machine using R-407C,” *HVAC&C Research*, vol. 9, pp. 451-466, 2003.
- [261] C. Sanama, X. Xia, “Modelling and experimental investigation of a vapor compression system under steady state regime,” *International Journal of Mechanical Engineering and Robotic Research*, vol. 11, pp.114-122, 2022.
- [262] F. Behrooz, N. Mariun, M. H. Marhaban, M. A. M. Radzi, A. R. Ramli, “Review of control techniques for HVAC systems-nonlinearity approaches based on fuzzy cognitive maps,” *Energies*, vol. 11, pp. 1-41, 2018.
- [263] A. Afram, F. Janabi-Sharifi, “Theory and application of HVAC control systems - A review of model predictive control (MPC),” *Building & Environment*, vol. 72, pp. 343-355, 2014.
- [264] B. Tashtoush, M. Molhim, M. Al-Rousan, “Dynamic model of an HVAC system for control analysis,” *Energy*, vol. 30, pp. 1729-1745, 2005.
- [265] M. Xu, S. Li, W. J. Cai, L. Lu, “Effects of a GPC-PID control strategy with hierarchical structure for a cooling coil unit,” *Energy Conversion & Management*, vol. 47, pp. 132-145, 2006.

## ***REFERENCES***

---

- [266] M. Xu, S. Li, “Practical generalized predictive control with decentralized identification approach to HVAC systems,” *Energy Conversion & Management*, vol. 48, pp. 292-299, 2007.
- [267] A. Thosar, A. Patra, S. Bhattacharyya, “Feedback linearization based control of a variable air volume air conditioning system for cooling applications,” *ISA*, vol. 47, pp. 339-349, 2008.
- [268] W. J. Zhang, S. F. Ding, C. L. Zhang, “Transient modeling of an air-cooled chiller with economized compressor. Part II: Application to control design,” *Applied Thermal Engineering*, vol. 29, pp. 2403-2407, 2009.
- [269] A. Parisio, D. Varagnolo, M. Molinari, G. Pattarello, L. Fabietti, K. H. Johansson, “Implementation of a Scenario-based MPC for HVAC Systems: an Experimental Case Study,” *IFAC Proceedings Volumes*, vol. 47, pp. 599-605, 2014.
- [270] D. Sotelo, A. Favela-Contreras, V. V. Kalashnikov, C. Sotelo, “Model predictive control with a relaxed cost function for constrained linear systems,” *Mathematical Problems in Engineering*, vol. 2020, pp. 1-10, 2020.
- [271] P. D. Morosan, R. Bourdais, D. Buisson, “Building temperature using a distributed model predictive control,” *Energy and Buildings*, vol. 42, pp. 1445-1452, 2010.
- [272] J. A. Candanedo, A. K. Athientis, “Predictive control of radiant floor heating and solar-source heat pump operation in a solar house,” *HVAC&R Research*, vol. 17, pp. 235-256, 2011.

## ***REFERENCES***

---

- [273] J. Rerhl, M. Horn, “Temperature control for HVAC systems based on exact linearization and model predictive control,” *IEEE International Conference on Control Applications (CCA)*, Denver, USA, 28 - 30 September, 2011.
- [274] J. Siroky, F. Oldewurtel, J. Cigler, S. Privara, “Experimental analysis of model predictive control for an energy efficient building heating system,” *Applied Energy*, vol. 88, pp. 3079-3087, 2011.
- [275] S. Privara, J. Siroky, L. Ferkl, J. Cigler, “Model predictive control of a building heating system: The first experience,” *Energy and Buildings*, vol. 43, pp. 564-572, 2011.
- [276] J. Ma, J. Qin, T. Salsbury, P. Xu, “Demand reduction in building energy systems based on economic model predictive control,” *Chemical Engineering Science*, vol. 67, pp. 92-100, 2012.
- [277] T. Salsbury, P. Mhaskar, S. J. Qin, “Predictive control methods to improve energy efficiency and reduce demand in buildings,” *Computer and Chemical Engineering*, vol. 51, pp. 75-77, 2013.
- [278] S. Zhan, A. Chong, “Data requirements and performance evaluation of model predictive control in buildings: A modeling perspective,” *Renewable and Sustainable Energy Reviews*, vol. 142, pp. 1-17, 2021.
- [279] T. Ferhatbegovic, P. Palensky, G. Fontanella, D. Basciotti, “Modelling and design of a linear predictive controller for a solar powered HVAC system,” *IEEE International Symposium on Industrial Electronics*, Hangzhou, China, 28 - 31 May, 2012.



## ***REFERENCES***

---

- [280] J. E. Braun, S. A. Klein, W. A. Beckman, J. W. Mitchell, "Methodology for optimal control of chilled water systems without storage," *ASHRAE Transactions*, vol. 95, pp. 652-662, 1989.
- [281] B. C. Ahn, J. W. Mitchell, "Optimal control development for chilled water plants using quadratic representation," *Energy and Buildings*, vol. 33, pp. 371-378, 2001.
- [282] F. Wang, H. Yoshida, K. Matsumoto, "Energy consumption for room air-conditioners using room temperatures simulations with one-minute intervals," *International Conference for Enhanced Building Operations, Shenzhen: HVAC Technologies for Energy Efficiency*, Shenzhen, China, 06 - 09 November, 2006.
- [283] B. Dong, "Non-linear optimal controller design for building HVAC systems," *IEEE International Conference Control Applications Part of 2010 IEEE Multi-conference on Systems and Control*, Yokohama, Japan, 08 - 10 September, 2010.
- [284] Y. L. Shen, W. J. Cai, S. Y. Li, "Normalized decoupling control for high-dimensional MIMO process for application in room temperature control HVAC systems," *Control Engineering Practice*, vol. 18, pp. 652-664, 2010.
- [285] E. Semsar-Kazerooni, M. Yazdampanah, C. Lucas, "Nonlinear control and disturbance decoupling of HVAC systems using feedback linearization and backstepping with load estimation," *IEEE Transactions on Control Systems Technology*, vol. 16, pp. 918-929, 2008.

## ***REFERENCES***

---

- [286] S. Huang, R. Nelson, "Rule development and adjustment strategies of a fuzzy logic controller for an HVAC system: Part one – analysis," *ASHRAE Transactions*, vol. 100, pp. 841-850, 1994.
- [287] S. Huang, R. Nelson, "Rule development and adjustment strategies of a fuzzy logic controller for an HVAC system: Part two – experiment," *ASHRAE Transactions*, vol. 100, pp. 851-856, 1994.
- [288] M. Arima, E. H. Hara, J. D. Katzberg, "A fuzzy logic and rough sets controller for HVAC systems," *IEEE WESCANEX 95. Communications, Power, and Computing. Conference Proceedings*, vol. 1, pp. 133-138, 1995.
- [289] R. N. Lea, E. Dohmann, W. Prebisky, Y. Jani, "An HVAC fuzzy logic zone control system and performance results," *5<sup>th</sup> IEEE International Conference on Fuzzy Systems*, New Orleans, USA, 08 - 11 September, 1996.
- [290] S. S. Ahmed, M. S. Majid, H. Novia, H. A. Rahman, "Fuzzy logic based energy saving technique for a central air conditioning system," *Energy*, vol., 32, pp. 1222-1234, 2007.
- [291] C. Guo, Q. Song, W. Cai, "A neural network assisted cascade control system for air handling unit," *IEEE Transactions on Industrial Electronics*, vol. 54, pp.620-628, 2007.
- [292] H. Mirinejad, S. H. Sadati, M. Ghasemian, H. Torab, "Control techniques on heating, ventilating and air conditioning (HVAC) systems," *Journal of Computer Science*, Vol. 4, pp. 777-783, 2008.

## ***REFERENCES***

---

- [293] H. Mirinejad, K. C. Welch, L. Spicer, “A review of intelligent control techniques in HVAC systems,” *2012 IEEE Energytech Conference*, Cleveland, USA, 29 - 31 May, 2012.
- [294] R. Z. Freire, G. H. C. Oliveira, N. Mendes, “Predictive controllers for thermal comfort optimization and energy savings,” *Energy and Buildings*, vol. 40, pp. 1353-1365, 2008.
- [295] G. Serale, M. Fiorentini, A. Capozzoli, D. Bernardini, A. Bemporad, “Model predictive control (MPC) for enhancing building and HVAC system energy efficiency: problem formulation, applications and opportunities,” *Energies*, vol. 11, pp. 1-35, 2018.
- [296] R. Kwadzogah, M. Zhou, “Model predictive control for HVAC systems - a review,” *IEEE International Conference on Automation Science and Engineering (CASE)*, Madison, USA, 17 - 20 August, 2013.
- [297] S. Wang, Z. Ma, “Supervisory and optimal control of building HVAC systems: a review,” *HVAC&R Research*, vol. 14, pp. 3-32, 2008.
- [298] M. Sen, R. Singh, R. Ramachandran, “A hybrid MPC-PID control system design for the continuous purification and processing of active pharmaceutical ingredients,” *Processes*, vol. 2, pp. 392-418, 2014.
- [299] S. Deshmukh, S. Samouhos, L. Glicksman, L. Norford, “Fault detection in commercial building VAV AHU: A case study of an academic building,” *Energy and Buildings*, vol. 201, pp. 163-173, 2019.
- [300] B. Wu, W. Cai, H. Chen, X. Zhang, “A hybrid data-driven simultaneous fault diagnosis model for air handling units,” *Energy and Buildings*, vol. 245, pp. 1-12, 2021.

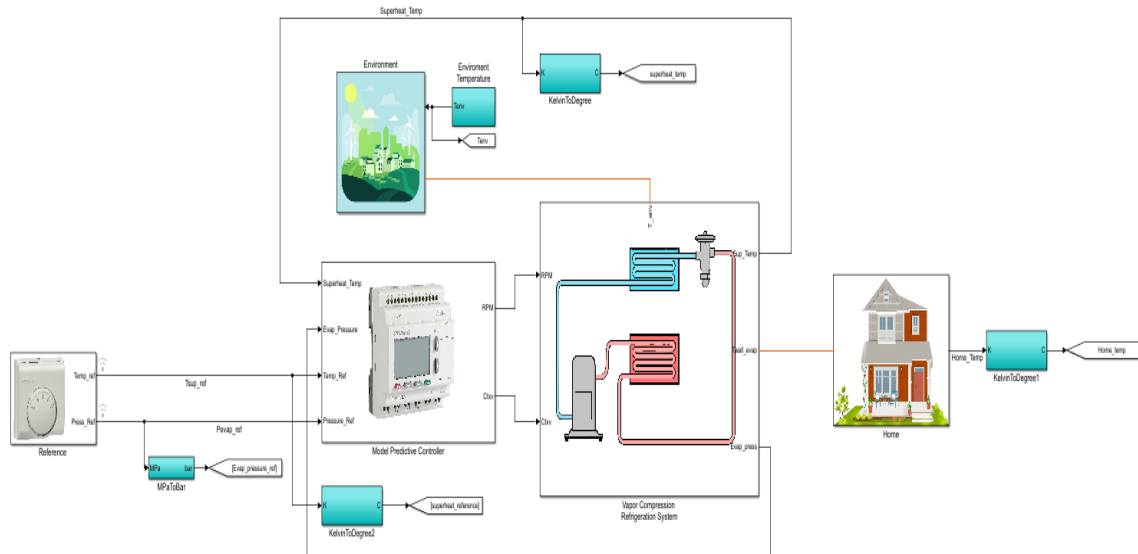
## ***REFERENCES***

---

- [301] M. L. Abell, J. P. Braselton, “Introductory Differential Equations,” *Elsevier Science*, vol. 5, ISBN 978-0-12-814948-5, 2019.
- [302] D. S. Naidu, C. G. Rieger, “Advanced control strategies for heating, ventilation, air-conditioning, and refrigeration systems - An overview: Part I: Hard control,” *HVAC&R Research*, vol. 17, pp. 2-21, 2011.
- [303] R. Z. Homod, “Automatic control for HVAC system,” *Masters Dissertation, University of Malaya*, Kuala Lumpur, 2009.
- [304] K. Zakova, M. Huba, “Theoretical Analysis of Ziegler-Nichols Conclusions,” *IFAC Proceedings Volumes*, vol. 30, pp. 195-200, 1997.
- [305] V. Ramasamy, R. K. Sidharthan, R. Kannan, G. Muralidharan, “Optimal tuning of model predictive controller weights using genetic algorithm with interactive decision tree for industrial cement kiln,” *Processes*, vol. 7, pp. 1-22, 2019.

# ADDENDUM

## A.1. SIMULINK MODEL OF A VC SYSTEM



## A.2. HEAT TRANSFER CORRELATIONS

Heat exchanger	Parameter	Formula	Description
	Chilton - Colburn factor	$J_{hx,dry} = 0.023 Re_{hx,dry}^{-0.2}$	<ul style="list-style-type: none"> <li><math>Re_{hx,dry}</math> : Reynolds number at the dry zone of the heat exchanger</li> </ul>
Dry zone	Prandtl number	$Pr_{hx,dry} = \frac{C_{air} \mu_{hx,dry}}{k_{hx}}$	<ul style="list-style-type: none"> <li><math>\mu_{hx,dry}</math> : dynamic viscosity of air at the dry zone of the heat exchanger in (kg/m.s)</li> <li><math>k_{hx}</math> : thermal conductivity of the heat exchanger in (kw/m °C)</li> </ul>

## ADDENDUM

---

	Reynolds number	$Re_{hx,dry} = \frac{\rho_{air} u_{hx,dry}}{\mu_{hx,dry}} l_{hx,dry}$	<ul style="list-style-type: none"> <li>○ <math>l_{hx,dry}</math> : length of the dry zone of the heat exchanger in (m)</li> </ul>
	Chilton - Colburn factor	$J_{hx,wet} = 0.023 Re_{hx,wet}^{-0.2}$	<ul style="list-style-type: none"> <li>○ <math>Re_{hx,wet}</math> : Reynolds number at the wet zone of the heat exchanger</li> </ul>
Wet zone	Prandtl number	$Pr_{hx,wet} = \frac{C_{air} \mu_{hx,wet}}{k_{hx}}$	<ul style="list-style-type: none"> <li>○ <math>\mu_{hx,wet}</math> : dynamic viscosity of air at the wet zone of the heat exchanger in (kg/m.s)</li> <li>○ <math>k_{hx}</math> : thermal conductivity of the heat exchanger in (kw/m °C)</li> </ul>
	Reynolds number	$Re_{hx,wet} = \frac{\rho_{air} u_{hx,wet}}{\mu_{hx,wet}} l_{hx,wet}$	<ul style="list-style-type: none"> <li>○ <math>l_{hx,wet}</math> : length of the wet zone of the heat exchanger in (m)</li> </ul>

### A.3. DERIVATION OF DISCRETIZED EQUATIONS

Conservation of mass and energy in the condenser:

$$\frac{\partial \rho}{\partial t} + \frac{\partial(\rho u)}{\partial x} = 0 \quad (\text{A.1})$$

$$\frac{\partial(\rho h)}{\partial t} + \frac{\partial(\rho u h)}{\partial x} + \delta \dot{Q}_{ref} = 0 \quad (\text{A.2})$$

$\delta \dot{Q}_{ref}$  is defined as follows:

$$\delta \dot{Q}_{ref} = \frac{\alpha}{N_{cells}} \frac{(T_{ref,cond} - T_{wall})}{\delta x} \quad (\text{A.3})$$

## ADDENDUM

---

$\alpha$  is the heat transfer coefficient ( $kw/m^2\text{°C}$ ).  $T_{ref,cond}$  is the refrigerant temperature in the condenser ( $\text{°C}$ ).  $T_{wall}$  is the wall temperature in the condenser ( $\text{°C}$ ).  $\delta x$  is the distance travelled by the refrigerant stream ( $m$ ).

Eq. (A.1) and (A.2) could be discretized across the  $i^{th}$ -control volume as follows:

$$\int_{cv} \left( \frac{\partial \rho}{\partial t} \right) dV_i + \int_{cv} \left( \frac{\partial(\rho u)}{\partial x} \right) dV_i = 0 \quad (\text{A.4})$$

$$\int_{cv} \left( \frac{\partial(\rho h)}{\partial t} \right) dV_i + \int_{cv} \left( \frac{\partial(\rho u h)}{\partial x} \right) dV_i + \int_{cv} (\delta \dot{Q}_{ref}) dV_i = 0 \quad (\text{A.5})$$

The volume integrals with spatial terms in (A.4) and (A.5) could be re-written as surface integrals by adopting the divergence theorem of Gauss. For a vector  $\lambda$  this theorem states:

$$\int_{cv} \frac{\partial \lambda}{\partial x} dV = \int_{cv} \text{div}(\lambda) dV = \int_A n \cdot \lambda dA \quad (\text{A.6})$$

$n \cdot \lambda$  represents the component  $\lambda$  in the direction of vector  $n$  normal to the bounding surface element  $dA$ . Applying Gauss's theorem, (A.4) and (A.5) can be written as follows:

$$\frac{\partial}{\partial t} \int_{cv} (\rho) dV_i + \int_{A_i} n \cdot (\rho u) dA_i = 0 \quad (\text{A.7})$$

$$\frac{\partial}{\partial t} \int_{cv} (\rho h) dV_i + \int_{A_i} n \cdot (\rho u h) dA_i + (\delta \dot{Q}_{ref} V)_i = 0 \quad (\text{A.8})$$

Re-arranging (A.7) and (A.8) yields to:

$$\frac{\partial(\rho V)_i}{\partial t} + [\rho u A_i]_{in}^{out} = 0 \quad (\text{A.9})$$

## ADDENDUM

---

$$\frac{\partial(\rho hV)_i}{\partial t} + [\rho u A_i h]_{in}^{out} + \delta \dot{Q}_{ref,i} A_i \delta x, i = 0 \quad (A.10)$$

By definition,

$$\rho u A_i = \dot{m} \quad (A.11)$$

$$\delta \dot{Q}_{ref,i} = \frac{\alpha_i}{N_{cells}} \frac{(T_i - T_{wall,i})}{\delta x, i} \quad (A.12)$$

Therefore,

$$[\rho u A_i]_{in}^{out} = -(\dot{m}_{cond,ref})_{in} + (\dot{m}_{cond,ref})_{out} \quad (A.13)$$

$$[\rho u A_i h]_{in}^{out} = -(\dot{m}_{cond,ref})_{in} h_{cond,in} + (\dot{m}_{cond,ref})_{out} h_{cond,out} \quad (A.14)$$

$$\delta \dot{Q}_{ref,i} A_i \delta x, i = \alpha_i \frac{A_i}{N_{cells}} (T_i - T_{wall,i}) = \dot{Q}_{ref,i} \quad (A.15)$$

Eq. (A.9) and (A.10) could therefore be re-written as follows:

$$\frac{\partial(\rho V)_i}{\partial t} - (\dot{m}_{cond,ref})_{in} + (\dot{m}_{cond,ref})_{out} = 0 \quad (A.16)$$

$$\frac{\partial(\rho hV)_i}{\partial t} - (\dot{m}_{cond,ref})_{in} h_{cond,in} + (\dot{m}_{cond,ref})_{out} h_{cond,out} + \dot{Q}_{ref,i} = 0 \quad (A.17)$$

Applying the chain rules with  $\rho = f(P, h)$ , (A.16) and (A.17) could be arranged as follows:



## ADDENDUM

---

$$V_i \left[ \left. \frac{\partial \rho_i}{\partial P} \right|_{h,i} \frac{dP_{cond}}{dt} + \left. \frac{\partial \rho_i}{\partial h_i} \right|_P \frac{dh_i}{dt} \right] = (\dot{m}_{cond,ref})_{in} - (\dot{m}_{cond,ref})_{out} \quad (A.18)$$

$$\begin{aligned} V_i \left[ \left( h_i \left. \frac{\partial \rho_i}{\partial P} \right|_{h,i} - 1 \right) \frac{dP_{cond}}{dt} + \left( h_i \left. \frac{\partial \rho_i}{\partial h_i} \right|_P + \rho_i \right) \frac{dh_i}{dt} \right] \\ = (\dot{m}_{cond,ref})_{in} h_{cond,in} - (\dot{m}_{cond,ref})_{out} h_{cond,out} - \dot{Q}_{ref,i} \end{aligned} \quad (A.19)$$

Inserting (A.18) into (A.19) yields to:

$$\begin{aligned} (\dot{m}_{cond,ref})_{in} h_i - (\dot{m}_{cond,ref})_{out} h_i - V_i \frac{dP_{cond}}{dt} + V_i \rho_i \frac{dh_i}{dt} \\ = (\dot{m}_{cond,ref})_{in} h_{cond,in} - (\dot{m}_{cond,ref})_{out} h_{cond,out} - \dot{Q}_{ref,i} \end{aligned} \quad (A.20)$$

Eq. (A.20) is for one control volume and it is equivalent to (3.6) and could be re-arranged as follows:

$$\begin{aligned} (\dot{m}_{cond,ref})_{in} h_i - (\dot{m}_{cond,ref})_{out} h_i - V_i \frac{dP_{cond}}{dt} + V_i \rho_i \frac{dh_i}{dt} \\ + (\dot{m}_{cond,ref})_{out} h_{cond,out} \\ = (\dot{m}_{cond,ref})_{in} h_{cond,in} - \alpha_i \frac{A_i}{N_{cells}} (T_i - T_{wall,i}) \end{aligned} \quad (A.21)$$

- Within  $(i - 1)^{th}$ -control volume:

Inlet conditions :  $(\dot{m}_{cond,ref})_{in}$  and  $h_{cond,in}$

## ADDENDUM

---

Centre or nodal point:  $m_{i-1}$  and  $h_{i-1}$

Outlet conditions:  $m_{i-1,i}$  and  $h_{i-1,i}$

Applying Eq. (A.21) within the  $(i - 1)^{th}$ -control volume yields to:

$$\begin{aligned}
 (m_{cond,ref})_{in} h_{i-1} - m_{i-1,i} h_{i-1} - V_{i-1} \frac{dP_{cond}}{dt} + V_{i-1} \rho_{i-1} \frac{dh_{i-1}}{dt} + m_{i-1,i} h_{i-1,i} \\
 = (m_{cond,ref})_{in} h_{cond,in} - \alpha_{i-1} \frac{A_{i-1}}{N_{cells}} (T_{i-1} - T_{wall,i-1})
 \end{aligned} \tag{A.22}$$

○ Within  $i^{th}$ -control volume:

Inlet conditions:  $m_{i-1,i}$  and  $h_{i-1,i}$

Centre or nodal point:  $m_i$  and  $h_i$

Outlet conditions:  $m_{i,i+1}$  and  $h_{i,i+1}$

Applying Eq. (A.21) within the  $i^{th}$ -control volume yields to:

$$\begin{aligned}
 m_{i-1,i} h_i - m_{i,i+1} h_i - V_i \frac{dP_{cond}}{dt} + V_i \rho_i \frac{dh_i}{dt} + m_{i,i+1} h_{i,i+1} \\
 = m_{i-1,i} h_{i-1,i} - \alpha_i \frac{A_i}{N_{cells}} (T_i - T_{wall,i})
 \end{aligned} \tag{A.23}$$

○ Within  $(i + 1)^{th}$ -control volume:

Inlet conditions:  $m_{i,i+1}$  and  $h_{i,i+1}$

Centre or nodal point:  $m_{i+1}$  and  $h_{i+1}$

## ADDENDUM

---

Outlet conditions:  $(\dot{m}_{cond,ref})_{out}$  and  $h_{cond,out}$

Applying (A.21) within the  $(i + 1)^{th}$ -control volume yields to:

$$\begin{aligned}
 m_{i,i+1}h_{i+1} - (\dot{m}_{cond,ref})_{out}h_{i+1} - V_{i+1}\frac{dP_{cond}}{dt} + V_{i+1}\rho_{i+1}\frac{dh_{i+1}}{dt} + (\dot{m}_{cond,ref})_{out}h_{cond,out} \\
 = m_{i,i+1}h_{i,i+1} - \alpha_{i+1}\frac{A_{i+1}}{N_{cells}}(T_{i+1} - T_{wall,i+1})
 \end{aligned} \tag{A.24}$$

Regrouping (A.22) to (A.24) into a system and re-arranging each equation yields to:

$$\left\{ \begin{aligned}
 & (\dot{m}_{cond,ref})_{in}h_{i-1} - m_{i-1,i}h_{i-1} - V_{i-1}\frac{dP_{cond}}{dt} + V_{i-1}\rho_{i-1}\frac{dh_{i-1}}{dt} + m_{i-1,i}h_{i-1,i} \\
 & \quad = (\dot{m}_{cond,ref})_{in}h_{cond,in} - \alpha_{i-1}\frac{A_{i-1}}{N_{cells}}(T_{i-1} - T_{wall,i-1}) \\
 & m_{i-1,i}h_i - m_{i,i+1}h_i - V_i\frac{dP_{cond}}{dt} + V_i\rho_i\frac{dh_i}{dt} - m_{i-1,i}h_{i-1,i} + m_{i,i+1}h_{i,i+1} \\
 & \quad = -\alpha_i\frac{A_i}{N_{cells}}(T_i - T_{wall,i}) \\
 & m_{i,i+1}h_{i+1} - (\dot{m}_{cond,ref})_{out}h_{i+1} - V_{i+1}\frac{dP_{cond}}{dt} + V_{i+1}\rho_{i+1}\frac{dh_{i+1}}{dt} - m_{i,i+1}h_{i,i+1} \\
 & \quad = -(\dot{m}_{cond,ref})_{out}h_{cond,out} - \alpha_{i+1}\frac{A_{i+1}}{N_{cells}}(T_{i+1} - T_{wall,i+1})
 \end{aligned} \right. \tag{A.25}$$

### A.4. MODEL TRANSFORMATION FROM PREDICTIVE TO CONTROL-ORIENTED

To convert the transient model into a control-oriented model more suitable for controller implementation the Navier-Stokes equations adopted for the transient model in the previous section would need to be considered with additional parameters to capture with more accuracy the phase changes undergone by the refrigerant.

Therefore, starting from the conservation equations for mass and energy we previously had as follows:

## ADDENDUM

---

$$\frac{\partial \rho}{\partial t} + \frac{\partial(\rho u)}{\partial x} = 0 \quad (\text{A.1})$$

$$\frac{\partial(\rho h)}{\partial t} + \frac{\partial(\rho u h)}{\partial x} + \delta \dot{Q}_{ref} = 0 \quad (\text{A.2})$$

We need to derive the governing equations of the refrigerant dynamics along within the evaporator and the condenser considering the phase changes. The transient pressure  $p$  needs to be considered to effectively capture the refrigerant dynamics therefore (A.2) could be written into generic energy equation as:

$$\frac{\partial(\rho h - p)}{\partial t} + \frac{\partial(\rho u h)}{\partial x} + \delta \dot{Q}_{ref} = 0 \quad (\text{A.26})$$

### A.4.1. Evaporator modelling

The refrigerant flow through the evaporator undergoes phase change due to energy gains, therefore it is divided in two zones namely, the two-phase and superheated zones. The refrigerant temperature is at saturation and is spatially invariant along the two-phase zone whilst it increases along the single-phase zone through the evaporator outlet.

Adopting time-invariant principle the following Leibniz equation could be adopted:

$$\begin{aligned} & \int_{x_1(t)}^{x_2(t)} \left( \frac{\partial g(x, t)}{\partial t} \right) dx \\ &= \frac{d}{dt} \int_{x_1(t)}^{x_2(t)} g(x, t) dx - g(x_2(t), t) \frac{dx_2(t)}{dt} \\ &+ g(x_1(t), t) \frac{dx_1(t)}{dt} \end{aligned} \quad (\text{A.27})$$

## ADDENDUM

---

Mass conservation equation along the two-phase zone could be integrated from  $x_1 = 0$  to  $x_2 = l_{evap,2ph}$  and expressed as:

$$A_{evap} \int_0^{l_{evap,2ph}} \left( \frac{\partial \rho_{evap,2ph}}{\partial t} \right) dx = (m_{evap,ref})_{in} - (m_{evap,ref})_{int} \quad (A.28)$$

with,

$$\rho_{evap,2ph} = \rho_{evap,liq}(1 - \bar{\gamma}_{evap}) + \rho_{evap,gas}\bar{\gamma}_{evap} \quad (A.29)$$

we have,

$$\begin{aligned} A_{evap} \int_0^{l_{evap,2ph}} \frac{\partial \rho_{evap,2ph}}{\partial t} dx &= \frac{d}{dt} \int_0^{l_{evap,2ph}} (\rho_{evap,liq}(1 - \bar{\gamma}_{evap}) + \rho_{evap,gas}\bar{\gamma}_{evap}) dx \\ &\quad - \rho_{evap,gas} \frac{dl_{evap,2ph}}{dt} \\ &= \frac{d}{dt} \left( l_{evap,2ph} \frac{1}{l_{evap,2ph}} \int_0^{l_{evap,2ph}} (\rho_{evap,liq}(1 - \bar{\gamma}_{evap}) \right. \\ &\quad \left. + \rho_{evap,gas}\bar{\gamma}_{evap}) dx \right) - \rho_{evap,gas} \frac{dl_{evap,2ph}}{dt} \\ &= l_{evap,2ph} \frac{d\rho_{evap,2ph}}{dp} \frac{dp}{dt} + (\rho_{evap,liq} - \rho_{evap,gas}) \frac{dl_{evap,2ph}}{dt} \end{aligned} \quad (A.30)$$

Therefore, the conservation of mass along the two-phase zone is expressed as:

## ADDENDUM

---

$$\begin{aligned}
 A_{evap} l_{evap,2ph} \frac{d\rho_{evap,2ph}}{dp} \frac{dp}{dt} + A_{evap} (\rho_{evap,liq} - \rho_{evap,gas}) \frac{dl_{evap,2ph}}{dt} \\
 = (m_{evap,ref})_{in} - (m_{evap,ref})_{int}
 \end{aligned} \tag{A.31}$$

Energy conservation equation along the two-phase zone could be integrated from  $x_1 = 0$  to  $x_2 =$

$l_{evap,2ph}$  and expressed as:

$$\begin{aligned}
 A_{evap} \int_0^{l_{evap,2ph}} \frac{\partial \rho_{evap,2ph} h_{evap,2ph}}{\partial t} dx - A_{evap} l_{evap,2ph} \frac{dp}{dt} \\
 = (m_{evap,ref})_{in} h_{evap,in} - (m_{evap,ref})_{int} h_{evap,int} + Q_{evap,2ph}
 \end{aligned} \tag{A.32}$$

where,

## ADDENDUM

---

$$\begin{aligned}
 & \int_0^{l_{evap,2ph}} \frac{\partial \rho_{evap,2ph} h_{evap,2ph}}{\partial t} dx \\
 &= \frac{d}{dt} \int_0^{l_{evap,2ph}} \rho_{evap,liq} h_{evap,liq} dx - \rho_{evap,gas} h_{evap,gas} \frac{dl_{evap,2ph}}{dt} \\
 &= \frac{d}{dt} \int_0^{l_{evap,2ph}} \left( \rho_{evap,liq} h_{evap,liq} (1 - \bar{\gamma}_{evap}) \right. \\
 & \quad \left. + \rho_{evap,gas} h_{evap,gas} \bar{\gamma}_{evap} \right) dx - \rho_{evap,gas} h_{evap,gas} \frac{dl_{evap,2ph}}{dt} \\
 &= \frac{d}{dt} \left( \rho_{evap,liq} h_{evap,liq} \int_0^{l_{evap,2ph}} (1 - \bar{\gamma}_{evap}) dx \right. \\
 & \quad \left. + \rho_{evap,gas} h_{evap,gas} \int_0^{l_{evap,2ph}} \bar{\gamma}_{evap} dx \right) \\
 & \quad - \rho_{evap,gas} h_{evap,gas} \frac{dl_{evap,2ph}}{dt} \tag{A.33} \\
 &= \frac{d}{dt} \left( l_{evap,2ph} \rho_{evap,liq} h_{evap,liq} (1 - \bar{\gamma}_{evap}) \right. \\
 & \quad \left. + l_{evap,2ph} \rho_{evap,gas} h_{evap,gas} \bar{\gamma}_{evap} \right) - \rho_{evap,gas} h_{evap,gas} \frac{dl_{evap,2ph}}{dt} \\
 &= l_{evap,2ph} \left( \frac{d(\rho_{evap,liq} h_{evap,liq})}{dt} (1 - \bar{\gamma}_{evap}) \right. \\
 & \quad \left. + \frac{d(\rho_{evap,gas} h_{evap,gas})}{dt} \bar{\gamma}_{evap} \right) \\
 & \quad + (1 - \bar{\gamma}_{evap}) (\rho_{evap,liq} h_{evap,liq} - \rho_{evap,gas} h_{evap,gas}) \frac{dl_{evap,2ph}}{dt}
 \end{aligned}$$

Therefore, (A.32) could be rewritten as:

## ADDENDUM

---

$$\begin{aligned}
 & A_{evap} l_{evap,2ph} \left( \frac{d(\rho_{evap,liq} h_{evap,liq})}{dt} (1 - \bar{v}_{evap}) \right. \\
 & \quad \left. + \frac{d(\rho_{evap,gas} h_{evap,gas})}{dt} \bar{v}_{evap} - \frac{dP_{evap}}{dt} \right) \\
 & \quad + A_{evap} (1 - \bar{v}_{evap}) (\rho_{evap,liq} h_{evap,liq} \\
 & \quad - \rho_{evap,gas} h_{evap,gas}) \frac{dl_{evap,2ph}}{dt} \\
 & = (m_{evap,ref})_{in} h_{evap,in} - (m_{evap,ref})_{int} h_{evap,int} \\
 & \quad + Q_{evap,2ph}
 \end{aligned} \tag{A.34}$$

### A.4.2. Condenser modelling

The condenser equations to be adopted for control-oriented modelling could be derived similarly to the evaporator from Navier-Stokes equations using Leibniz equations however, three zones instead of two should be considered namely, superheat, two-phase and subcool zones.

### A.4.3. Derivation of steady state equations

Considering (A.20) as follows:

$$\begin{aligned}
 & (\dot{m}_{cond,ref})_{in} h_i - (\dot{m}_{cond,ref})_{out} h_i - V_i \frac{dP_{cond}}{dt} + V_i \rho_i \frac{dh_i}{dt} \\
 & = (\dot{m}_{cond,ref})_{in} h_{cond,in} - (\dot{m}_{cond,ref})_{out} h_{cond,out} - \dot{Q}_{ref,i}
 \end{aligned} \tag{A.20}$$

At steady state operating conditions, all time derivatives must be equal to zero therefore:

$$\begin{aligned}
 & (\dot{m}_{cond,ref})_{in} h_i - (\dot{m}_{cond,ref})_{out} h_i \\
 & = (\dot{m}_{cond,ref})_{in} h_{cond,in} - (\dot{m}_{cond,ref})_{out} h_{cond,out} - \dot{Q}_{ref,i}
 \end{aligned} \tag{A.35}$$



## ***ADDENDUM***

---

At steady state condition the refrigerant mass flow rate at the condenser inlet and outlet could be assumed identical and equal to the refrigerant mass flow rate at the compressor or thermostatic expansion valve and therefore:

$$\dot{m}_{comp}(h_{cond,out} - h_{cond,in}) = \dot{Q}_{ref,i} = Q_{cond} \quad (A.36)$$

Eq. (A.36) is equivalent to (3.4) and similar approach could be adopted for the evaporator equation in Table 3.3. Darcy-Weisback correlation is adopted for pressure drop estimation within the condenser and evaporator to determine (3.5) assuming constant HTC, friction factor and neglected water-side pressure drop. Mass flow rate through the expansion valve was correlated following ASHRAE guidelines considering isenthalpic process and constant valve flow coefficient. The refrigerant mass flow rate through the compressor was correlated following [145].